Lincoln University
Te Whare Wānaka o Aoraki

DECLARATION

This dissertation/thesis (please circle one) is submitted in partial fulfilment of the requirements for the Lincoln University Degree of **Bachelors of Agricultural Sciences with Honours**.

The regulations for the degree are set out in the Lincoln University Calendar and are elaborated in a practice manual known as House Rules for the Study of Doctor of Philosophy or Masters Degrees at Lincoln University.

Supervisor's Declaration

I confirm that, to the best of my knowledge:

- the research was carried out and the dissertation was prepared under my direct supervision;
- except where otherwise approved by the Academic Administration Committee of Lincoln University, the research was conducted in accordance with the degree regulations and house rules;
- the dissertation/thesis (please circle one)represents the original research work of the candidate;
- the contribution made to the research by me, by other members of the supervisory team, by other members of staff of the University and by others was consistent with normal supervisory practice.
- external contributions to the research (as defined in the House Rules) are acknowledged. (Delete if not applicable)

Supervisor **Dr. Clive Kaiser** _____ Date 24/11/22

Co-supervisor **Dr. Seona Casonato** _____

Candidate's Declaration

I confirm that:

- this dissertation/thesis (please circle one) represents my own work;
- the contribution of any supervisors and others to the research and to the dissertation/thesis (please circle one) was consistent with normal supervisory practice.
- external contributions to the research (as defined in the House Rules) are acknowledged. (Delete if not applicable)

Candidate **Charan Yuvaraj Sivakumar** _____ Date 24/11/22

Pre-Publication of Parts of this dissertation/thesis (please circle one)

Either:

1 We confirm that no part of this dissertation has been submitted for publication in advance of submission of the dissertation/thesis (please circle one) for examination.

Candidate Charan Yuvaraj Sivakumar _____ Date 24/11/22

Supervisor Dr. Clive Kaiser _____ 24/11/22

Co-supervisor Dr. Seona Casonato _____ Date 24/11/22

Or:

2 Parts of this dissertation/thesis (please circle one) have been submitted and/or accepted for publication in advance of submission of the dissertation/thesis (please circle one) for examination.

In this case, please set out on a separate page information on:

- which sections have been submitted, which have been accepted and which have appeared;
- which journals they have been submitted to;
- who are the co-authors.

Candidate _____ Date 24/11/22

Supervisor _____ Date 24/11/22

Development of a field bioassay for the rapid detection of *Candidatus* Liberibacter solanacearum (Lieft.) in potato (*Solanum tuberosum* L.) leaves and tubers

A dissertation/thesis

submitted in partial fulfilment

of the requirement for the Degree of

Bachelor of Agricultural Science with Honours

at

Lincoln University

by

Charan Yuvaraj Sivakumar

Lincoln University

2022

Abstract of a Thesis submitted in partial fulfilment of the requirement for the Degree of Bachelor of Agricultural Science with Honours.

Development of a field bioassay for the rapid detection of *Candidatus* Liberibacter solanacearum (Lieft.) in potato (*Solanum tuberosum* L.) leaves and tubers

By

Charan Yuvaraj Sivakumar

Candidatus Liberibacter solanacearum (CaLso) is a gram-negative, phloem limited bacteria, vectored by Tomato Potato Psyllid (*Bactericera cockerelli* Sulc.). Upon transmission, the bacterium spreads throughout the phloem and eventually infects underground tubers. Infected tubers exhibit a brown flecking throughout the peri-medullary region, which upon deep-frying (cross-section of tuber) in oil exhibit a characteristic zebra pattern, giving them the name 'Zebra Chip'. This is a huge concern for growers and the potato industry as this cosmetic damage in fresh tubers and bitter fried crisps renders them unmarketable. Additionally, the CaLso infected potato plants are a source of primary inoculum for TPP, thus increasing its risk of spread. Currently the only diagnostic method to determine whether a plant is infected with CaLso is by the time-consuming and expensive polymerase chain reaction (PCR) method.

An rapid, inexpensive bioassay of 3% iodine solution was prepared, with previous findings suggesting that CaLso infected plants have a high concentration of starch in the aerial parts. In this study 24 'Russet Burbank' leaves and tubers were tested with 3% iodine solution, and confirmation of CaLso was done with a single-step PCR and nested PCR. 100% of ZC-symptomatic plants stained blackish-purple in the leaves and tubers, with 87.5% confirming CaLso positive by PCR. A 12.5% inaccuracy, with one false-positive (stained but PCR negative) was observed in *Rhizoctonia solani*-symptomatic plants. Of the visibly healthy-looking plants, 2 false-positives and 2 false-negatives (no stain but PCR positive)

were observed. The results suggested: (1) although the false-positives and false-negatives observed with visibly healthy-looking plants made the 3% iodine starch test less accurate on symptomless plants, this is less of a concern as roguing of a small number of healthy looking false-positives is an insignificant economic loss erring on the side of caution; (2) the bioassay is effective on ZC-symptomatic plants, and should be used by growers to test and rogue infected plants to prevent further spread of CaLso; (3) *R. solani*-symptomatic plants are not a precursor for CaLso.

Keywords: *Candidatus* Liberibacter asiaticus, amylopectin, Huanglongbing, Haplotype B, qPCR, gel electrophoresis, phloem pugging.

TABLE OF CONTENTS

LIST OF TABLES

List of tables in Appendix

LIST OF FIGURES

List of figures in Appendix A

List of figures in Appendix B

LIST OF APPENDICES

1 INTRODUCTION

Originating from the Andes in South America (Navarre *et al.,* 2014), potatoes (*Solanum tuberosum* L.) are a staple crop feeding millions of people around the world. Potatoes are rich in antioxidants as well as vitamins and minerals, making them an important nutritional crop (Brown, 2005). Domestication of this crop in regions away from its epicentre has made it susceptible to pests and pathogens (Navarre *et al.,* 2014), leading to economic losses. Of the diseases, Zebra Chip (ZC) first reported in 1994 near Saltillo, Mexico (Secor and Rivera-Varas, 2004) is a relatively new disease, causing economic losses to potato Industries (Munyaneza, 2012). ZC has been documented in commercial potato fields of the USA, Canada, Mexico, Central America, New Zealand, and South America (Prager *et al*., 2022).

Apart from being consumed locally, since 2007 over half of the potatoes grown in New Zealand are processed mainly as French fries and crisps. The New Zealand potato industry is worth NZD 1,088 million and processed potatoes account for 67% of the value (Anon *et al*., 2020). ZC infected tubers show very dark blotches in freshly cut tubers, and strips or streaks when fried (Wallis *et al*., 2014). The cosmetic damage in fresh tubers and the bitter fried crisps are unmarketable, which causes an economic loss to farmers and Industry (Munyaneza, 2012; Munyaneza *et al.,* 2008; Secor *et al.,* 2009). *Candidatus* Liberibacter Solanacearum (CaLso) was identified as the etiological agent of ZC disease. It is a fast-moving, phloem-limited, gram-negative, unculturable bacterium transmitted from infected to healthy plants by psyllid vectors (Bove, 2006). In potatoes, tomato/potato psyllid (TPP) (*Bactericera cockerelli* Sulc. (Hemiptera: Triozidae)) is a common phloem-feeding vector (Munyaneza, 2012).

Underground symptoms of infected plants include: - infected tubers showing collapsed stolons, browning of vascular tissue, necrotic flecking of internal tissues and streaking of the medullary ray tissues. These symptoms make ZC more distinct from other potato diseases. Foliar symptoms, which include leaf curling and scorching, shortened internodes, aerial tubers and eventually plant death are similar to that of psyllid yellows, purple top, heat stress and *Rhizoctonia solani* (Vereijssen *et al.,* 2015; Munyaneza *et al.,* 2010). These similarities in foliar symptoms can lead to misidentification, while also making ZC identification difficult.

Upon Infection with CaLso, the above ground symptoms take 3-4 weeks to appear (Wenninger *et al.,* 2022). This is problematic for the farmers as it goes undetected and reduces their chance of roguing their fields using visual symptoms. Industrially approved methods of detection include conventional and quantitative real-time polymerase chain reaction (PCR) (Liefting *et al.,* 2008). Apart from being expensive, commercial PCR laboratories in Canterbury, New Zealand, can be time-consuming and may take up to 3 weeks for results of disease identification (Kirkwood, *pers comm*[1]). To help achieve a simple, fast and cost-effective diagnosis, an iodine starch test (IST) might be an option. IST is a bioassay that was developed in Japan (Takushi *et al.,* 2006) to aid as a quick field test for Huanglongbing (HLB) (also called the citrus greening disease) caused by *Candidatus* Liberibacter asiaticus (CLas). The bioassay is based on the discovery by Schneider (1968), where HLB-infected leaves showed enormous concentrations of starch. IST on HLB-infected leaves show a dark-brown black stain when compared to healthy plants (Takusi *et al.,* 2006). Similarly, CaLso infected plants had high starch accumulation in the aerial parts of plants and a high reducing sugars concentration in tubers (Buchman *et al*., 2012; Wallis *et al.,* 2015). This creates a definitive opportunity to develop an IST that can work on CaLso-infected potato plants, where no previous experiments have been conducted.

1.1 Aims and Objectives

With no prior cultural control methods to aid farmers in roguing CaLso infected potato plants, this experiment aimed to develop an inexpensive bioassay to detect CaLso infected potato plants with Zebra Chip disease in-field. To achieve this, the following objectives were developed:

1. Develop a bioassay by refining and adjusting the procedure outlined by Etxeberria *et al.* (2009), to suit potato leaves and tubers.
2. Evaluate the accuracy of the bioassay developed by comparing positive or negative IST on 'Russet Burbank' potatoes symptomatic of Zebra Chip, those symptomatic of *R. solani*

[1] Kirkwood, Iain. Research Manager Potatoes New Zealand.

infection, as well as healthy looking potato plants, against PCR to confirm the presence or absence of CaLso in all plants.

2 REVIEW OF THE LITERATURE

To perform and evaluate the efficiency of the iodine starch test (IST) on Zebra Chip (ZC) infected potatoes, it is vital to have an overview on the morphology and microstructure of the tubers and the leaf lamina, phenology and host physiological changes in *Candidatus* Liberibacter solanacearum (CaLso) infected potato plants, current detection methods of ZC and previous work done in performing an IST on plants infected with Liberibacter species. This information will help in conducting experiments to achieve the objective to develop a bioassay for CaLso infected potato plants.

2.1 Potato (Solanum *tuberosum* L.)

2.1.1 Taxonomy

Potato, a dicotyledonous plant in the family Solanaceae, is of the genus *Solanum*, which has approximately 1400 species (Frodin, 2004; Hawkes, 1999). Of the cultivated species, 72% are diploids, 12% are tetraploids and the rest are triploids, pentaploids and hexaploids (Reddy *et al.,* 2018). *Solanum tuberosum* L. is a tetraploid, which is the most commonly cultivated potato species in all continents but Antarctica. Hawkes *et al*. (1990), reported that there are seven species of the genus *Solanum* that have been cultivated.

2.1.2 Morphological Description

Potatoes are herbaceous plants with rosetted, prostate and erect growth habits (Navarre *et al.,* 2014), which vary between and within species. They can be grown from either tubers or true seeds. Plants grown from tubers have adventitious roots arising from subterranean stems, while plants grown from seeds form a slender tap root, with branched lateral roots (Huaman *et al.,* 1968). The stem system of a cultivated potato plant consists of aboveground stems and leaves, and subterranean stolons, and associated belowground tubers. The plant usually has one main stem if grown from a true seed, whereas a number of stems can be produced if grown from a tuber. Stems are green in colour, round to angular in cross section with straight, undulated or dentate wings formed at angular margins (Huaman *et al.,* 1968).

Tubers are the main storage organ for carbohydrate and nutrients of the plant. Under favourable conditions, tuberization is induced through the formation of a graft-transmissible signal from the leaves to the growing stolon. Tubers form when the terminal end of a stolon becomes enlarged (Gregory, 1956; Jackson *et al.,* 1998). External morphology of a tuber includes: - scale leaves, internodes, nodes and the periderm (skin) (Navarre *et al.,* 2014). The periderm has small pores and lenticels, essential for gas exchange. Beneath the periderm lies the cortex composed of storage parenchyma tissues, within which is a ring of vascular tissue surrounding a central pith composed of parenchyma tissue (Navarre *et al.,* 2014; Hauman *et al.,* 1968) (Figure 2.1).

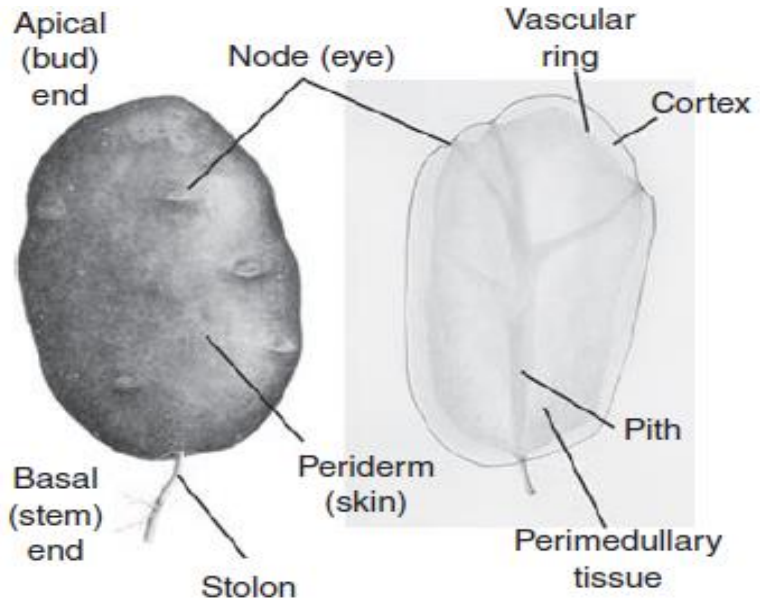

Figure 2.1 Anatomy of a potato tuber (image from Navarre *et al.,* 2014)

McCauley & Evert (1988) studied the morphology of 'Russet Burbank' and found that compound leaves are arranged spirally on the stem of the plant. Compound leaves have a midrib (rachis) and several leaflets (Figure 2.2). The distal, terminal leaflet is the largest and secondary leaflets appear progressively smaller as one moves towards the proximal leaflet. Secondary leaflets are arranged oppositely along the rachis. Between each pair of secondary leaflets, a small pair of interjected leaflets occurs. Each secondary leaflet is attached to the rachis by a petiolule. Interjected leaflets are sessile (Figure 2.2 B). The petiole accounts for less than 20% of the total leaf length (McCauley & Evert, 1988) while ensheathing one-third of the stem circumference with its base and wings (Artschwager, 1918).

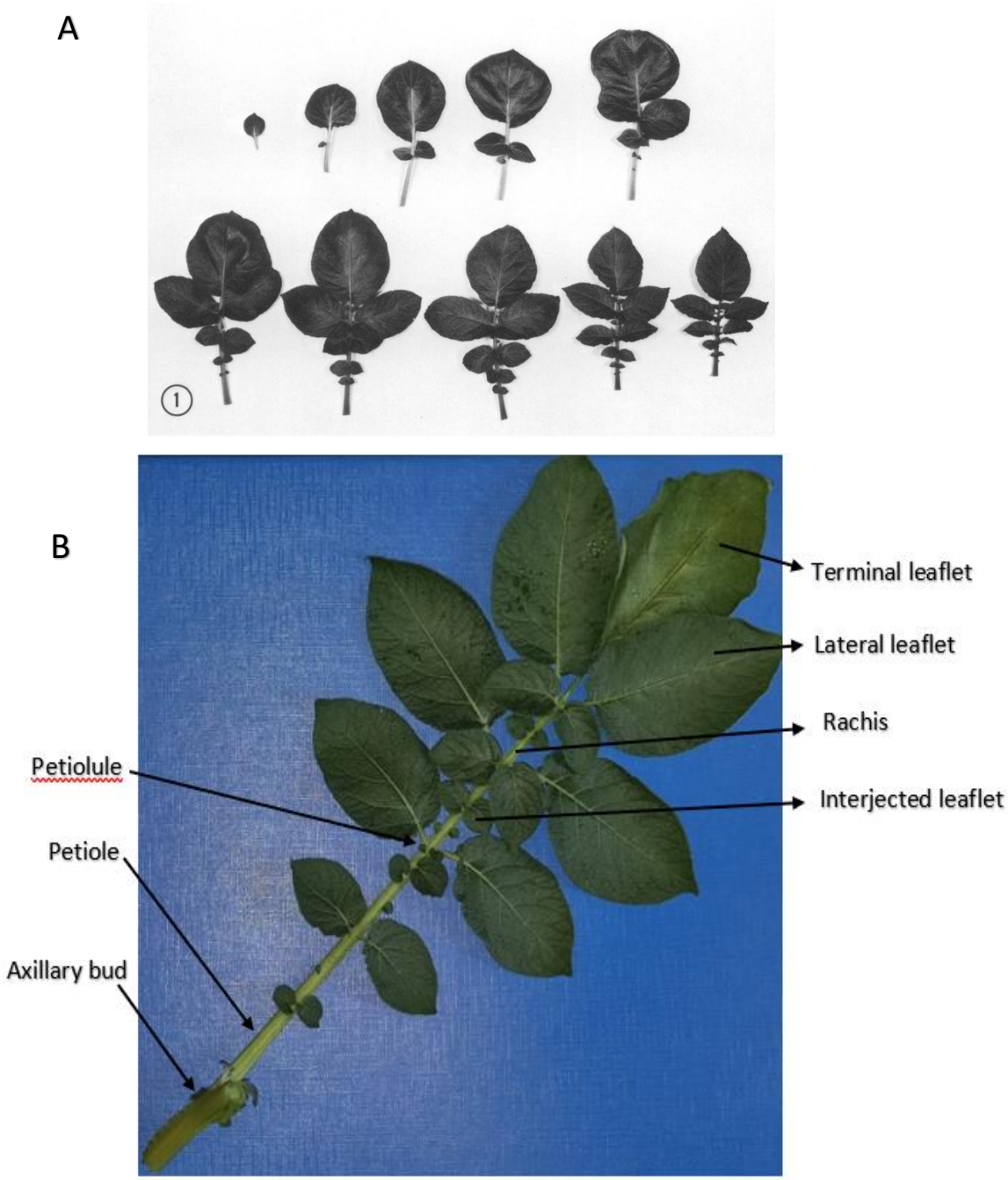

Figure 2.2. (A). First ten leaves from the main shoot of a potato plant (image from McCauley & Evert, 1988). (B). Different parts of a potato compound leaf.

2.1.3 Microstructure of potato tuber

Potato tubers have two ends, namely the bud (distal) end and the stem (proximal) end. The stem end is attached to the stolon with fewer eyes than the bud end. The outer skin of the

potato consists of a layer of corky periderm which is approximately 10 cells deep (Fedec *et al*., 1997; Miranda & Aguilera, 2006). These cells are dead, empty with a thick cell wall than that observed in parenchyma cells. Cortex under the periderm consists of a thin layer of parenchyma tissue. This part of the tuber is where cells appear to be the largest (146-189 µm) and are seen to contain a large number of round and oval shaped starch granules (Fedec *et al.,* 1997; Gancarz *et al.,* 2014). High in starch content, the vascular storage parenchyma lies within the cells of the cortex. The xylem and phloem can be found in minute bundles forming a narrow discontinuous ring known as the vascular ring. These bundles are located between the cortex and the vascular area (Figure 2.3) (Troncoso *et al.,* 2009).

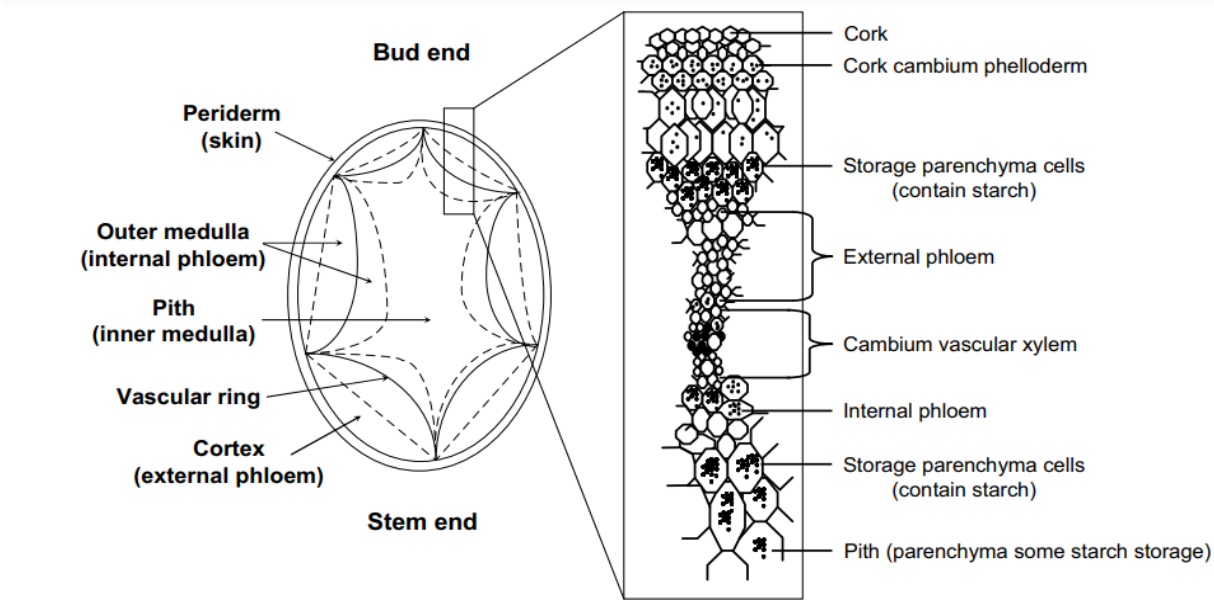

Figure 2.3. Cross-section of a potato tuber (Troncoso *et al.,* 2009).

2.1.4 Cross-section and vasculature of the potato leaf

Leaves are an important and efficient organ of a plant as they manufacture photosynthates to be exported to various plant parts through the vascular system. A cross section of the terminal leaflet of the potato (Solanum *tuberosum* L. 'Russet Burbank') using a scanning electron microscope (SEM) performed by McCauley & Evert (1988b) is presented in Figure 2.4. Cells of the upper epidermis of the leaf lamina are less sinuous than the lower epidermis. Mesophyll of potato leaves have one layer of palisade cells and three to four layers of spongy parenchyma (Figure 2.4) (McCauley & Evert, 1988b; Chaffey, 2014). Bordering the palisade

layer, are slightly branched spongy cells that form a layer of cells called the collecting cells. These cells along with the palisade cell, contain prominent starch grains. The lower layer of spongy cells have smaller starch grains (Figure 2.4 B). The intercellular air space makes up to 30-33% of the laminar volume. Mesophyll of the leaf is permeated by numerous vascular bundles that are continuous with the vascular system of the stem (Chaffey, 2014). The largest vein along the axis of the leaf is the midvein. Smaller lateral veins are connected to the midvein and each lateral vein is connected to smaller veins, from which other smaller veins diverge (Chaffey, 2014). The midvein and some lateral veins of the potato leaf contain both abaxial and adaxial phloem, while the vein endings have only abaxial phloem (Artschwager, 1918; Esmarch-Bromberg, 1919; McCauley & Evert, 1988b). These veins can be present in the intercellular spaces where individual veins can undulate upwards and downwards through the mesophyll (McCauley & Evert 1988b).

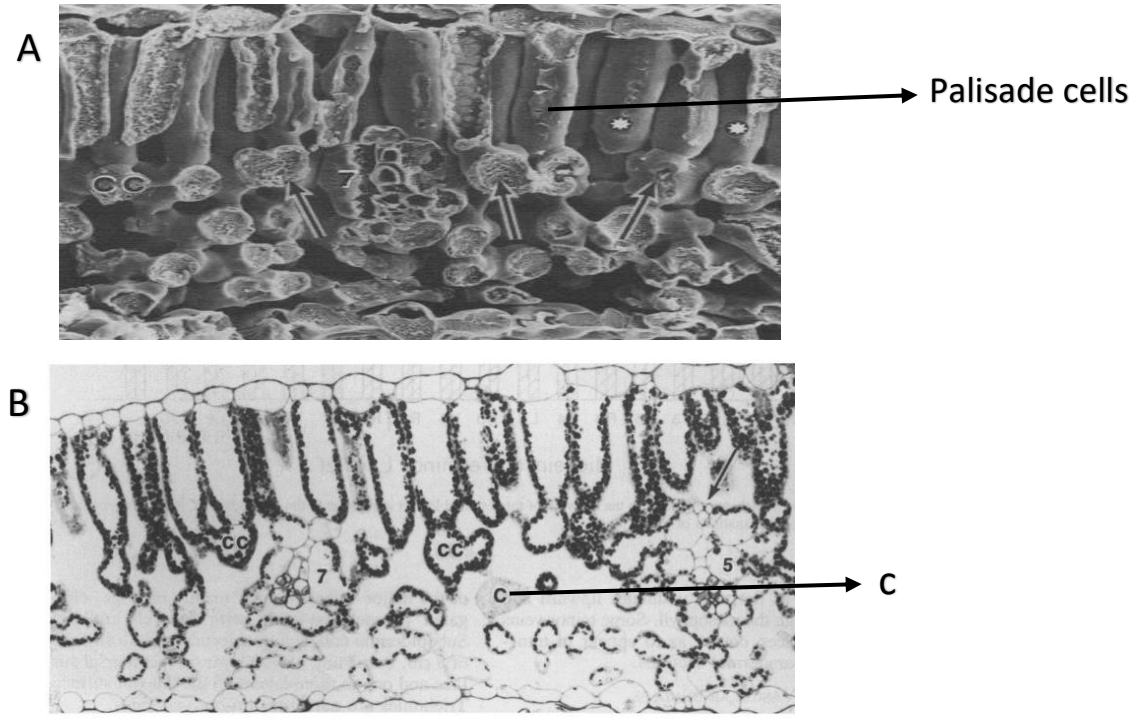

Figure 2.4. A) SEM of the terminal leaf lamina. (cc) indicates a layer of collecting cells which separates the palisade cells from the remaining layers of spongy cells (below); x 400. B) Cross section of the leaf lamina. A gradual decrease in size of starch grains can be noted from palisade cells to lowermost layer of spongy cells. The arrow indicates the adaxial phloem of the quintenary vein exposed to the intercellular

space. ‘c’ indicates the crystal sand-containing cell; x309 (from McCauley & Evert. 1988b)

The vasculature of the leaf lamina is similar in all leaflets of the potato leaf, regardless of their position. The primary vascular system of the potato stem is made up of six bundles, three small and three large (Figure 2.5-A) (McCauley & Evert, 1988a). At each node two of the three large bundles give rise two lateral leaf traces and one of the three small bundle gives rise to a median leaf trace. The three leaf traces enter the petiole of the leaf, where each of the lateral leaf traces split into upper and lower laterals (LL) (Figure 2.5-B). Before entering the terminal leaflets, the lower laterals converge on the median bundle to form a single vascular crescent (Figure 2.5). This arrangement of the crescent shaped vascular bundles along the petiole-rachis axis and at the petiolule, has be described similarly for leguminous leaves, apple leaves, and numerous other species (Watari, 1934; MacDaniels & Cowart, 1944; Ashworth, 1963; Howard, 1974). The vascular crescent progresses acropetally through the midvein into the terminal leaflet. Portions of the midvein diverge outwards and continue as secondaries into the lamina. At the tip of the terminal leaflet, the midvein consists of a singular vascular bundle which is a continuation of the median bundle. Lin *et al.* (2015) showed an abundance of phloem associated cells to be present in the “LL” region in the petioles (Figure 2.5-B). This information is vital to understanding starch accumulation in the leaves, a result of CaLso infection (discussed in section 2.3.3).

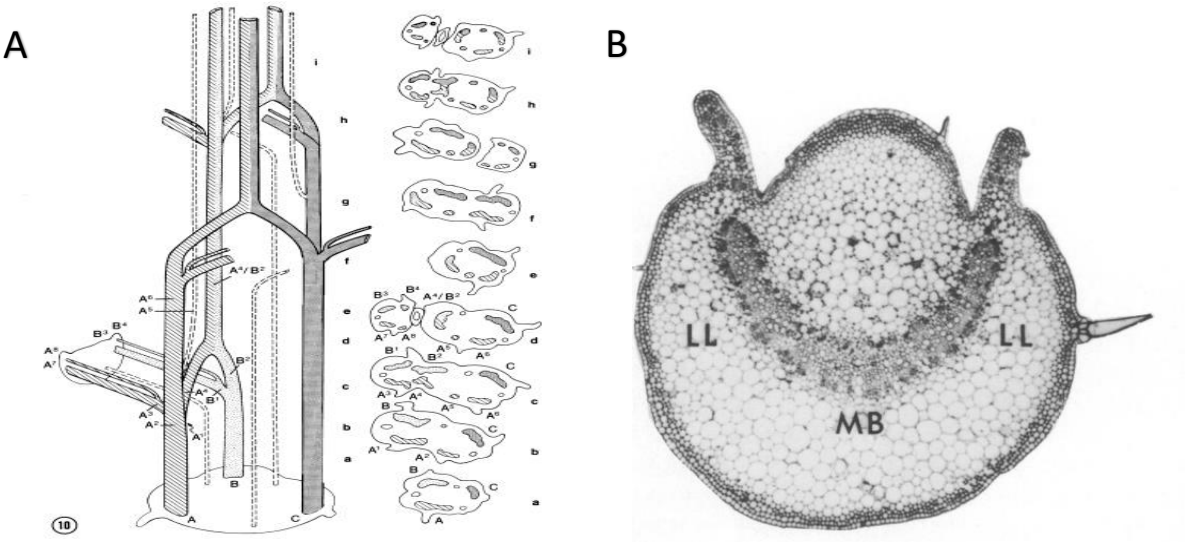

Figure 2.5. A) Transectional view of the vascular bundle in the stem of a potato plant. B) Transverse section of potato petiole, where **LL** is the lateral leaflet and **MB** is the median bundle (images from McCauley & Evert, 1988a).

2.2 Zebra Chip (ZC)

Zebra Chip disease in potatoes was first observed in the commercial fields of Lower Rio Grande Valley in Texas, USA in 2000 (Secor and Rivera-Varas 2004). Following this, it was subsequently observed in Nebraska, Kansas, Colorado, Arizona, Nevada, California, and New Mexico (Munyaneza *et al.,* 2007). In 2008, symptoms of ZC were observed in potato tubers harvested in South Auckland, New Zealand (Liefting *et al.,* 2008b). The disease in New Zealand has led to yield reductions of up to 60%, while harvested tubers produce less dry matter than uninfected tubers. The disease is caused by *Candidatus* Liberibacter solanacearum L. (CaLso), a phloem-limited bacteria that spreads from infected to healthy plants through psyllid insect vectors or through grafting (Munyaneza *et al.,* 2012a; Haapalainen *et al.,* 2014). Native to North America, *B. cockerelli* (also known as Tomato potato psyllid (TPP)) is the known vector for the transmission and movement of the bacterium in a wide range of Solanaceous and Convolvulaceae crops and weeds (Table 2.1). The pathogen with its vector are a problem for potato growers as TPP can spread over thousands of kilometres naturally or through human assistance (Teulon *et al.,* 2009).

ZC is characterised by dark flecking and streaking of the medullary ray tissues, which upon frying is very distinct. This aspect of the disease is what makes them unmarketable both for processing as well as for fresh market sale (Figure 2.6) (Pitman *et al.,* 2011). Foliar symptoms of infected plants include, upward rolling of the basal portion of young leaves, shortened internodes, chlorosis, small leaves, purple top, enlargement of the stems, swollen axillary buds, aerial tubers and early plant senescence (Figure 2.6) (Crosslin *et al.,* 2010; Pitman *et al.,* 2011; Rondon *et al.,* 2012). These symptoms may also resemble those of other potato conditions such as psyllid yellows, purple top, heat stress and *Rhizoctonia solani* (Vereijssen *et al.,* 2015; Munyaneza *et al.,* 2010). This can make foliar identification confusing, leading to possible misidentification.

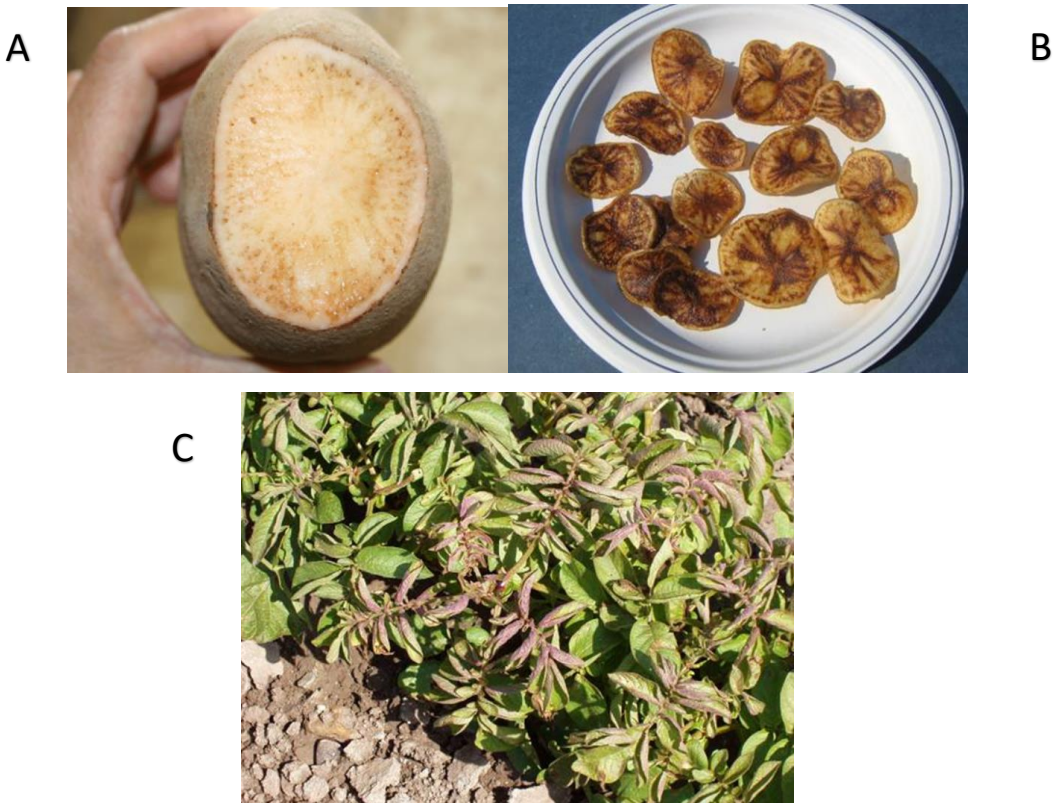

Figure 2.6. A) Fresh tuber symptoms (image from Rondon *et al.,* 2012). B) Zebra Chip symptoms upon frying the tubers (image from Crosslin *et al.,* 2010). C) Foliar symptoms of ZC disease (image from Crosslin *et al.,* 2010)

2.3 *Candidatus* Liberibacter solanacearum (CaLso)

2.3.1 Taxonomy, Morphology and Haplotypes

The genus "Liberibacter" contains at least seven species in the order *Rhizobiales* of the α2 subdivision of the Gram-negative Proteobacteria, in the Rhizobeaceae family. These bacteria are phloem-limited, thus are transmitted by phloem-feeding psyllids infecting plant species determined by the psyllids host range. Liberibacter species are also obligate parasites that multiplying only inside their eukaryotic plant and psyllid hosts (Sengoda *et al.,* 2014).

These fastidious "*Candidatus* Liberibacter" pathogens and their vectors have attracted tremendous attention amongst growers, the agricultural industry, the scientific communities and the government, as they cause economically important plant diseases and have been geographically expanding worldwide (Prager *et al.,* 2022). CaLso is an important Liberibacter species infecting commercially grown Solanaceous plants. CaLso examined under an electron

microscope, has a rod-shaped morphology being 0.2 µm wide and 4 µm long (Liefting *et al.,* 2009a; Secor *et al.,* 2009).

Distinguished based on variations in SSR, 16S or MLST sequences, CaLso occurs in seven distinct haplotypes recorded so far (Nelson *et al.,* 2011, 2012; Grimm *et al.,* 2019; Mauck *et al.,* 2019). Of the seven, Haplotypes A, B, F and G have been found to infect potato and other solanaceous plants. With regards to disease severity observed, Haplotype B infects potato plants with more severe symptoms than Haplotype A (Thomson *et al.,* 2015). Haplotypes F and G were recently discovered, thus less information of their infectivity is available. In New Zealand, the bacterium has been recorded to only occur as Haplotype A (Grimm *et al.,* 2019). This knowledge on exiting haplotypes can help in contingency plans upon infection of a field.

2.3.2 Pathways of movement

2.3.2.1 *Bactericera cockerelli*

The insect *B. cockerelli* is thought to be native to South-Western USA and Northern Mexico (Butler and Trumble, 2012; Munyaneza, 2012). They are known to disperse within crops by jumping and flying (Cameron *et al*., 2013) however, if caught by winds when in air they can disperse more than 100 kilometres (Nelson *et al*., 2014). *B. cockerelli* have been found in regions of North America, Central America and Oceania (EPPO 2013). Currently four haplotypes of *B. cockerelli* have been discovered. The Central (Texas, Nebraska), North-western (Washington and Idaho), Southwestern haplotype (Colorado, New Mexico) and Western (South California and Baja, Mexico) (Liu et al., 2006; Swisher *et al*., 2012; Swisher et al., 2014).

2.3.2.2 Host plants

Following its first report in the New Zealand in May 2006, TPP is believed to have entered New Zealand from Western USA (Thomas *et al.,* 2011). A wide range of host plants for the psyllid and CaLso in New Zealand are outlined in Table 1. Apart from the weeds mentioned below, Cooper *et al.* (2019) found 13 genera of weed species the psyllid over winters on, in the Pacific Northwest. Research conducted by evaluating the gut of TPP in the Pacific Northwest found the insect to feed on up to 37 genera in 17 plant families (Reyes Carrol *et al.,* 2021). Though the psyllid has a wide range of host plants, they overwinter and complete

their life cycle only on a few, such as the Chinese boxthorn, African boxthorn, field bindweed and sweet potato (Cooper *et al.,* 2019). Kaur *et al.* (2018) showed that although TPP are able to develop on sweet potatoes, the development rate is slow accompanied by nymphal mortality compared to field bindweed. Mustafa *et al.* (2021) concluded that, although TPP feed on Convolvulaceae, their feeding behaviours involve a shorted phloem feeding time when compared to feeding on Solanaceous hosts. Instances of phloem salivation and ingestion were observed to occur more on Solanaceae hosts when compared to Convolvulaceae. This could potentially explain Convolvulaceae not being a host for CaLso as observed in Table 2.1.

Perennials weeds are important to know as they are an earlier source of threat, overwintering a large population of TPP (infected/uninfected) in spring before leaf emergence in potatoes fields, and in autumn, post-harvest (Wang *et al.,* 2017; Barnes *et al.,* 2015; Cooper *et al.,* 2019). Thus, an established population of infected psyllids overwintering host plants would maintain the pathogen at a certain level, infecting susceptible crops the following season making them a primary source of inoculum for acquisition by uninfected psyllids in the ZC disease cycle.

Table 2.1. Tomato Potato Psyllid and CaLso host plants in New Zealand .

Type	**Common Plant Name**	**Species**	**CaLso Host**	**Reference**
Commercial Crops	Potato (cultivated/volunteers)	Solanum *tuberosum*	Yes	Cooper *et al.* (2019)
	Chilli pepper	*Capsicum annuum*	Yes	Wang *et al.* (2017)
	Tobacco	*Nicotiana tabacum*	Yes	Wang *et al.* (2017)
	Cape gooseberry	*Physalis peruviana*	Yes	Wang *et al.* (2017)
	Tamarillo	Solanum *betaceum*	Yes	Wang *et al.* (2017)
	Tomato	Solanum *lycopersicum*	Yes	Cooper *et al.* (2019)
	Eggplant	Solanum *melongena*	Nf	Martin *et al.* (2008)
	Sweet potato*	*Ipomoea batatas*	Nf	Kaur *et al.* (2018)
Weeds	Apple of peru	*Nicandra physolades*	Nf	Barnes *et al.* (2015)

African boxthorn	*Lycium ferocissimum*	Yes	Barnes *et al.* (2015)
Bittersweet nightshade	Solanum *dulcamara*	Yes	Cooper *et al.* (2019)
Chinese boxthorn	*Lycium barbarum*	Nf	Cooper *et al.* (2019)
Field bindweed*	*Convolvulus arvensis*	Nf	Cooper *et al.* (2019)
Ground cherry	*Physalis pubescebs*	Yes	Hortan *et al.* (2015)
Jerusalem Cherry	Solanum *Pseudocapsicum*	Yes	Vereijssen *et al.* (2015)
Poroporo	Solanum *laciniatum*	Nf	Barnes *et al.* (2015)
Thorn-apple	*Datura stramonium*	Yes	Vereijssen *et al.* (2015)

Note: Nf denotes not found.

* Denotes Convolvulaceae; all other plants are Solanaceae

2.3.2.3 Acquisition of the pathogen

Vector-borne plant pathogens have two primary stages of transmission. This includes pathogen acquisition and inoculum, which determine the vector efficiency in spreading the pathogen (Rashed *et al.,* 2012). The acquisition of CaLso by uninfected TPP occurs during its feeding activities in the phloem tissue of an infected plant (Cooper *et al.,* 2019; Pager *et al.,* 2022). Infected plants that serve as a primary source of inoculum for psyllid acquisition include, infected seed potatoes, infected volunteer potatoes and infected host plants (Table 2) (Prager *et al.,* 2022).

The process of ingestion also involves discharging salivary contents into the phloem through stylet penetration (Sandanayaka *et al.,* 2014; Mustafa *et al.,* 2015a). Sandanayaka *et al.* (2014), using an electrical penetration graph (EPG), found that acquisition of CaLso is limited to phloem ingestion given the TPP has a minimum acquisition access period threshold of 36.6 minutes, with 6.9 minutes of phloem ingestion period. This complements the work of Rashed *et al.* (2012) who found that highest acquisition success of CaLso by TPP was influenced by access to stem tissues, where phloem cells are most abundant. Acquisition success was not as high with restricted access to only leaflets and petioles. Mustafa *et al.* (2015a) also confirmed that the acquisition of the pathogen by TPP is limited to phloem feeding. This

process of feeding is also how the pathogen is transmitted to a heathy plant (Sandanayaka *et al.,* 2014; Sengoda *et al.,* 2014).

2.3.2.4 Transmission of the pathogen

The two main modes by which insects transmit bacterial pathogens are circulative and non-circulative transmission (Nault 1997). Non-circulative mode involves the pathogen attaching to the insects inner cuticular walls of the oral region lamina, which includes the style bundle canals and the pre-oral section (Killiny *et al.,* 2017). The pathogen does not pass into the mid-gut of the insect in this mode of transmission and is only delivered to the plant through regurgitation with saliva during feeding (Harris *et al*., 1996; Backus *et al.,* 2015). On the other hand, circulative mode of transmission involves the pathogen translocated to specific location in the insect, including the ventriculus, filter changer, or the hinge gut to the reach the hemolymph (Cicero *et al.,* 2017; Mustafa *et al.,* 2021). It is from hemolymph, the pathogen transmits and colonises the salivary gland prior to inoculating the host plant during feeding. Transmission of CaLso by TPP follows a propagative, circulative mode of transmission (Sengoda *et al.,* 2014; Cicero *et al.,* 2017).

The psyllid gut is the first organ CaLso encounters (Tang *et al.,* 2020), but transmission of CaLso after acquisition is only possible after the bacteria colonizes the salivary gland of the vector (Sengoda *et al.,* 2014; Prager *et al.,* 2022). Cicero *et al.* (2017), whose study focused on colonization and intrusive invasion of TPP by CaLso, concluded that in an adult TPP, although CaLso was found in regions of the midgut (i.e. between the basal lamina and basal epithelial cell membrane, in the basal laminar perforations, on the outer basal laminar surface, in the ventricular lumen, epithelial cytosol and in the filter chamber periventricular spaces), it was most abundantly visible in the salivary gland pericellular spaces and in the epidermal cell cytosol, in the head. Molki *et al.* (2019), confirmed the pathogens growth in TPP, while also concluding that CaLso alters TPP physiology to a more conducive environment for its survival and subsequent transmission. Bacterial titre in TPP increases under conditions of high pH and lower oxygen tension values in the gut.

A study by Sengoda *et al.* (2014) found that a latent period of 2 weeks at temperatures ranging from 24-28°C is required for CaLso to colonize the salivary gland. Also, using florescence *in situ* hybridization (Figure 2.7), they found that CaLso copy numbers increased from week 0 to

week 2 before reaching a plateau with copy numbers comparable to those in infected psyllid colonies. As a standard, copy numbers over 10,000 in the salivary gland of TPP increased its probability to infect a healthy plant (Sengoda *et al.,* 2014).

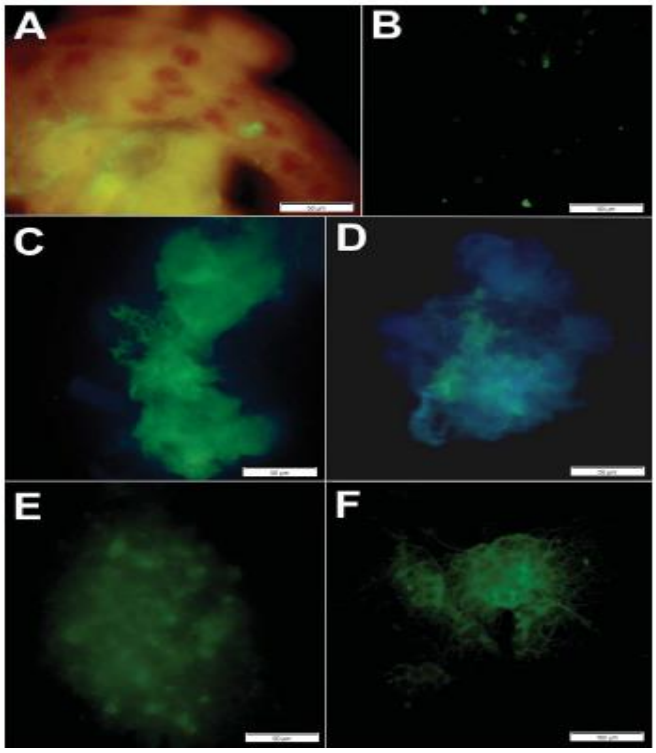

Figure 2.7. CaLso infection (green fluorescence) observed in (A) alimentary canal, (B) hemolymph, (C) and (D) salivary glands, and (E) and (F) bacteriomes dissected from *Bactericera cockerelli* adults. Blue or yellow auto-fluorescence shows organ boundaries (Sengoda *et al.,* 2014).

TPP can test positive for CaLso under PCR due to the pathogen colonizing their hemolymph, reproductive organs, syncytium of bacteriomes and salivary glands (Cooper *et al.,* 2013), but transmission occurs only by colonizing the salivary gland (Rashed *et al.,* 2012). Reasons for failure in colonizing the salivary gland can be because the immune system of the TPP could potentially prevent the movement of the pathogen through the midgut wall or from colonizing the salivary gland (Sengoda *et al.,* 2014). Upon colonizing, CaLso is only transmitted to the uninfected plant through salivary exudates while phloem feeding (Sengoda *et al.,* 2014).

An infected TPP is capable of inoculating a potato plant within 48 hours (Rashed *et al.,* 2012) with the fastest being 6 hours (Buchman *et al.,* 2011). With TPP being exposed to the whole

plant, the efficiency of CaLso transmission using multiple TPP was found to be high with an inoculation success rate of 100% within an hour, when compared to a single TPP resulting in an inoculation success rate of 70% within six hours (Buchman *et al.,* 2011). These results on vector density are also supported by the study conducted by Rashed *et al.* (2012). Thus, vector density does play an important role in CaLso transmission in potatoes, although a single TPP can still infect a plant given sufficient time and pathogen titre.

Nymphs harbour the pathogen but are not efficient in transmitting it (Buchman *et al.,* 2011). Sengoda *et al.* (2014) found that inefficiency of the nymphs to transmit the pathogen, may be because CaLso is less likely to colonise the salivary glands of the nymph than the adults. Cooper *et al.* (2014), using fluorescence *in situ* hybridisation, found higher CaLso colonisation in the salivary glands of adults when compared to nymphs. No differences in transmission of CaLso by male and female adults were observed in the study. In contrast, Casteel *et al.* (2012) found the opposite stating that the nymphs carrying CaLso through vertical transmission, were efficient vectors. The difference seen might be the result of vector efficiency on different host plants, as Casteel *et al.* (2012) used tomato plants while the former used potato plants as hosts. There is potential for further research to find the transmission efficiency of TPP at different life stages in different hosts.

Cicero *et al.* (2017) found two morpho types of the bacterium in TPP. One possessing pili and flagella like appendages, found in the midgut, while the other was rod shaped with a rough, granular cystol found in the gut, salivary gland and other oral region tissues. Though it is unknown where these structures are formed in the insect, it can be assumed that the pili and flagella are associated with motility, and would help CaLso reach the salivary gland, from where it can infect a healthy plant during feeding. There is scope for future research in understanding the pathogen form in TPP, which could potentially help in eradicating the disease.

2.3.3 Symptom development upon transmission

Upon transmission, the bacterium is found to translocate unevenly in the plant (Levy *et al.,* 2011; Prager *et al.,* 2022). Using PCR detection, Wen *et al.* (2009), found greater concentration of CaLso in the stolons and tubers than in the foliar parts. Additionally, petioles had a higher concentration of CaLso than the midvein and the leaf lamina. This uneven

distribution could be limited to the vascular architecture within the plant, as claimed by Cooper *et al.* (2014). It takes around 3-4 weeks until foliar symptoms develop in the plant following CaLso transmission (Alvarado *et al.,* 2012; Rashed *et al.,* 2014). In tubers, symptoms can appear as early as 2 weeks after infection, although it can be limited to the timing of infection in relation to the plants growth stage (Buchman et al 2012; Rashed *et al.,* 2013; Rashed *et al.,* 2014). Prager *et al.* (2022) concluded that polyphenol oxidases and phenolic compound accumulation in tubers upon infection were the reason for them to quickly turn brown around the vascular ring and the medullary ray tissue on exposure to air.

Infestations as early as leaf emergence in plants can lead to no tuber production (Buchman *et al.,* 2012). Contrastingly, Rashed *et al.* (2013) found less susceptible cultivars to produce tubers with infestation as early as 7-11 days post leaf emergence. This difference could be due to sampling differences. A destructive sampling approach at continuous intervals was used by Buchman *et al.* (2012) compared to Rashed *et al.* (2013) who sampled tubers at the end of the trial. Though tubers are produced at infestations post leaf emergence, tuber quality is highly affected, together with reduced yield (Rashed *et al.,* 2013). Potato plants when infested 2-6 weeks prior to harvest, were asymptomatic, but can test positive for CaLso with a visible reduction in tuber quality (Buchman *et al.,* 2012; Rashed *et al.,* 2013). Infection close to harvest makes it difficult to eradicate infected plants as they lack visual symptoms (Wenninger *et al.,* 2020; Rashed *et al.,* 2014).

Biotic factors also play an important role in symptom development as the rate of symptom development increases under favourable environmental conditions (Munyaneza *et al*., 2012). The shortest disease incubation period for symptom development was observed on an average of 20.7 days at 20-25 °C, while with unfavourable temperatures of 27-32 °C or above, it was observed at 30 days (Rashed *et al.,* 2013). The severity of foliar and tuber symptoms is also affected by an increase in temperature (Rashed *et al.,* 2013; Prager *et al.,* 2022).

Apart from temperature, severity and timing of symptom development is also influenced by CaLso titer in the host plant (Wallis *et al.,* 2014; Rashed *et al.,* 2015), vector density (Rashed *et al.,* 2015), and timing of infection. A single CaLso-infected TPP has the potential to infect many plants, and also infect a whole colony of uninfected TPP. A colony of TPP can infect a plant with more CaLso titer and more severity in symptoms at an earlier stage of plant

development (Rashed *et al.,* 2015). Alvarado *et al.,* (2012) concluded that CaLso titer in the TPP colony directly influenced the rate of disease development in plants. Contrasting results were observed in previous studies by Buchman *et al.* (2011) and Rashed *et al.* (2012), where neither vector density nor titre of the pathogen affected the rate of symptom development. Although this might be true, it is clear that an infected TPP with access to a plant can infect it. However, symptom development requires sufficient incubation time of CaLso in the plant. Thus, with multiple factors at play causing delayed foliar symptom development, it makes it difficult for a farmer to detect infected plants at an earlier stage of infection.

Early detection can help in roguing infected plants as well as to control ZC epidemic on the farm, which will help reduce the chance of having the entire crop rejected upon ZC inspection postharvest. It is also important to note that all the studies mentioned above were conducted in greenhouses using laboratory reared TPP. All the TPP used were positive for CaLso, but this is not always be the case *in vivo*. With respect to TPP under field conditions, Vereijssen *et al.* (2018), stated that not all TPP are positive for CaLso and CaLso titer in the TPP vary. This makes it is highly likely that transmission rates are highly variable under field conditions. Research determining TPP infectivity and distribution under field conditions will help determine the epidemic and guide control options.

With respect to vegetative transmission, the study by Pitman *et al.,* 2011 showed that 93.6% of CaLso-infected seed tubers sprouted. Of the sprouted tubers, 3.4 % were symptomatic while the 70% were asymptomatic. Furthermore, 27.4 % of these sprouted tubers did not test positive for Liberibacter. A recent study by Grimm *et al.* (2020) in the Pacific Northwest found that CaLso A and CaLso B infected seed tubers exhibiting severe ZC symptoms showed successful late emergence with reduced yield. CaLso was not detected in the leaves nor in any tubers of the 2-year study. Potential reasons for contrasting results can include, different potato cultivars used, difference in environmental conditions such as soil temperature, weather events or growing degree days (Grimm *et al.,* 2020). Pitman *et al.* (2011) stated symptoms can proliferate upon suitable environmental conditions such as temperature, which could also add up as a reason for the difference. Although using a small percentage of infected daughter tubers is considered acceptable in the USA fields as stated by Grimm *et al.* (2020), the same cannot be said for it in New Zealand unless proven or stated so. Thus, symptomless CaLso-infected plants are a primary inoculum for TPP and pose a serious

economic threat to farmers and the industry if not detected and rogued out on- farm. More research in identifying temperature thresholds and cultivars that can transmit CaLso vegetatively, will provide a better understanding of subsequent infection from daughter tubers, which can help in effective management.

2.3.4 Host physiology and starch accumulation

Understanding plant physiological changes upon infection with CaLso can help understand symptom development. This part of the review focuses on starch accumulation in infected plants for relevance with the Iodine starch test discussed later in the review. Levy *et al.* (2011) found that CaLso, translocated to the main stem from infected leaves in seven days. Movement of bacteria was seen to follow the carbohydrate transport route from source to sink in the phloem. New developing leaves, stolons and roots showed a high titre of CaLso in studies done by Levy *et al.* (2011). Similar results were also found by Wen *et al.* (2009). Upper parts of the stem contained abnormal starch as a result of damage to the phloem vessels, thus impairing the transport of sucrose from the source leaves to the roots (Gao *et al.,* 2016). Furthermore, Gao *et al.* (2016) also found that leaves infected at 4-week growth stage had more starch accumulation in the leaves than leaves infected at 6 or 10-weeks growth stage. The results confirm previous findings which determined that insect injury to stem tissues cause reduced translocation of photo-assimilates through the phloem causing increase carbohydrate levels in leaves of injured plants (Ladd and Rawlins, 1965; Nielsen *et al.,* 1999; Pirone *et al.,* 2005). CaLso-infected leaves had lower concentrations of reduced sugars than non-infected plants (Gao *et al.,* 2009; Wallis *et al.,* 2014), which according to Gao *et al.* (2014), could be because of decreased photosynthesis due to necrosis of leaf tissues. The concentration of soluble sugars could have been used by CaLso for energy or by the host for defence responses or converted into starch (Gao *et al.,* 2009). Alternatively, the author postulates that lower soluble sugars might be due to feedback inhibition.

Candidatus Liberibacter asiaticus (CLas), is also a phloem limited gram-negative bacteria of the same genus as CaLso, which causes Huanglongbing (HLB) in citrus trees. Upon infection in the pre-symptomatic stages, CLas was detected in the newly grown flushed in sweet orange and grapefruit trees (Folimonova & Anchor, 2010). Similar to CaLso infection in potatoes, CLas infections of sweet oranges leads to vascular phloem necrosis and starch accumulation in

leaves as a result of callose deposition in the sieve plate pores (Achor *et al.,* 2010; Koh *et al.,* 2012). The accumulation of starch and sugars in leaves, led to chloroplast disruption, leaf chlorosis and nutrient deficiencies in the sink organs (Achor *et al.,* 2010). The information confirming starch accumulation in CaLso infected leaves and its similarity in CLas affected leaves is important for understanding and performing the IST discussed in Section 2.5.

Tubers of plants Infected as early as 4 weeks of plant growth showed reduction in tuber size, suggesting lack of sugar translocation from source leaves to the sink for tuber development (Rashed *et al.,* 2013). While CaLso-infection after 6 to 10 weeks of plant growth showed no reduction in tuber size but a reduction in tuber quality associated with increased sugar concentrations. Early CaLso infection, in weeks 3-5 resulted in reduced yield and higher concentration of glucose in tubers when compared to infections closer to harvest. Starch concentrations in tubers however, were not affected when compared to non-infected plants (Gao *et al.,* 2009).

The severity of the symptoms on early CaLso-infected tubers were more when compared to asymptomatic tubers of plants infected within a few weeks before harvest (Rashed *et al.,* 2016). This could be because at an earlier stage infection, plant defence responses are elevated leading to increased amounts of phenolic compounds, amino acids, salicylic acid and defence related proteins in the tubers with increased sugars (Navarre *et al.,* 2009; Wallis *et al.,* 2012). Thus, a shift in resource allocation from initiating tuber and plant growth to defence would explain reduced tuber size, yield and quality. Research by Wallis *et al.* (2012), found concentrations of six amino acids, ten phenolics, glucose, fructose, peroxidase, and polyphenol oxidase to have consistently increased over a course of 9 weeks, post infection in both basal (stem) and apical (budding) sides of a potato tuber. The study concluded that the increase in these compounds where positively associated with tuber symptoms. Study by Wallis *et al.* (2014) also confirms that CaLso infected tubers show a greater level of individual disaccharides and monosaccharides as a result of conversion of starch to reducing sugars.

The reported increase in glucose content is important to consider as the increased concentration is above the industrial required concentration for making crisps and fries (Buchman *et al.,* 2012; Wallis *et al*., 2012). The increased amount of glucose and shifts in some amino acid concentrations causes potatoes to turn brown upon frying. Information on the

accumulation of glucose in the tubers with reduced starch accumulation, can be used in understanding and developing the IST (Section 1.5).

2.4 Detection and Diagnosis

2.4.1 Polymerase chain reaction (PCR)

This part of the section will review and discuss PCR based techniques used for the detection of CaLso in potatoes. The different PCR techniques used in detecting the pathogen in various Solanaceous species as well as in TPP include conventional PCR, multiplex PCR, nested PCR (nPCR), quantitative PCR (qPCR), multiplex real time PCR (mrtPCR), multi-locus sequence typing (MLST), loop-mediated isothermal amplification (LAMP), simple sequence repeat (SSR) and restricted fragment length polymorphism (RFLP) (Mirmajlessi *et al.,* 2019). Of these techniques, the most commonly used techniques such as the PCR, qPCR, multiplex PCR and nPCR are reviewed below.

Identification of CaLso infected plants can be made through visual symptoms as discussed in the previous sections, while confirming the presence of the pathogen in the plants need to be done to confirm the disease. All identified Liberibacter species have been unculturable, except Liberibacter *crescens* (cultured axenically in artificial media) (Pierson *et al.,* 2022). Since Liberibacter is unculturable, industrially accepted identification relies on DNA sequencing and phylogenetic analysis (Liefting *et al.,* 2009a). Different haplotypes have been detected by determining the genetic variability using single-nucleotide polymorphism (SNP) analysis (Liefting *et al.,* 2009a; Secor *et al.,* 2009; Wen *et al.,* 2009; Nelson *et al.,* 2011; Alfaro-Fernández *et al.,* 2017; Monger & Jeffries 2018; Mirmajlessi *et al.,* 2019), genotyping the PCR products amplified using a SSR or MLST markers (Glynn *et al.,* 2012; Lin *et al.,* 2012; Mirmajlessi *et al.,* 2019).

The effective detection of the pathogen upon infection mainly depends on the pathogen titre in the host plant (Mirmajlessi *et al.,* 2015) and using appropriate primer sets for identifying the target DNA region of the pathogen. Using primer sets with accurate primer sequences, can give a highly accurate and sensitive diagnosis of PCR (Henson & French, 1993). For detection of CaLso, the 16S ribosomal RNA gene, the 16S/23S intergenic spacer region and

the 50S ribosomal protein genes have been described as useful target genes for designing primers and probes (Maiden *et al.,* 1998; Lopez *et al.,* 2009; Nelson *et al.,* 2011).

2.4.1.1 DNA isolation and extraction

The important steps before performing PCR include plant sampling and DNA extraction. Plant sampling is important and critical in the pre-analytic step as CaLso is unevenly distributed and can be detected in symptomless plants at a very low concentration (Levy *et al.,* 2011; Li *et al.,* 2011). Thus, selecting a symptomatic leaf and increasing sample numbers can help ease the diagnosis.

Effective DNA isolation technique is important for efficient extraction of pure and uncontaminated DNA of good quantity (Gupta, 2019). DNA extraction involves purifying DNA from a sample using physical and/or chemical methods. The purification process involves DNA separation from cell membranes, proteins and other cellular components (Gupta, 2019). Manual methods and/or commercially available kits are used for extraction. DNA extraction is a critical step with purified DNA improving the diagnostic results of a PCR (Li *et al.,* 2009). By performing spectrophotometry, the yield and quality of the DNA extracted can be assessed (Gupta, 2019). A A_{260}/A_{280} ratio of 1.8 is considered good quality, while any value less than 1.7 indicates protein contamination and a less titre of the DNA (Gupta, 2019).

Schena *et al.* (2013) reported the presence of PCR inhibitors in plant tissue samples that can potentially reduce the PCR reaction sensitivity. A low DNA titre of the pathogen and a non-optimal DNA extraction method, coupled with a PCR inhibitor can also reduce the reaction sensitivity for detection (Mirmajlessi *et al.,* 2019). Multainu *et al.* (2018) found that the inhibitory substances can be removed using lyophilisation, template dilution and other column-based protocols. The removal of inhibitory compounds, while being simple in the rapid extraction is what makes commercial kits to be widely used (Mimajlessi *et al.,* 2019). Some of the widely used methods for DNA extraction using commercially available commercial kits are stated in studies mentioned in Table 2.2. However, other methods can also be effective, such as a Chelex ® 100 resin method. Simon *et al.* (2020), with dried blood spots as samples, showed a Chelex ® 100 method can be used to extract a high quantity of a high-quality genomic DNA (gDNA). This method is recommended by the authors for a diverse range of studies that require a high-quality DNA.

Table 2.2. Systematic publication review on the PCR methods used in detecting CaLso in potatoes.

PCR-based method used	Origin	Reference
PCR	USA, Mexico, Guatemala	Secor *et al.* (2009)
PCR + mrtPCR (TaqMan)	USA	Li *et al.* (2009) *
PCR + qPCR (TaqMan) + multiplex PCR	USA	Wen *et al.* (2009) *
PCR	USA	Sengoda *et al.* (2010)
USA	USA	Levy *et al.* (2011)
PCR	Hondurus	Rehman *et al.* (2010)
PCR + nPCR + multiplex PCR	New Zealand	Pitman *et al.* (2011)
PCR	USA	Ravindran *et al.* (2011)
PCR	USA	Crosslin *et al.* (2012a, b)
SSR	USA, Mexico	Lin *et al.* (2012) *
PCR	USA	Munyaneza *et al.* (2012b)
PCR + qPCR (SYBRGreen)	USA	Wallis *et al.* (2012)
MLST	USA, Mexico, New Zealand	Glynn *et al.* (2012) *
LAMP + PCR	USA	Ravindran *et al.* (2012)
SSR + PCR	USA	Wen *et al.* (2013)
PCR + nPCR + Semi-nested, qPCR (SYBRGreen) + qPCR (TaqMan)	New Zealand	Beard *et al.* (2013)
PCR	USA	Cating *et al.* (2015)
qPCR (TaqMan)	Spain	Antolinez *et al.* (2017)
Note: *original PCR method used; PCR: conventional PCR; mrtPCR: multiplex real-time PCR; qPCR: quantitative PCR; multiplex PCR; nPCR: nested PCR; MLST: multi-locus sequence typing; LAMP: loop-mediated isothermal amplification; SSR: simple sequence repeat;		

PCR assay is performed after DNA extraction, where a specific segment of the pathogens DNA is amplified. This involves preparing a master mix with various chemical components such as $MgCl_2$, buffer (pH: 8.3–8.8), deoxynucleoside triphosphates (dNTPs), PCR primers, target DNA,

and thermostable DNA polymerase (Clark *et al.,* 2013). PCR is performed in a thermocycler and involves, denaturation of the double stranded (ds) DNA template at 92–95°C, annealing of the primers 50–70°C and extension of the dsDNA molecules at around 72°C. These steps are repeated for 30-40 cycles in the thermocycles (Gupta. 2019).

2.4.1.2 qPCR and PCR

From the different methods stated (Table 2), qPCR allows for the detection of the pathogen with the highest sensitivity, and also provides a reliable estimate on pathogen load (Palacio-Bielsa *et al.,* 2009) with a cycle threshold and quantity values. The amplicon detection in qPCR is based on fluorescent signalling (Mirmajlessi *et al.,* 2015b), which makes it more desirable for large scale processes as it reduces time by eliminating the requirement for post-amplification processes (Bustin *et al.,* 2009). Tatineni *et al.* (2008) and Tiexeira *et al.* (2008) showed that the use of an qPCR is 10-100 times more sensitive in detecting CLas in HLB infected leaves. Similarly, sensitivity of CaLso detection using qPCR over PCR have been reported by Li *et al.* (2009), Wen *et al.* (2009) and Ravindran *et al.* (2011). Viability of CaLso can also be achieved using an qPCR assay, wherein proidium monoazide (PMA) can be used as a DNA-intercalating agent to help detect suppressed dead CaLso cells (Bertolini *et al.,* 2015), which otherwise could be detected as a positive result in a PCR.

PCR, though not as sensitive as qPCR, is widely used to detect CaLso. Detection sensitivity of PCR assay depends on the primer sets used. Primer sets have different levels of detection sensitivity and can be seen in the studies at different laboratories in table 1. In New Zealand, Liefting *et al.,* 2009 designed the primers OA2 and used it with primer OI2c (Jagoueix *et al.,* 1996) to amplify a 1160 bp fragment of the 16S rRNA sequence in infected tomato and pepper plant (Figure 2.8). The results showed amplification in CaLso infected plants. Following this study, experimentation by Li *et al.* (2009) on infected tubers found that performing PCR targeting 16S rRNA with the primers LsoF/OI2c were 10 times more sensitive than with OA2/OI2c primers, when using the identical cycling parameters. Similarly, greater detection rate of 69.5% from 49.1% was achieved in a study by Ravinder *et al.* (2011), using different primer sets such as Lso TXF/R or Lp FragF/R, targeting 16S-23S-ITSrDNA, when compared to LsoF/OI2c primer sets targeting 16S rDNA. In a study on CaLso infected carrots, Fukiwara and Fujikawa (2016) designed six new primer sets to amplify CaLso in carrots, where four primer

sets detected CaLso in the range of 10^2 to 10^8 CaLso cells/µl in carrot seeds. Thus, an increased sensitivity of PCR assays can be achieved with the right selection of primer sets. However, PCR has a few limitations which include, preparing and optimizing the PCR assay with the right annealing temperature, ineffective detection of the pathogen in low titre samples which may require further diluting of the samples (Li *et al.,* 2009), and the time-consuming procedure in optimizing the right master mix for the PCR assay. With respect to PCR inhibitors (such as non-target DNA) that can inhibit effective detection, Cating *et al.* (2015) used high-fidelity enzymes that increased detecting sensitivity in symptomatic potatoes by 30-40%. Thus, making it a potential option to optimize PCR assay.

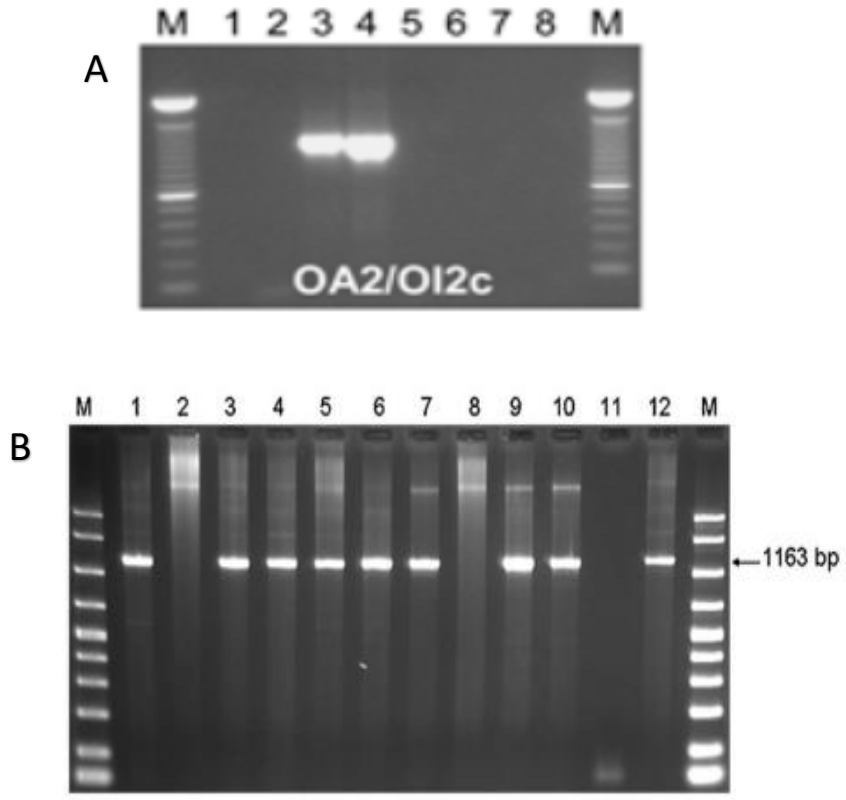

Figure 2.8. (A) Gel electrophoresis results of 1160bp amplicon using OA2 and OI2c primers to detect CaLso infected tomato and pepper plants (image from Liefting *et al.,* 2009a). (B) DNA extracts of various tissues using LsoF/OI2c primers: midribs and petioles, leaf blades, whole stalk, stalk epidermis, stalk cortices, root epidermis, root cortices, aerial tubers, small tubers and medium tubers (lanes 1 to 10) of potato plants affected by zebra chip in the field in Texas. Lanes 11 and 12 were no

template and positive controls. Marker (M) was the Extra ladder (Invitrogen) (Li *et al.,* 2009).

2.4.1.3 Multiplex PCR

The multiplex PCR method uses multiple primers in one reaction mixture. This allows several different DNA sequences to amplify. Using the same conditions of the ZCf/OI2c or OA2/OI2c primer sets described by Liefting *et al.* (2009a), Wen *et al.* (2009) developed a multiplex PCR for CaLso detection, where different primers including Btub1F/R plus ZCf/OI2c and Btub2F/R plus OA2/OI2c were used on different solanaceous hosts (Figure 2.9). The amplifications were confirmed by eliminating false negatives with amplification of the potato β-tubulin (Btub) DNA region with two specific primer sets. Similarly, the use of this method was proven efficient by Pitman *et al.* (2011). Elnifro *et al.* (2000) states that, although this method is reliable and reduces false negatives, it is time consuming.

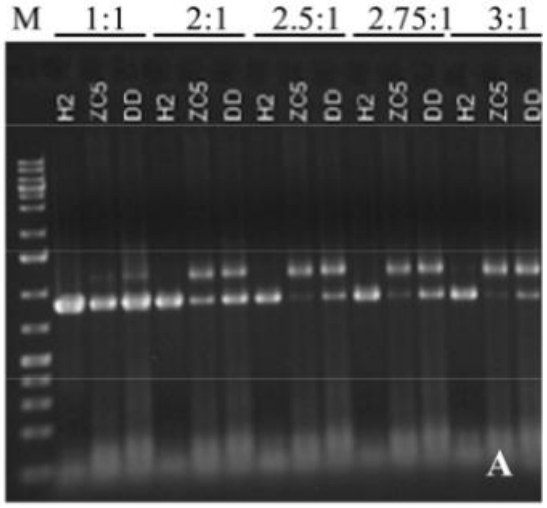

Figure 2.9. Multiplex PCR performed using Platinum Ta qDNA polymerase. Primer ratios of 0.4 µM for ZCf/OI2c and varying concentrations of β-tubulin1 F-R (0.4, 0.2, 0.16, 0.145, and 0.133 µM). H2: healthy potato tissue, and ZC5 and DD represent two zebracomplex–afflicted plants from two different locations. DNA marker: O'Gene Ruler 1 kb DNA Ladder Plus (Glen Burnie, MD). (Image from Wen *et al.,* 2009).

2.4.1.4 Nested PCR

The nPCR is a technique that increases the detection sensitivity while reducing the effect of PCR inhibitors (Miramajlessi *et al.,* 2019). Pitman *et al.* (2011), showed an increase in

detection sensitivity with nPCR in potato plants with low CaLso titre, using internal and external primers targeting the 16S rDNA. Pitman *et al*. (2011) first performed PCR with the OA2 and OI2c primers (as stated in Liefting *et al.* (2009a)), followed by a PCR with PCR products with primers Lib16S01F and Lib16S01R to amplify 580 bp (Figure 2.10). This method proved to be more sensitive with low titre samples than PCR and multiplex PCR. The only drawback observed was the increased risk of cross contamination between reaction mixtures (Miramajlessi *et al.,* 2019). Bread *et al.* (2013), demonstrated a single-step semi-nested PCR technique using CaLso infected TPP, potatoes and tomatoes. This techniques was found to circumvent the risk of nPCR. This technique involves the use of a single tube containing a primer pair flanked by a third primer (forward or reverse) which allows the reaction to take place in a single round. The primers used in this technique targets the 16S rDNA. The results from Bread *et al.* (2013) showed that the technique is 50 and 20 times more sensitive than cPCR and nPCR respectively.

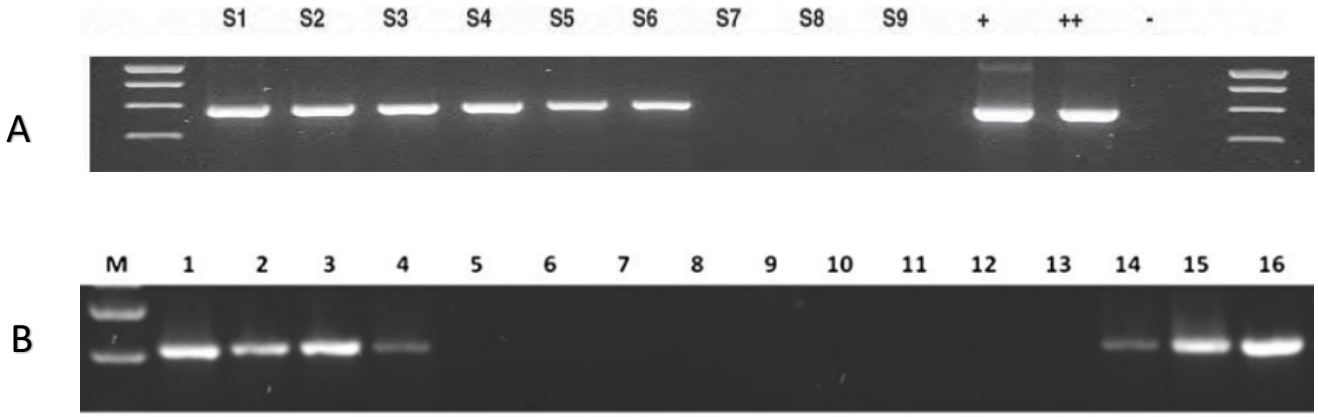

Figure 2.10. (A) nPCR results by Pitman *et al.,* 2011 using cPCR products with Lib16S01F-Lib16S01R primers. The amplification observed is at 580bp. (B) semi-nested PCR with OA2-Lib16S01F Lib16S01R for Ca. Liberibacter species. Lane 14 with an amplification at 580bp shows the potato sample infected with CaLso (Beard *et al.,* 2012).

DNA quality in any study for CaLso identification in potatoes can be assessed by using primers specific to the plant material. This was shown by Pitman *et al.* (2011) and Beard *et al.* (2013), where the primers 28Sf and 28Sr (Werren *et al.,* 1195) were used to amplify a 280 bp product for potatoes and tomatoes. Though these primers are used for quality analysis it can help

determine the efficiency of results against amplification from other primers as observed by Pitman *et al.* (2011).

However, a PCR assay has several drawbacks, relative to inexpensive detection methods. Some drawback include equipment cost which are depend on the components used, the need for highly trained personnel, the time required to conduct the whole process, and the difficulty in carrying out the detection reactions in field conditions (Prager *et al.,* 2022). Thus, this uncovers a void for a faster inexpensive detection method, to save time, yield and an economic loss for a farmer.

2.4.2 Other detection methods

Some other methods that could be used in the detection of CaLso in infected plants include:

a. Transmission electron microscope (Liefting *et al.,* 2009a, b). In terms of cost, this method is farm more expensive that PCR and would require specialized personnel to perform it.
b. Hyperspectral imaging, a method that was shown to have a potential in a non-destructive method of detection by Garhwal *et al.,* 2020. The model performance showed 92% accuracy in ZC potato identification, with a huge scope for research to help in removing diseased tubers.
c. Loop-mediated amplification technology (LAMP), a rapid field detection system devised by Keremane *et al.* (2015) for the detection of CLas in infected psyllids causing HLB. The method involves performing the LAMP assay in a Smart-DART^{TM} unit connected to a smart phone, with results showing up in 30 minutes. The method was developed for early identification of infected psyllids for effective control. This method could potentially be used by farmer, fieldman or extension workers in potato or other Solanaceous crop fields for accurate detection.

2.5 Iodine starch test (IST)

Industrially accepted identification of the bacteria relies on the use of PCR (Liefting *et al.,* 2009). A simple and rapid, on field diagnosis method can help in eliminating infected plants during field inspections. One such on field method developed was the Iodine starch method for the detection of citrus HLB. Following the initial findings of high starch accumulation in

the leaves infected with citrus HLB by Schneider (1968), Onuki *et al*. (2002) proved large starch granule accumulation in the infected leaves using histological staining. Starch turns blue when it reacts with iodine (Takushi *et al.,* 2007). Le Thi Thu Hong *et al.* (2003), subsequently developed an iodine reaction technique wherein symptomatic leaf samples were picked and ground with distilled water and reacted with 2 µl of iodine solution on a reaction film (NCM, Nitrocellulose membrane). The interpretation of the results were based on colour change. No change in colour of the iodine solution meant a negative reaction and a colour change to blue meant a positive reaction, stating the plant was infected.

Following this, Takusi *et al.* (2007) found HLB infected leaves of citrus trees to have 400-500 mg/kg of starch when compared to normal leaved having 85.6 mg/kg. They developed a method where the surface of the leaves were scratched with an abrasive paper and the abrasive paper was added into a bag with 50 mM of iodine solution (Figure 2.11). The IST conducted had a 90% agreement with PCR. Using a different abrasive paper but by following the same method as Takushi *et al.* (2007), Eng (2007) conducted an IST on the CLas infected mandarins (74.5%-89.5% agreement) and pummelo (12.5%-51.7% agreement). The researcher concluded that the accuracy of the test is highly dependent on the correct selection of infected leaves as well as the quality and concentration of the iodine solution used.

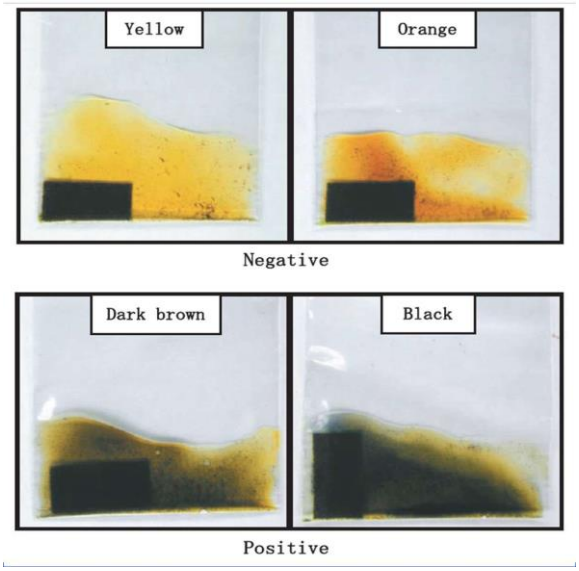

Figure 2.11. Scratch method indicating positive samples (infected leaves) with a blue-black colour while the negative (healthy leaves) are yellow/orange. (Takushi *et al.,* 2007)

Zhang Liping in 2009 conducted an iodine starch test as Takushi *et al.* (2007) and Eng *et al.* (2007), but followed a different method where the infected leaves were ground and mixed with an equivalent amount of water (Mao *et al*., 2018). 4µl of the mixed sample was aliquoted on a reaction film for 5 minutes and then treated with iodine. The colour change was evaluated similar to Takushi *et al.* (2007). The results of the test were 93.3% in agreement with PCR. Though these techniques worked with a consistency at >90% in agreement with PCR, they have a few drawbacks, which could include the interference of chlorophyll in the colour change, and the use of water to grind the samples as starch is insoluble in water, making water a variable leading to inaccuracy in the colour change. Sampling and grinding the leaf samples in the field will also be harder to do in bad weather condition such as strong winds and it also uses an 'x' amount of iodine solution to be used and thrown away. These disadvantages make the methodology followed by Takushi *et al*. (2007) and Eng *et al*. (2007) less appealing to be used in the field conditions.

Etxeberria *et al.* (2009), modified the methods stated in the studies above, wherein a cross section of the lamina, about 2 mm away from the midrib was cut from HLB symptomatic leaves (Figure 2.12). The cut section of the leaf was immersed in an iodine solution (1 part iodine mixed with 10 parts water) for 1.5 to 2 minutes.

Figure 2.12. A of HLB symtomatic (vein corking) leaf properly sectioned 2 mm away from the mid rib for the iodine test. The arrow indicated the cross section of the leaf used for the test (Etxeberria *et al.,* 2009).

The immersed section was later examined for dark staining (Figure 2.13) using a hand lens or a magnifying glass. The researchers concluded that the test indicated high starch accumulation in leaves, but also stated that it didn't mean the leaves were HLB positive. Reasons stated were that some citrus cultivars naturally have high starch concentration, physical damages in the phloem could lead to starch accumulation, and diseases other than HLB could also lead to starch accumulation in citrus leaves. The researchers state that this would not indicate HLB positive leaves consistently, however it can be used in determining leaves to be submitted for PCR, while reducing the number of negative samples submitted.

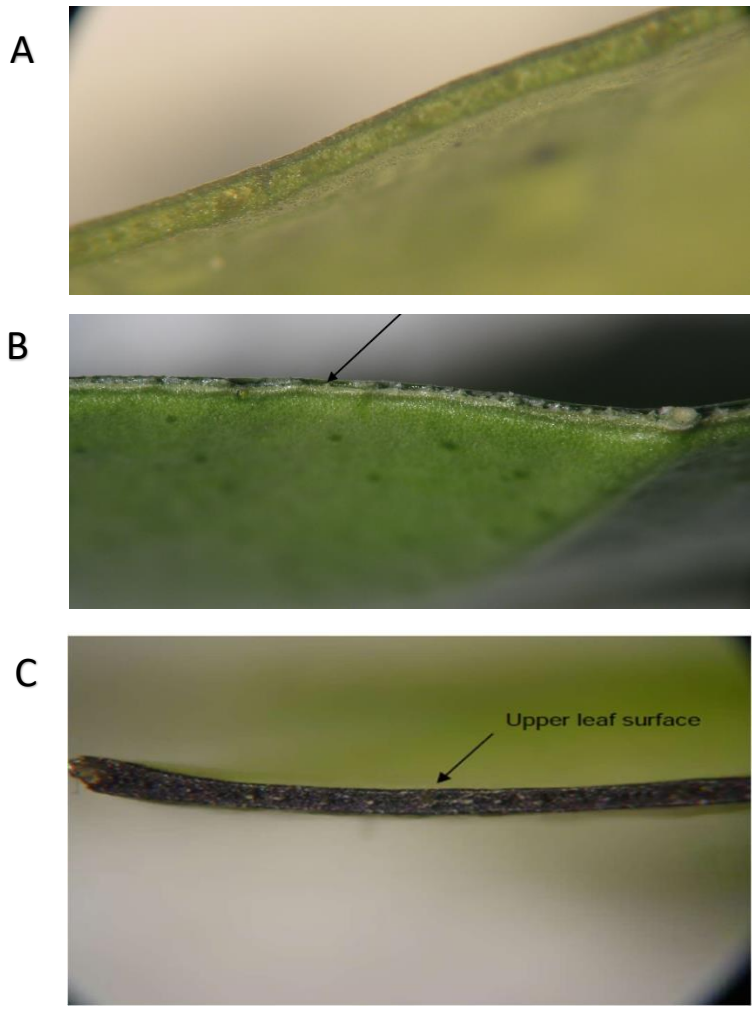

Figure 2.13. Healthy citrus leaf showing no (A) or very little (B) staining upon iodine testing. HLB infected leaf stains very dark grey to black along the cut surface when immersed in iodine for 2 minutes (Etxeberria *et al.,* 2009).

Although this method has been recommended for leaf sampling for PCR testing, a few important aspects from its methodology can be considered in developing an IST for CaLso infected potato plants. This includes, (a) leaf sampling i.e., to select symptomatic leaves or symptomatic sections of asymptomatic leaves, (b) iodine solution should be diluted, as an undiluted solution would react with even smaller quantities of starch, and (c) if conditions as not right on the field for testing, the leaves should be stored under refrigerated conditions for no more than 24 hours. This aspect of sample selection is also consistent with the work done by previous researched discussed above. Thus, making it even more important to consider while developing an IST (Etxeberria *et al.,* 2009).

A few advantages of the IST that make it desirable include its cost effectiveness for detection, reduction in manpower requirement, and a need of a high-level expertise to perform it is not required. These advantages make it easy for growers to carry out the tests themselves on the field.

2.6 Discussion and Conclusions

TPP pose a huge threat to potato growers and the industry as it acquires and transmits CaLso from infected to healthy plants and results in ZC disorder. Given the exceptionally high population of vectors in any given season as well as infected plants, as first shield of defence in preventing the spread of the disease it is vital for growers to eradicate volunteer potatoes, weeds that are potential hosts as well as infected plants. Although one way to control ZC is through TPP eradication, complete eradication is highly unlikely, and managing TPP populations at low levels is the best that can be expected. Furthermore, once a TPP adult acquires the pathogen, it can travel several hundred kilometres making control impossible. More importantly, eradication of ZC infected potato plants, including volunteers, should be the focus of eradication efforts.

CaLso infected plants take 3-4 weeks to show foliar symptoms, and a minimum of 2 weeks to show symptoms in tubers. This is problematic for the farmers as during symptom development, ZC goes undetected with no chance of roguing them out of the field, based on visual symptoms. Currently the only recognised method of CaLso detection involves the use of PCR. In general it takes 3 weeks for a grower to receive PCR results. During this time TPP could acquire and infect multiple plants. Another drawback observed in using PCR is sampling

quantity. PCR is cost-prohibitive for growers as it costs NZD 649.75 per sample (Ministry of Primary Industry, 2022).

Upon acquisition, CaLso moves from the infected leaves to the main stem in seven days. This motility of CaLso could be aided by its pili and flagella through the phloem vessels. CaLso, similar to CLas, is known to cause phloem necrosis in the stem, which leads to a high starch accumulation in the aerial parts of the plant in comparison to uninfected plants. Tubers, however, have a high concentration of reducing sugars, amino acids and compounds related to plant defence. High concentration of starch in the aerial parts of the plant provide an opportunity to utilise IST, similar to that developed to detect HLB infected leaves. With studies showing >90% agreement of IST with PCR, an opportunity lies in detecting CaLso infected potatoes with IST.

Etxeberria *et al.* (2009) developed a more feasible, inexpensive, and accurate field bioassay, when compared to Takushi *et al.* (2007) and Eng (2007). Here, a grower can assess multiple plants with less effort and waste (iodine solution). The only drawback observed in that study was the 2 minutes immersion period per sample and future investigations should determine whether it is possible to reduce this time. In addition to testing leaves, confirmation of tuber infection by iodine staining would also be useful. However, if proven to be highly accurate, ZC positive confirmation of the leaves would be sufficient evidence for roguing of entire plants in the field. This would have a dramatic impact on reducing primary inoculum in potato fields and volunteer plants.

3 EXPERIMENT 1 - DEVELOPING THE BIOASSAY

3.1 Introduction

Upon infection with *Candidatus* Liberibacter solanacearum (CaLso), potato plants exhibit an abnormal amount of starch in the aerial parts of the plant. This is the result of phloem vessel damage by the bacterium, as it travels from source (leaves) to the sink (tubers/roots) (Gao *et al.,* 2009; Levy *et al*., 2011; Wallis *et al*., 2012; Wallis *et al*., 2014). Similar observations were made in *Candidatus* Liberibacter asiaticus (CLas) infected citrus trees causing Huanglongbing disease (HLB) (Gonzalez *et al*., 2012). With prior success in detecting CLas infected citrus trees (HLB), there lies an opportunity to detect CaLso infected potato plants as well. Of the methods discussed in Chapter 1, section 2.5, Etxeberria *et al.* (2008) demonstrated a detection method that is rapid and suitable for an in-field scenario. The method outlined in that study will be replicated and modified to suit potato leaves and tubers. Furthermore ZC-symptomatic potatoes will be compared against *R. solani*-symptomatic and visibly healthy, presumably uninfected potato plants.

3.2 Materials and Methods

In total, 24 'Russet Burbank' potato plants were collected from a potato field on the 10th of March (2021/22 growing season), which was approximately two weeks before commercial harvest. The potato field was located on Hamptons Road, Pendarves 7777, New Zealand (coordinates: -43.931081,171.972751). Of these 24 plants, eight were symptomatic of ZC infection, eight were symptomatic to *R. solani* infection and eight were visibly healthy plants, that were not suspected of being infected. All plants were selected based on foliar symptoms and tubers were dug to confirm presence or absence of flecking of the peri-medullary region.

3.2.1 Preliminary test with 6% Iodine solution

Lugol's 500 mL iodine solution (Iodine 5% (w/v), potassium iodide 10% (w/v), 85% Purified water) was used for this experiment. Following the procedure outlined in Etxeberria *et al.* (2008), a preliminary test was performed with the iodine solution diluted to 6% with water. Tubers and lateral leaflets were selected at random from the 24 samples collected.

Symptomatic (yellow in colour) (Figure 3.1) and asymptomatic leaves (green in colour) were tested. A sharp, clean razor blade was used to cut a section 1 mm away from the midrib, down the length of the midrib (Figure 3.1). That section was then trimmed to approximate a rectangle, thus exposing a large cross-section of the lamina. The section was immersed in 6% iodine solution for 2 minutes and then rinsed with distilled water for 5 seconds (Etxeberria *et al.,* 2008). The cut edges of the section (leaf lamina) were examined using a 200X magnifying lens (Koolertron mini phone microscope with LED light, Home Entertainment Systems, FL, USA) attached to a smart phone camera. Similarly, with tubers, a cross-section was cut from about 2 cm away from the basal end and immersed in the 6% iodine solution once for 2 minutes, rinsed with clean water for 5 seconds and immediately photographed.

Figure 3.1. A symptomatic potato leaf from a Zebra Chip symptomatic plant sectioned for the iodine (6%) starch test. The arrow indicated the section of the leaf to be used for testing.

3.2.2 3% Iodine solution

The 6% iodine solution was further diluted to 3% with water, due to lack of results. Where possible, affected leaflets (refer Figure 2.2) from diseased plants and from healthy looking plants were selected and sections excised as per section 3.2.1 (Figure 3.2). The cut section of the leaflet was immersed in the diluted 3% iodine solution for 30 seconds and rinsed in distilled water for 5 seconds. The cut edge of the leaf was examined for staining and photographed using a 200X magnifying lens (Koolertron mini phone microscope) attached

to a smart phone camera. Samples were collected in a snap lock bag and immediately frozen (-20°C), until PCR analysis to (Chapter 4).

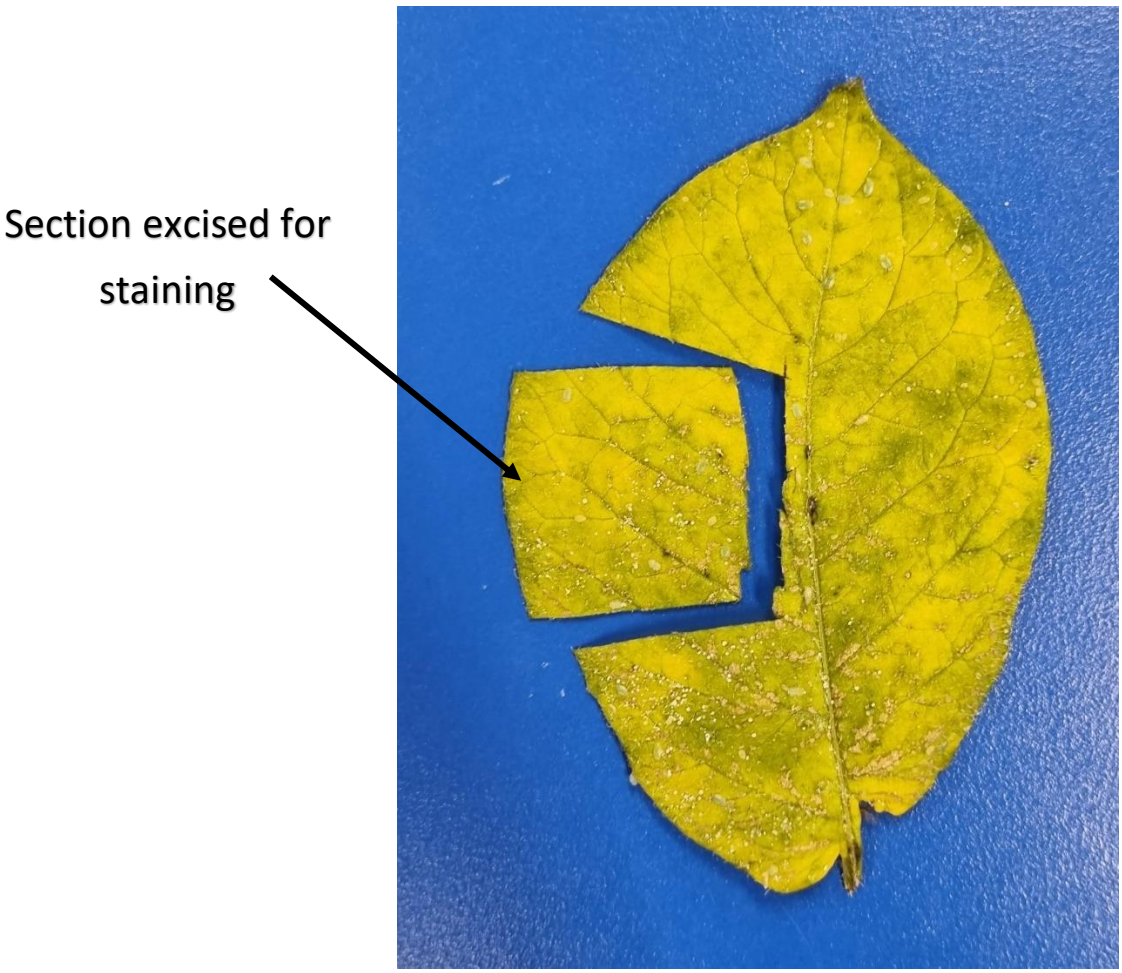

Figure 3.2. A potato leaflet from a Zebra Chip symptomatic plant used for iodine starch test (3% iodine solution). The arrow indicated the section of the leaf used for staining.

From each tuber sample, a cross section of 20 mm away from the basal end were cut for IST (Figure 3.3). The cut end of the tuber was immersed in the diluted 3% iodine solution for 10 seconds and rinsed with distilled water for 5 seconds. The cut edge was immediately stained and photographed. One section near the vascular ring region and one from within the peri-medullary tissue region of the tuber (Figure 3.3) were excised from each tuber sample, which was then frozen at -20°C, until PCR analysis was performed (Chapter 4).

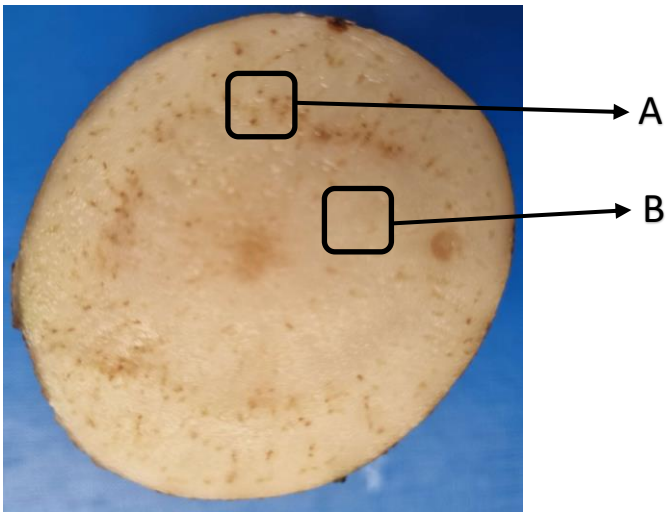

Figure 3.3. Liberibacter symptomatic sample 1, tuber cross-section from the basal end used for staining with 3% iodine. **A** (piece near the vascular ring region) and **B** (piece from around the peri-medullary tissue region) are the two pieces used for PCR.

3.2.3 Preliminary investigation on the midrib and petiolule

Two 'Russet Burbank' potato plants grown in the greenhouse at Lincoln University, New Zealand, were used fort this preliminary investigation. Of the two plants, one was infected with CaLso using CaLso infected TPP and the other was visibly healthy, presumably uninfected. A leaflet from each of the plants were taken to check for potential staining with the standardised 3% iodine solution. This experiment was conducted to check for alternative staining options and also to check for the presence of CaLso in the midrib and petiolule region of the leaflet. The midrib (Figure 3.4-A) of each leaflet was excised in the middle into two halves. One half was immersed in 3% iodine solution (section 3.2.2) for 30 seconds and rinsed with distilled water for 5 seconds. Similarly, the lower cut edge of the petiolule of each leaflet (Figure 3.4-B) was also immersed in the 3% iodine solution for 30 seconds and rinsed with clear water for 5 seconds. The immersed sections were examined for staining and photographed using a 200X magnifying lens (Koolertron mini phone microscope with LED light) attached to a smart phone camera. The samples along with a cross-section of the leaf lamina were collected in snap lock bags and frozen until used for PCR analysis to check for the presence or absence of CaLso (Chapter 4).

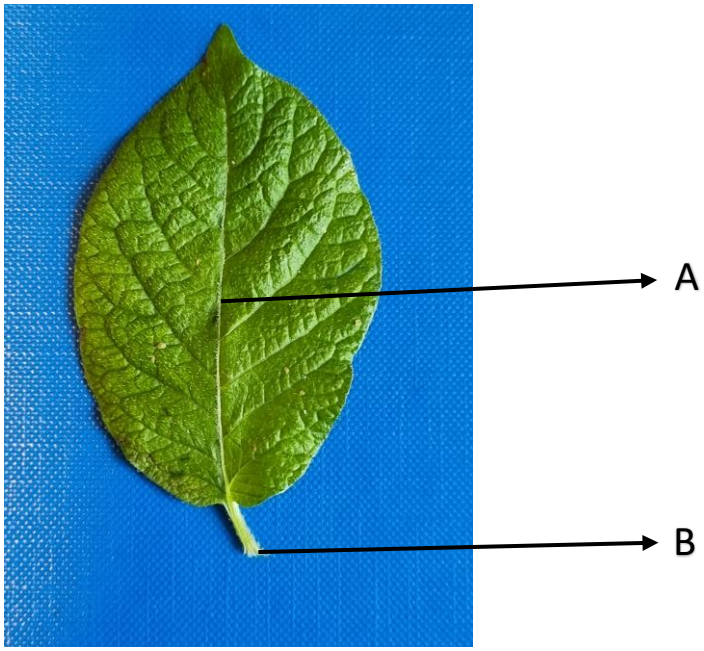

Figure 3.4. (**A**) indicated the leaf midrib to be excised and (**B**) indicates the petiolule region used for staining with 3% iodine solution.

3.3 Results

3.3.1 Preliminary test with 6% iodine solution

All tested leaf samples showed a dark black staining with 6% iodine (Figure 3.5-A, B). The cut section of symptomatic yellow leaflets showed a greyish stain (Figure 3.5-A), while the green symptomless leaves showed a dark black staining (Figure 3.5-B). All cell layers of the leaf laminas were observed to be completely stained in all samples tested. Similarly, all tubers showed a complete black staining upon immersion (Figure 3.5-C).

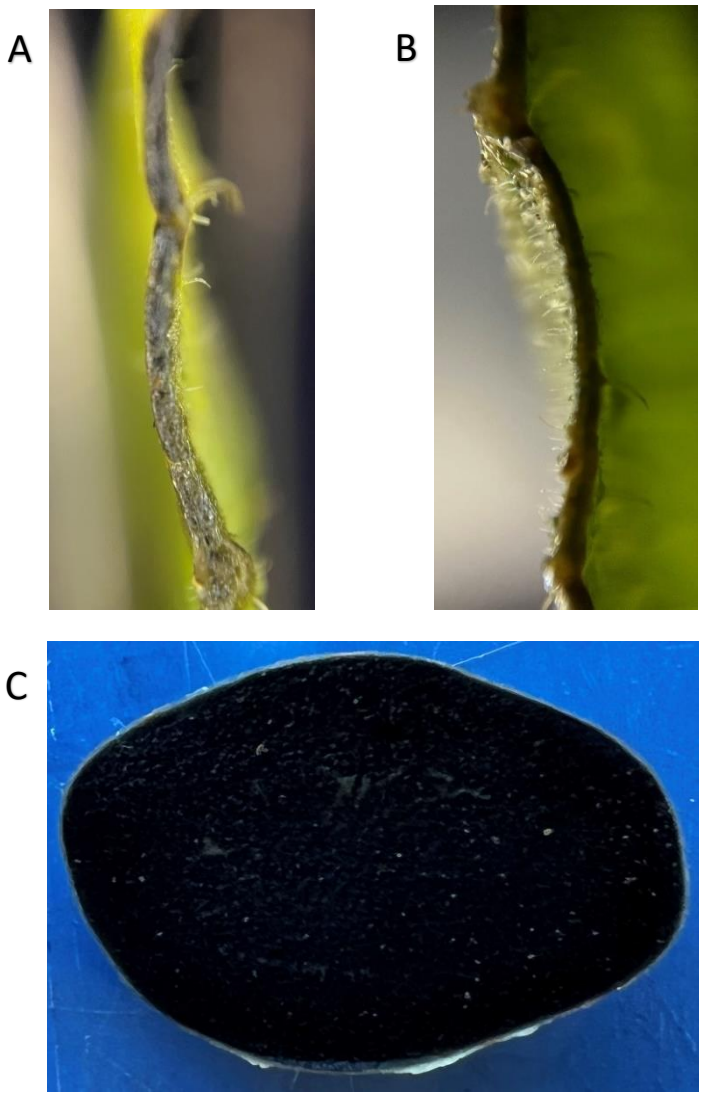

Figure 3.5. ZC-symptomatic tuber and leaflet cross sections were immersed in 6% iodine solution. (**A**) Grey staining is observed along the lamina of the cut section, of the symptomatic yellow leaflet. (**B**) A very dark black staining is observed along the lamina of the cut section of the symptomless green leaf. (**C**) The tuber cross section is completely stained black.

3.3.2 3% Iodine solution

From the ZC-symptomatic plants, all eight leaflet and tuber sections showed a dark blackish-purple stain along the leaf laminas and, around the outer peri-medullary region through to the skin of the potato tubers respectively (Figure 3.6) (Appendix A).

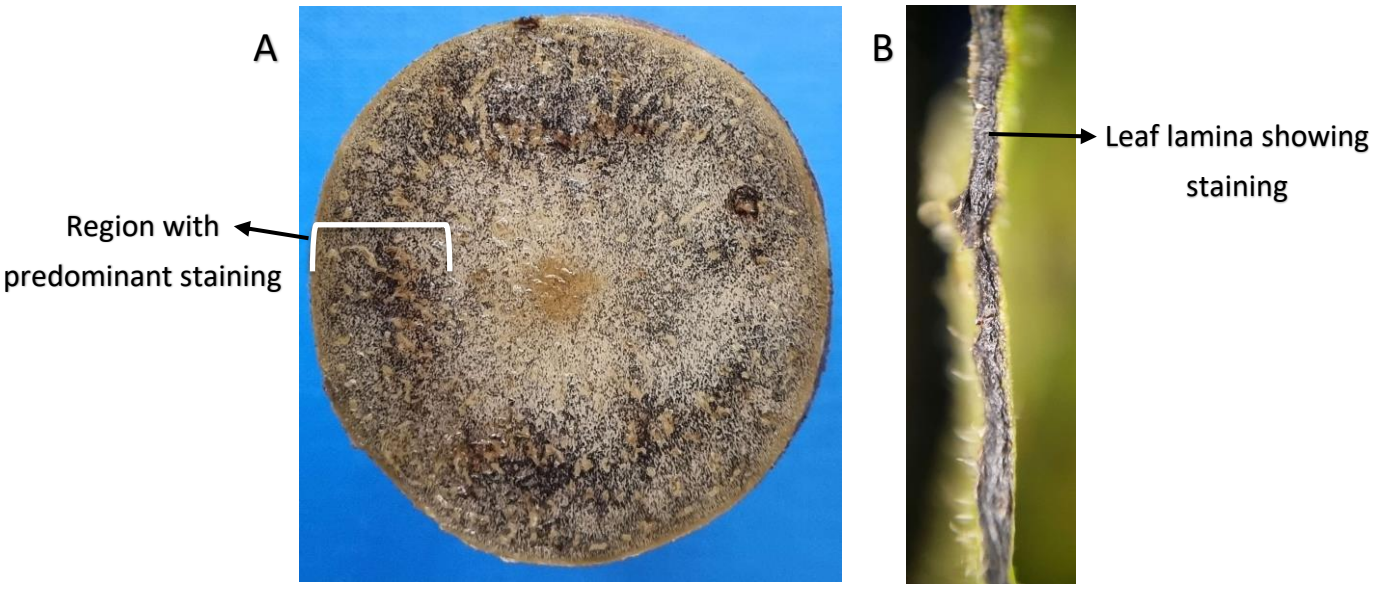

Figure 3.6. IST of *Liberibacter* symptomatic sample 1, tuber and leaf lamina. **A**) Tuber with predominant blackish-purple stain; **B**) Leaf sample with a blackish-purple staining along the leaf lamina (all cell layers are observed to be stained).

In visibly healthy-looking plants (Appendix A), sample number 2 (stained darkest) (Figure 3.7) and sample number 6 (stained darker) showed a blackish-purple stain around the outer peri-medullary region through to the skin of the potato tubers. The other six samples showed a light blueish-purple stain. With regards to the leaves, only samples 2 and 6 showed a dark blackish-purple stain.

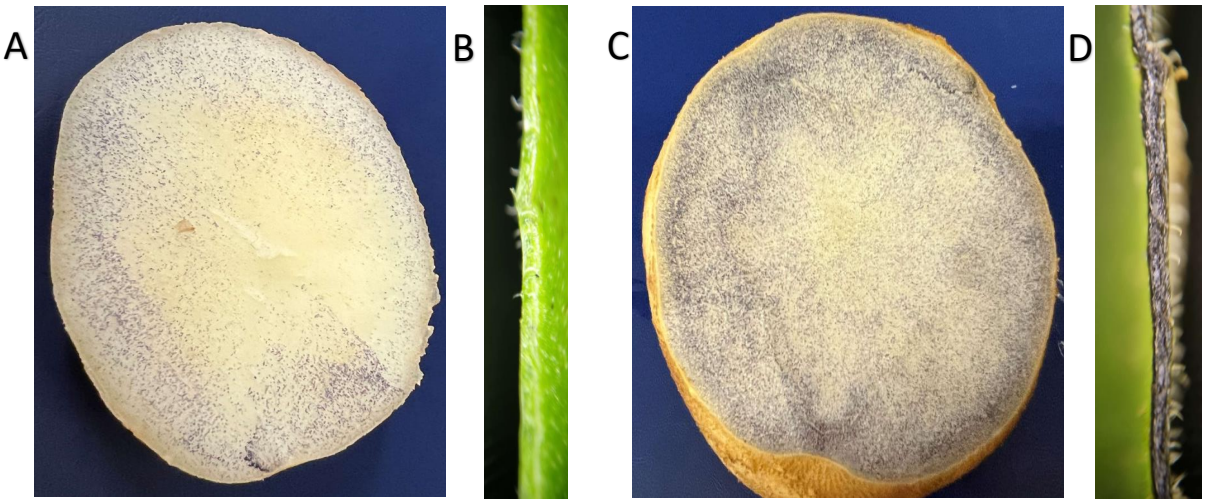

Figure 3.7. IST of visibly healthy-looking plant tubers and leaf laminas of samples 1 and 2. **A** and **B** of sample 1 shows light blueish-purple stain on the tuber and no stain

on leaf lamina respectively. **C** and **D** of sample 2 shows a dark blackish-purple staining on the tuber and along the leaf lamina respectively.

In *R. solani* symptomatic plants (Appendix A), all samples (n=8), except sample 7 (n=1) had no staining along the leaf lamina, and the tubers showed a light blueish-purple stain from the vascular region through to the periderm (Figure 3.8).

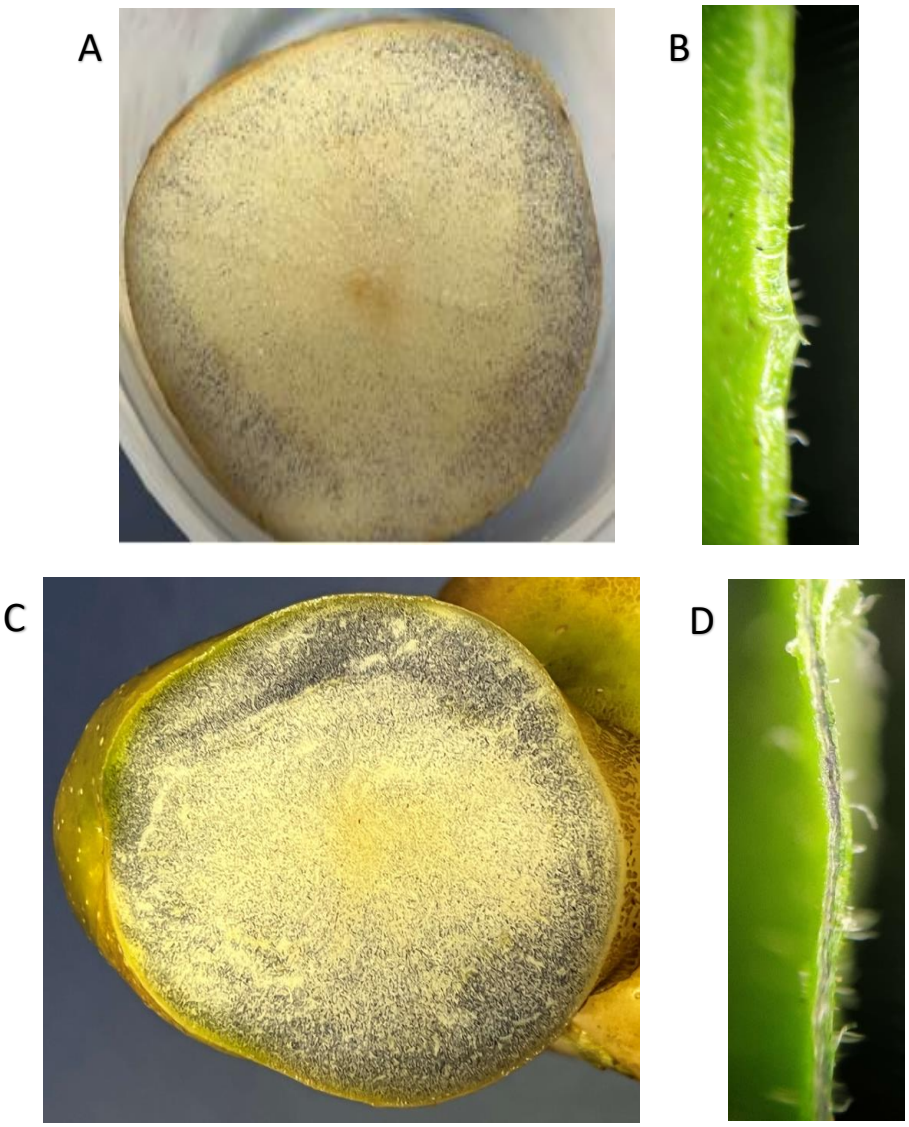

Figure 3.8. IST of *Rhizoctonia* symptomatic samples 1 and 7, tubers and leaf laminas. No staining observed along the leaf lamina of sample 1 (**B**), while a light blueish-purple stain is seen between the outer vascular ring and the periderm of the tuber (**A**). Images **C** and **D** shoe the IST results of sample 7, with a dark blackish-purple staining on the tuber and leaf lamina respectively.

Thus, 100% (n=8) of ZC-symptomatic, 12.5% (n=1) of *R. solani* symptomatic and 25% (n=2) of healthy-looking plant samples showed a dark blackish-purple staining along the leaf laminas and on tubers (Table 3.1).

Table 3.1. Leaf lamina and tubers of the 24 samples that stained positive and negative with 3% iodine solution.

Sample Type	Sample Number	Iodine Staining		General comments
		Leaf lamina	Tuber	
ZC-symptomatic Plants	L1	+	+	
	L2	+	+	
	L3	+	+	
	L4	+	+	
	L5	+	+	
	L6	+	+	
	L7	+	+	
	L8	+	+	
Rhizoctonia solani symptomatic plants	R1	-	-	
	R2	-	-	
	R3	-	-	
	R4	-	-	
	R5	-	-	
	R6	-	-	
	R7	+	+	Mild blackish-purple stain observed along the leaf lamina.
	R8	-	-	
Visibly healthy-looking plant	S1	-	-	
	S2	+	+	
	S3	-	-	
	S4	-	-	
	S5	-	-	
	S6	+	+	Mild blackish-purple stain observed on the tubers.
	S7	-	-	Mild staining observed on one side of the leaf lamina.

3.3.3 Preliminary investigation of midrib and petiolule

The midrib and petiolule of a ZC-infected potato plant showed a dark blackish-purple stain with 3% iodine, while that of the visibly healthy plant showed no staining (Figure 3.9). The observed stain in the midrib and petiolule was along the phloem region (refer Figure 2.5).

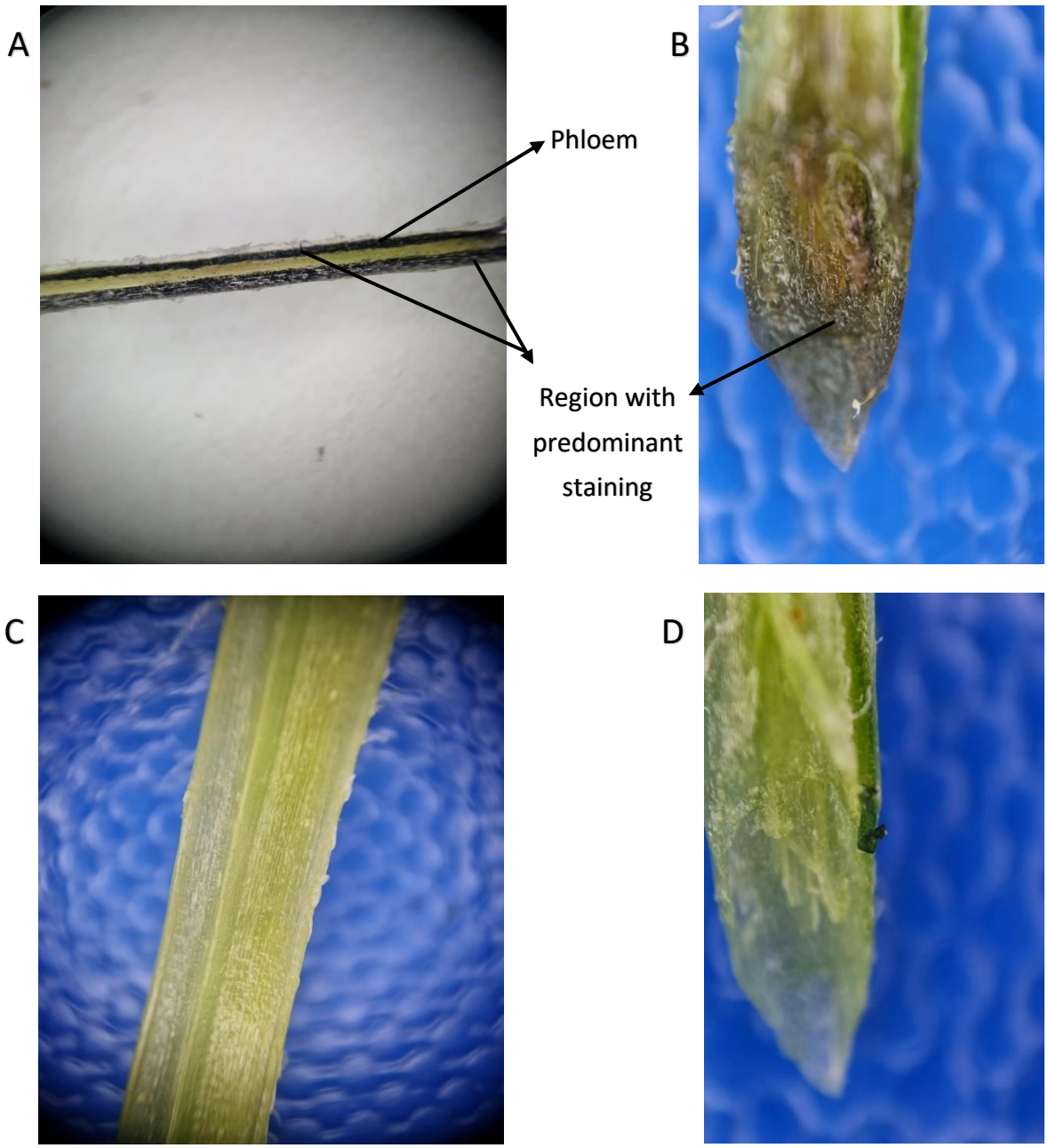

Figure 3.9. IST of midrib and petiolule of ZC infected and uninfected healthy 'Russet Burbank' potato plants. Midrib (**A**) and petiolule (**B**) of ZC infected plants show

predominant black staining. No staining is observed along the midrib (**C**) and petiolule (**D**) of uninfected healthy plants.

3.4 Discussion

3.4.1 6% and 3% IST

Initial test results with 6% iodine on tubers and leaf samples were overstained and no differences could be seen between any samples. It is assumed that the concentration of the iodine solution was too high. As per Etxeberria *et al.* (2008) the iodine concentration was diluted to 3%. Leaves and tubers stained with 3% iodine exhibited differences in colour and intensity of stains ranging from light blueish-purple to dark blackish-purple, as well as no staining. This blackish-purple stain was also observed along the leaf lamina similar to that in HLB-infected citrus leaves (Etxeberria *et al.,* 2008). In tubers, the 3% stain was observed around the outer peri-medullary region through to the skin of the potato tubers. A colour difference in staining amongst different tuber samples was also a confirming indicator that the 3% iodine concentration is ideal for testing 'Russet Burbank'. This thus led to standardising the 3% iodine solution as a suitable bioassay to check for staining in 'Russet Burbank' tubers and leaf lamina for CaLso detection in this study. Furthermore, the time in iodine solution was significantly reduced from 2 minutes to 30 seconds for leaves, and 10 seconds for tubers.

Starch is a natural product of photosynthetic CO_2 fixation in green tissues. It has two components, the highly branched insoluble amylopectin and the small linear chain amylose (Shannon & Garwood, 1984). When reacted with iodine, amylose turns blue and amylopectin turns purple. However, a colour change to either blue or purple indicates the presence of starch. Upon CaLso infection potato plants have a lower concentration of reduced sugar either as a result of decreased photosynthesis due to necrosis of phloem tissues by the bacterium (Gao *et al*., 2016) or the concentration of soluble sugars could have been used by CaLso for energy or by the plant for defence responses or converted into starch (Gao *et al.,* 2009). CLas, a phloem limited bacteria of the same genus as CaLso, causes a similar decrease in reducing sugars and an increase in starch concentration, in the aerial parts of the plant. The reasons for this increase include vascular phloem necrosis and callose deposition in the sieve plate pores (Achor *et al.,* 2010; Koh *et al.,* 2012). Phloem

plugging and phloem necrosis could also be a reason for starch accumulation in potato leaves upon CaLso infection (Levy *et al*., 2011; Gao *et al*., 2016). Furthermore, CaLso follows the carbohydrate transport route from source (leaves) to sink (tuber/roots) in the phloem (Levy *et al*., 2011). Thus, it may be hypothesized that all ZC-symptomatic, one *R. solani*-symptomatic, as well as two visibly healthy-looking plant, which all stained blackish-purple along the leaf lamina in 3% iodine, may be infected with CaLso. PCR results of these samples are presented in Chapter 4.

In the study by Gonzalez *et al*. (2012), phloem that was blocked by mechanical damage had starch that were biochemically different from that found in HLB infected leaves, which had more amylopectin. This observation could probably be the same in CaLso-infected potato plants as, CaLso is from the same genus, while also being phloem-limited. Increase in amylopectin concentration may be the reason for the observed difference in staining colour in tubers. Here, all tuber samples that showed a blackish-purple stain may indicate a higher amylopectin concentration and CaLso infection. Similar staining observations and hypothesis may be made with the leaf samples. For confirmation, amylopectin concentrations in each sample would need to be determined, but this was not within the scope of this study.

With regards to the staining region in tubers, most staining was observed around the outer peri-medullary region (mostly the vascular region) through to the periderm. This observation was consistent in all tuber samples. This stained region between the outer peri-medullary region through to the periderm, consists of storage parenchyma cells that contain starch granules (refer section 2.1.3) (Troncoso *et al.,* 2009; Fedec *et al.,* 1997; Gancarz *et al.,* 2014). When transmitted to a leaf from an infected TPP, CaLso moves through the phloem from source (leaves) to sink (tubers/roots) and is known to have a higher titre in stolons and tubers (Levy *et al.,* 2011). This suggests that CaLso islocated in the phloem bundles (refer section 2.1.3) of tubers, as tubers are the final sink in potato plants. The darker blackish-purple staining observed in this region could be due to CaLso biochemically changing the composition of starch to amylopectin and reducing sugars. In addition, the light blueish-purple stain could be the result of amylose staining, but this was not within the scope of the study.

3.4.2 Preliminary investigation on midrib and petiolule

When a CaLso-infected potato plant was compared with a visibly healthy, presumably uninfected plant. Preliminary 3% IST results of the CaLso-infected potato plant showed a dark blackish-purple stain along the phloem region of the midrib and the petiolule (Figure 3.9-A, B) (refer section 2.1.4), which suggests that it was infected with CaLso. Confirmation of infection by PCR is presented in Chapter 4. In the visible healthy, presumably uninfected plant no staining was observed in the midrib nor the petiolule (Figure 3.9-C, D), which suggests no CaLso infection. Confirmation of this by PCR is presented in Chapter 4.

4 EXPERIMENT 2 – ACCURACY OF THE BIOASSAY

4.1 Introduction

Polymerase chain reaction (PCR) is a crucial tool to detect and identify many plant pathogens, especially those that are non-culturable, such as CaLso (Jagoueix *et al*., 1994). To confirm the accuracy of a 3% iodine solution used to stain CaLso-positive potato plants, verification with an approved and accurate testing method such as the PCR was undertaken. Some previous work done in detecting CaLso using different primers and PCR methods are outlined in Chapter 1, section 2.4. Of these methods, the conventional single-step PCR method with OA2 and OI2c primers, and the nested PCR method with Lib16S01F and Lib16S01F primers were used to determine the presence or absence of CaLso. The methods were adapted from the study by Pitman *et al*. (2011). The nested PCR was conducted due to its improved sensitivity in detection in comparison to the single-step PCR (Pitman *et al*., 2011; Beard *et al*., 2012). This chapter assesses and evaluates: (1) PCR results and (2) accuracy of the 3% iodine starch test (IST) by comparing the staining results with PCR.

4.2 Materials and Methods

4.2.1 DNA isolation and extraction

All 28 tuber and leaf samples (Chapter 3) collected, were frozen with liquid nitrogen and subsequently ground into fine particles for DNA extraction, with a sterilised mortar and pestle (autoclaved at 121°C). The ground samples were stored in 1.7 ml Eppendorf tubes at -20°C until further processing was required.

DNA of each tuber and leaf sample was extracted using the Chelex® resin method (Henderson *et al*., 2019). A sterile scoopula was used to remove approximately 1 mm^3 of the sample which was then suspended in 300 µL of 10% Chelex solution (Chelex®100 resin, 50-100 mesh, sodium form, Bio-Rad), in a 1.7 mL Eppendorf tube. The suspension was vortexed for 2 sec and incubated at 100°C for 10 min on a heating block (Total Lab-Systems Ltd). Following this, vapour pressure inside the tube was released, the suspension vortexed again and subsequently incubated at 100°C for a further 10 min. The mixture was then

centrifuged at 12,300 X *g* for 10 min and 150 µl of the resulting supernatant was transferred into a 1.7 ml tube. DNA quality and yield concentration was measured using the NanoDrop spectrophotometer (NanoDrop Lite, Thermo Scientific) and stored at -20°C until used.

DNA ng/µl value from the Nanodrop output was used to dilute the concentration to a 10 ng/µl in a 50 µl sample. NanoDrop spectrophotometer (NanoDrop Lite, Thermo Scientific) was used to confirm the concentration of DNA to 10±2 ng/µl.

4.2.2 PCR amplification

The presence or absence of CaLso in each leaf and tuber sample was made from PCR amplification using the primers OA2 (5' GCGCTTATTTTTAATAGGAGCGGCA 3') and OI2c (5' -GCCTCGCGACTTCGCAACCCAT 3') (Liefting *et al.,* 2008) in a single-step PCR. Primers Lib16S01F (5' TTCTACGGGATAACGCACGG 3') and Lib16S01R (5' CGTCAGTATCAGGCCAGTGAG 3') (Liefting *et al.,* 2009a) were subsequently used in a nested PCR. Amplification Protocol outlined by Pitman *et al.* (2011) was followed to run the PCR.

4.2.2.1 Single-step PCR

A single step PCR was performed using primers OA2 and OI2c to amplify a fragment from the 16S rRNA gene region of the bacteria CaLso (Pitman *et al*., 2011). PCR was performed in a total reaction volume of 20 µL containing 10 µl of Dream Taq (Green PCR Masters Mix; Thermo Scientific), 0.2 µl of each 10 µM primer (Final concentration 0.1 µM; Integrated DNA Technologies PTE, Singapore), 2 µl of DNA (10 ng/µl) and 7.6 µl of ultra-pure water (Life Technologies, Thermo Fisher Scientific Inc., USA). A non-template control was included for each reaction to check for contamination.

PCR was performed in a Sensoquest PCR thermal cycler (Biomedizinische Elektronik) with the following amplification conditions: Initial denaturation at 95°C for 5 min, followed by 35 cycles of denaturation at 95°C for 30s, annealing at 66°C for 30s, and extension at 72°C for 1 min and a final extension step of 72°C for 10 minutes (Pitman *et al.,* 2011). PCR products were subjected to electrophoresis on a 1% agarose gel (Bioline, Bioline USA Inc., USA) stained with GelRed R (Nucleic Acid stain, 10,000X in water (Biotium)), and was undertaken in a 0.5 x TBE buffer at 90 V for 30 min. The product size was visualised with

the aid of a 1 kb plus DNA ladder (InvitrogenTM, Life Technologies, Thermo Fisher Scientific Inc., USA). The expected product size was 1160 base pair (bp) (Pitman *et al*., 2011)

4.2.2.2 Nested PCR

Following the first round of PCR using the OA2 and OI2c primers, a nested PCR was performed using the primer Lib16S01F and Lib16S01R to produce an amplification of 580 bp (Liefting *et al.,* 2009a and Pitman *et al.,* 2011). PCR was performed in a total reaction volume of 20 µL containing 10 µl of Dream Taq (Green PCR Masters Mix; Thermo Scientific), 0.2 µl of each 10 µM primer (Final concentration 0.1 µM; Integrated DNA Technologies PTE, Singapore), 1 µl from the first PCR reaction as template and 8.6 µl of ultra-pure water (Life Technologies, Thermo Fisher Scientific Inc., USA). A non-template control was included for each reaction to check for contamination. Pitman *et al.* (2011), used 1 µl (of a 1 in 20 dilution) from the single-step PCR product as a template, but in this experiment 1 µl from the first reaction was directly used as the results obtained showed no difference (Appendix B, Table 5).

The PCR was performed in Sensoquest PCR thermal cycler (Biomedizinische Elektronik) with the following amplification conditions: Initial denaturation at Initial denaturation at 95°C for 5 min, followed by 35 cycles of denaturation at 95°C for 30s, annealing at 66°C for 30s, and extension at 72°C for 1 min and a final extension step of 72°C for 10 minutes (adapted from Pitman *et al.,* 2011). PCR products were subjected to electrophoresis on a 1% agarose (Bioline, Bioline USA Inc., USA) stained with GelRed R (Nucleic Acid stain, 10,000X in water (Biotium)), and was undertaken in a 0.5 x TBE buffer at 90 V for 30 min. The product size was visualised with the aid of a 1 kb plus DNA ladder (InvitrogenTM, Life Technologies, Thermo Fisher Scientific Inc., USA). The expected product size was 580 bp (Pitman *et al*., 2011).

The following samples were sent for sequencing at the Lincoln University Sequencing Facility: the single-step PCR product of the inner tuber region of ZC-symptomatic sample 1, nested PCR product of the outer tuber region of ZC-symptomatic sample 1 and nested PCR product of the outer tuber region of the visibly healthy-looking plant sample 4 (Appendix B). The chromatographs obtained were viewed using Geneious Prime 2021.2 (Biomatters, New Zealand). The sequences obtained from the single-step PCR product of the inner tuber

region of ZC-symptomatic sample 1, nested PCR product of the outer tuber region of ZC-symptomatic sample 1 and nested PCR product of the outer tuber region of the healthy looking plant sample 4 were trimmed to 955 bp, 571 bp and 582 bp respectively to remove any inconclusive regions and ambiguous nucleotides submitted during contig alignment. Basic Local Alignment Search Tool (BLAST) in the GenBank nucleotide database from the National Center of Biotechnology Information website (NCBI; www.ncbi.nlm.nih.gov) was used to BLAST the consensus sequences of the contig alignment against other sequences obtained within the BLAST.

Similar steps were followed, to check for the presence or absence of CaLso using a single-step and nested PCR in the midrib and petiolule of visibly healthy (presumably uninfected) and CaLso infected potato plants.

4.3 Results

Leaf lamina and tubers of the 24 plant samples

4.3.1.1 Identification of CaLso

An average 260/280 ratio of 1.3 was obtained from the nanodrop results of the extracted DNA of leaves and tubers from each sample. From the gel electrophoresis results, the single-step PCR yielded a fragment amplification between 1,000 bp and 1,500 bp (Figure 4.1-A). This amplification was observed in only 6 out of 8 ZC-symptomatic samples (only tubers). The second round of amplification, using the nested PCR resulted in a 580 bp amplification (Figure 4.1-B) in 7 out of 8 ZC-symptomatic samples (only tubers) and a 700 bp amplification (Figure 4.1-C) in 2 out of 8 healthy looking plant samples (only tubers). No amplification of fragments from the DNA of *R. solani* symptomatic potato tubers were observed. No amplification was seen in any of the leaf samples from either the single-step nor nested PCR.

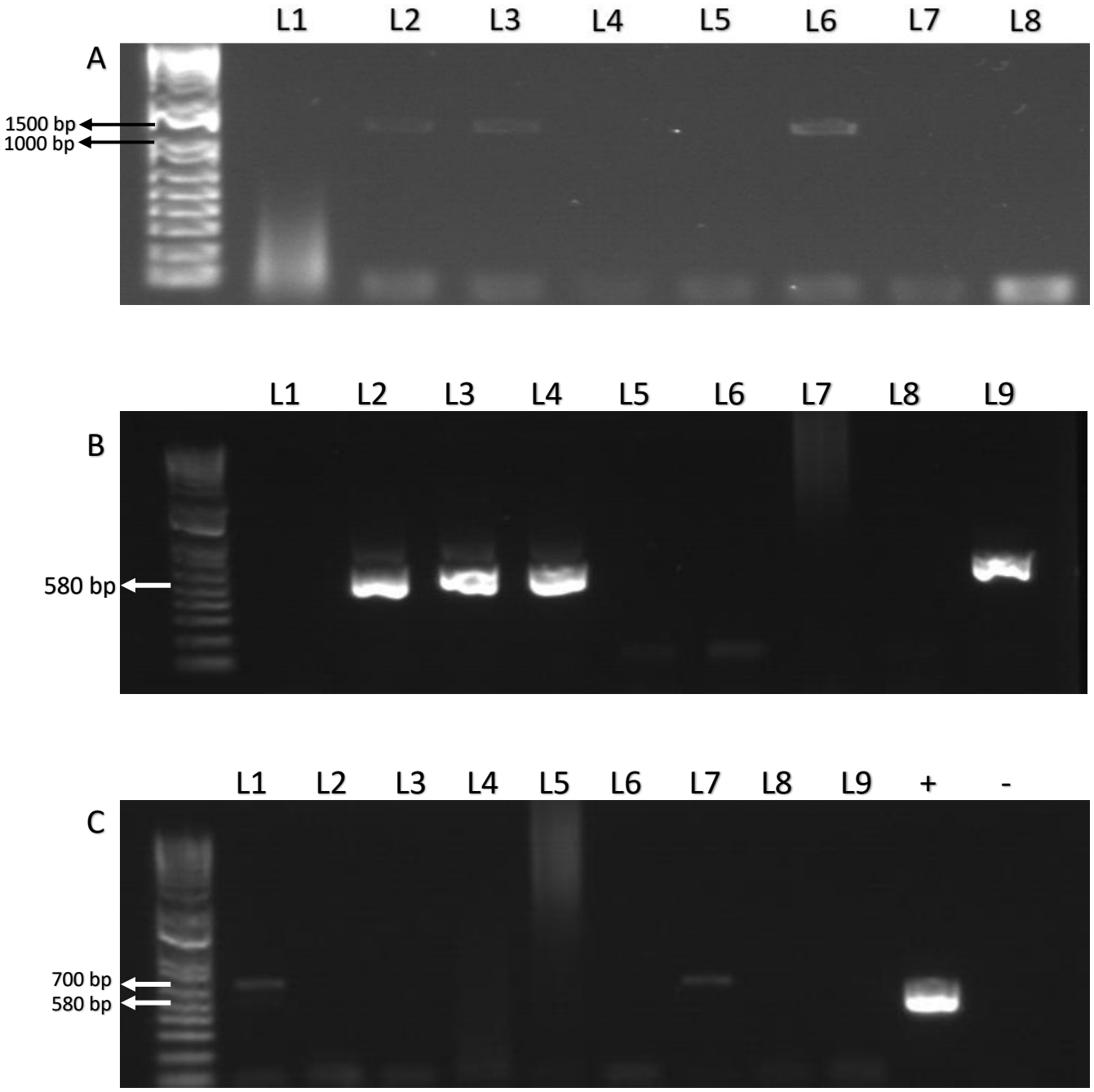

Figure 4.1. Agarose gel electrophoresis results of: (**A**) Single-step PCR products amplified from the DNA extracts of tuber and leaf lamina of ZC-symptomatic samples with primers OA2 and OI2c (Lane 1, 4 and 7 are of leaf lamina samples 1, 2 and 3; Lane 2, 3, 5, 6 and 8 are outer and inner region of tuber samples 1, 2 and 3); (**B**) Nested PCR products amplified from DNA extracts of ZC-symptomatic tubers and leaf lamina with primers Lib16S01F and Lib16S01R (Lane 1, 6 and 7 are of leaf lamina samples of sample 6, 7 and 8; Lane 2, 3, 4, 5, 8 and 9 are outer and inner region of tuber samples 6, 7 and 8). The agarose gels show an amplification product

between 1000bp and 1,600 bp for the single-step PCR (**A**) and 580 bp for the nested PCR (B). The agarose gel electrophoresis of nested PCR (**C**) products from DNA extracts of visibly healthy-looking plant tubers (Lane 1: outer tuber region of sample 1; lane 7: outer tuber region of sample 4) with primers Lib16S01F and Lib16S01R, show an amplification of 700bp. In image **C**, lanes 2-6, 8 and 9 are nested PCR products of tubers and leaf samples from visibly healthy looking plants, + denotes the positive control and – denotes the negative control. All amplifications were assessed with a 1 kb plus ladder.

Sequences produced had a high similarity to the sequence of CaLso within NCBI (Table 4.1). The amplified product between 1,000 bp - 1,500 bp region from the single-step PCR showed a >98.75 % identity, 580 bp region from the nested PCR showed a >99.82% identity and the 700bp region from the nested PCR showed an identity of 98.80 % to CaLso (Table 4.1).

Table 4.1. BLASTn results showing high similarity (>98%) of the amplified regions of the single-step and nested PCR to CaLso.

PCR product used for sequencing	Description	Query length	Query Cover	Gaps	Identity	Accession
Single-step PCR product (1,000 bp – 1,500 bp amplification) of ZC-symptomatic plant, sample 1 (inner tuber region)	A new 'Candidatus Liberibacter' species in *Solanum betaceum* (tamarillo) and *Physalis peruviana* (cape gooseberry) in New Zealand	955	100%	1% (11/957)	98.85%	EU935004.1
	Candidatus Liberibacter solanacearum isolate AB171 16S ribosomal RNA gene, partial sequence		100%	1% (11/957)	98.85%	MH843709.1

	Candidatus Liberibacter solanacearum clone OR-psyllids-1 16S ribosomal RNA gene, partial sequence		100%	1% (11/957)	98.75%	JX624245.1
Nested PCR product (700 bp) of healthy-looking plant, Sample 4 (outer tuber region)	*Candidatus* Liberibacter solanacearum strain FI 15-108 16S ribosomal RNA gene, partial sequence	582	99%	0% (5/583)	98.80%	MG701016.1
	Candidatus Liberibacter solanacearum clone OR-psyllids-1 16S ribosomal RNA gene, partial sequence		99%	0% (5/583)	98.80%	JX624245.1
Nested PCR product (580 bp) of ZC-symptomatic plant, Sample 1 (outer tuber region)	*Candidatus* Liberibacter solanacearum clone OR-psyllids-1 16S ribosomal RNA gene, partial sequence	571	100%	0% (0/570)	100%	JX624245.1
	Candidatus Liberibacter solanacearum strain 16-004 16S ribosomal RNA gene, partial sequence		99%	0% (0/570)	99.82%	MG701016.1

4.3.1.2 Comparing PCR product sequences against previous studies

Edited sequences from single-step PCR product of ZC-symptomatic sample 1 (inner tuber region) showed substantial differences in nucleotides arrangement when compared to sequences from accessions, JX624245.1 (Nelson *et al*., 2013), EU935004.1 (Liefting *et al*., 2008) (the sequence length was trimmed to 1,281 bp from 2,073 bp as the consensus of the sequenced sample was 955 bp long) and HM246509.2 (Pitman *et al*., 2011), using muscle alignment in Geneious Prime 2021.2 (Biomatters, New Zealand) (Figure 4.2). Similarly, the edited sequences from the nested PCR products, ZC-symptomatic sample 1 (outer tuber region) (**Figure 4.3**) and healthy looking plant sample 4 (outer tuber region) (Figure 4.4) aligned (multiple alignment tool in Geneious Prime 2021.2 (Biomatters, New Zealand)) with sequences from accessions JX624245.1 (Nelson *et al*., 2013), MG701016.1 (Haapalainen *et al*., 2018) and HM246509 (Pitman *et al*., 2011), showed one and six differences in nucleotide arrangement respectively. Some minor differences in nucleotides arrangement amongst the sequences obtained from the accessions were also observed from the alignment results (Figure. 4.2, 4.3 and 4.4).

```
                          10         20         30         40         50         60
Consensus ZC_1_ITR  CAGCCCTATA AAGACCCAAC ATCTAGATAA AATC--TAAA CTTGATGGCA ACTAGAGGTA
JX624245.1          ---------- --GCGCTTAT TTTTA-ATAG GAGCGGCAGA CGGGTGAGTA ACGCGTGGGA
EU935004.1          CATGCAAGTC GAGCGCTTAT TTTTA-ATAG GAGCGGCAGA CGGGTGAGTA ACGCGTGGGA
MH843709.1          ---------C GAGCGCTTAT TTTTA-ATAG GAGCGGCAGA CGGGTGAGTA ACGCGTGGGA
Pitman Accession    ---------- --GCGCTTAT TTTTA-ATAG GAGCGGCAGA CGGGTGAGTA ACGCGTGGGA
                      ** *** * *  ** ** * * *  *   * * * *** *   ** *** *    ** *  *
                          70         80         90         100        110        120
Consensus ZC_1_ITR  ---------- ------GGGG TTGCGCTCGT TGCGGGACTT AACCCAACAT CT--CACGAC
JX624245.1          ATCTACCTTT TTCTACGGGA TAACGCACG- ---GAAACGT GTGCTAATAC CGTATACGCC
EU935004.1          ATCTACCTTT TTCTACGGGA TAACGCACG- ---GAAACGT GTGCTAATAC CGTATACGCC
MH843709.1          ATCTACCTTT TTCTACGGGA TAACGCACG- ---GAAACGT GTGCTAATAC CGTATACGCC
Pitman Accession    ATCTACCTTT TTCTACGGGA TAACGCACG- ---GAAACGT GTGCTAATAC CGTATACGCC
                    ********** ******   *  **   *  * *** **  *  *** *  * *  ****   **
```

```
                          130        140        150        160        170        180
Consensus ZC_1_ITR  ACGAGCTGAC GACAGCCATG C--------- ---AGCACCT GT-------- ----------
JX624245.1          CTGAGAAGGG GAAAGATTTA TTGGAGAGAG ATGAGCCCGC GTTAGATTAG CTAGTTGGTG
EU935004.1          CTGAGAAGGG GAAAGATTTA TTGGAGAGAG ATGAGCCCGC GTTAGATTAG CTAGTTGGTG
MH843709.1          CTGAGAAGGG GAAAGATTTA TTGGAGAGAG ATGAGCCCGC GTTAGATTAG CTAGTTGGTG
Pitman Accession    CTGAGAAGGG GAAAGATTTA TTGGAGAGAG ATGAGCCCGC GTTAGATTAG CTAGTTGGTG
                    **   ** **   *  *** * ********** ***   * **   ******** **********

                          190        200        210        220        230        240
Consensus ZC_1_ITR  --ATAAAGGT CTCCGAAAAG AAAATACCAT CTCTGAT--- --------AT CGTCCTCTAT
JX624245.1          GGGTAAATGC CTACCAAGGC TACGATCTAT AGCTGGTCTG AGAGGACGAT CAGCCACACT
EU935004.1          GGGTAAATGC CTACCAAGGC TACGATCTAT AGCTGGTCTG AGAGGACGAT CAGCCACACT
MH843709.1          GGGTAAATGC CTACCAAGGC TACGATCTAT AGCTGGTCTG AGAGGACGAT CAGCCACACT
Pitman Accession    GGGTAAATGC CTACCAAGGC TACGATCTAT AGCTGGTCTG AGAGGACGAT CAGCCACACT
                    ***    * *   * *  *** * **** *   **   * *** ********    **  * **

                          250        260        270        280        290        300
Consensus ZC_1_ITR  ATGTCAAGGG CTGG---TAA GGTTCTGCGC GTTGCATCGA --------AT TAAACCACAT
JX624245.1          GGGACTGAGA CACGGCCCAG ACTCCTACGG GAGGCAGCAG TGGGGAATAT TGGACAATGG
EU935004.1          GGGACTGAGA CACGGCCCAG ACTCCTACGG GAGGCAGCAG TGGGGAATAT TGGACAATGG
MH843709.1          GGGACTGAGA CACGGCCCAG ACTCCTACGG GAGGCAGCAG TGGGGAATAT TGGACAATGG
Pitman Accession    GGGACTGAGA CACGGCCCAG ACTCCTACGG GAGGCAGCAG TGGGGAATAT TGGACAATGG
                    ** * *** *  ** **** * ** *  *  *  **   * ** ********    **  * ***

                          310        320        330        340        350        360
Consensus ZC_1_ITR  GCTCCACCGC TTGTGCGGGC ---CCCCGTC AAT------- TCCTTTGAGT TTTAA---TC
JX624245.1          GGGCAACC-C TGATCCAGCC ATGCCGCGTG AGTGAAGAAG GCCTTAGGGT TGTAAAGCTC
EU935004.1          GGGCAACC-C TGATCCAGCC ATGCCGCGTG AGTGAAGAAG GCCTTAGGGT TGTAAAGCTC
MH843709.1          GGGCAACC-C TGATCCAGCC ATGCCGCGTG AGTGAAGAAG GCCTTAGGGT TGTAAAGCTC
Pitman Accession    GGGCAACC-C TGATCCAGCC ATGCCGCGTG AGTGAAGAAG GCCTTAGGGT TGTAAAGCTC
                     ** *   *   ** * * *  ***  *      * ******* *    * *    *   ***
```

```
                          370        380        390        400        410        420
Consensus ZC_1_ITR  TTGC------ ---------G ACCGTACTCC CCAGGCGGAG T----GCTTA ATGCGT----
JX624245.1          TTTCGCCGGA GAAGATAATG ACGGTA-TCC GGAGAAGAAG TCCCGGCTAA CTTCGTGCCA
EU935004.1          TTTCGCCGGA GAAGATAATG ACGGTA-TCC GGAGAAGAAG TCCCGGCTAA CTTCGTGCCA
MH843709.1          TTTCGCCGGA GAAGATAATG ACGGTA-TCC GGAGAAGAAG TCCCGGCTAA CTTCGTGCCA
Pitman Accession    TTTCGCCGGA GAAGATAATG ACGGTA-TCC GGAGAAGAAG TCCCGGCTAA CTTCGTGCCA
                      * ****** *********    *   *    **  ** *    ****   *  * *   ****

                          430        440        450        460        470        480
Consensus ZC_1_ITR  -TAGCTGCGC CACT--GAAT GGTAAAACCA ----CCCCAA CAGCTAGCAC TCATCGTTTA
JX624245.1          GCAGCCGCGG TAATACGAAG GGGGCGAGCG TTGTTCGGAA TAACTGG--- ---GCGTAAA
EU935004.1          GCAGCCGCGG TAATACGAAG GGGGCGAGCG TTGTTCGGAA TAACTGG--- ---GCGTAAA
MH843709.1          GCAGCCGCGG TAATACGAAG GGGGCGAGCG TTGTTCGGAA TAACTGG--- ---GCGTAAA
Pitman Accession    GCAGCCGCGG TAATACGAAG GGGGCGAGCG TTGTTCGGAA TAACTGG--- ---GCGTAAA
                    **   *   * * * **   *   **** * * ***** **   * *  ********** * **

                          490        500        510        520        530        540
Consensus ZC_1_ITR  CAGCGTGGAC TACCAGGGTA TCTAAATCCT GTTTGCTCCC CACGCTTTCG CGCCTCAGCG
JX624245.1          GGGCGCG--- TAGGCGGGTA ATTAAGTTAG GGGTGAAATC C-------CA AGGCTCAACC
EU935004.1          GGGCGCG--- TAGGCGGGTA ATTAAGTTAG GGGTGAAATC C-------CA AGGCTCAACC
MH843709.1          GGGCGCG--- TAGGCGGGTA ATTAAGTTAG GGGTGAAATC C-------CA AGGCTCAACC
Pitman Accession    GGGCGCG--- TAGGCGGGTA ATTAAGTTAG GGGTGAAATC C-------CA AGGCTCAACC
                    **   * ***   ***      **   * ***  **  ****   ******* * * *    * *

                          550        560        570        580        590        600
Consensus ZC_1_ITR  TCAGTATCAG GCCCAGTGAG CCCGCCTTCG CCACTGGGTG TTC------- ----------
JX624245.1          T--------- ------TGGA ACTGCCTTTA ATACTGGTTA TCTAGAGTTT AGGAGAGGTG
EU935004.1          T--------- ------TGGA ACTGCCTTTA ATACTGGTTA TCTAGAGTTT AGGAGAGGTG
MH843709.1          T--------- ------TGGA ACTGCCTTTA ATACTGGTTA TCTAGAGTTT AGGAGAGGTG
Pitman Accession    T--------- ------TGGA ACTGCCTTTA ATACTGGTTA TCTAGAGTTT AGGAGAGGTG
                     ********* ******  ** * *     ** **     * *  ********* **********
```

```
                          610        620        630        640        650        660
Consensus ZC_1_ITR  -------CTC CCGAAATATC TGCGAATTTC ACCTCTACAC TCNGGAATTC CA--------
JX624245.1          AGTGGAATTC CGAGTGTAGA GGTGAAATTC GCAGATATTC GGAGGAACAC CAGTGGCGAA
EU935004.1          AGTGGAATTC CGAGTGTAGA GGTGAAATTC GCAGATATTC GGAGGAACAC CAGTGGCGAA
MH843709.1          AGTGGAATTC CGAGTGTAGA GGTGAAATTC GCAGATATTC GGAGGAACAC CAGTGGCGAA
Pitman Accession    AGTGGAATTC CGAGTGTAGA GGTGAAATTC GCAGATATTC GGAGGAACAC CAGTGGCGAA
                    ********    *****  ** * *   *    * ***  *** ***    **    ********

                          670        680        690        700        710        720
Consensus ZC_1_ITR  -----CTCAC CTCTCCTAAA CTCTAGAT-- ---------- ---------- AACCAGTATT
JX624245.1          GGCGGCTCAC TGGCCTGATA CTGACGCTGA GGCGCGAAAG CGTGGGGAGC AAACAGGATT
EU935004.1          GGCGGCTCAC TGGCCTGATA CTGACGCTGA GGCGCGAAAG CGTGGGGAGC AAACAGGATT
MH843709.1          GGCGGCTCAC TGGCCTGATA CTGACGCTGA GGCGCGAAAG CGTGGGGAGC AAACAGGATT
Pitman Accession    GGCGGCTCAC TGGCCTGATA CTGACGCTGA GGCGCGAAAG CGTGGGGAGC AAACAGGATT
                    *****      **** ** *    *** * ** ********** **********   *   *

                          730        740        750        760        770        780
Consensus ZC_1_ITR  AAA------G GCAGTTC--- ----CAAGGT TGAGCCTTGG ---------G ATTT------
JX624245.1          AGATACCCTG GTAGTCCACG CTGTAAACGA TGAGTGCTAG CTGTTGGGTG GTTTACCATT
EU935004.1          AGATACCCTG GTAGTCCACG CTGTAAACGA TGAGTGCTAG CTGTTGGGTG GTTTACCATT
MH843709.1          AGATACCCTG GTAGTCCACG CTGTAAACGA TGAGTGCTAG CTGTTGGGTG GTTTACCATT
Pitman Accession    AGATACCCTG GTAGTCCACG CTGTAAACGA TGAGTGCTAG CTGTTGGGTG GTTTACCATT
                     * ******   *   * *** *****  * *     *** *  *********  *   ******

                          790        800        810        820        830        840
Consensus ZC_1_ITR  ------CACC CCTAAC---T TAATTAC-CC GCCTA----- ------CGCG CCCTTTACGC
JX624245.1          CAGTGGCGCA GCTAACGCAT TAAGCACTCC GCCTGGGGAG TACGGTCGCA AGATTAAAAC
EU935004.1          CAGTGGCGCA GCTAACGCAT TAAGCACTCC GCCTGGGGAG TACGGTCGCA AGATTAAAAC
MH843709.1          CAGTGGCGCA GCTAACGCAT TAAGCACTCC GCCTGGGGAG TACGGTCGCA AGATTAAAAC
Pitman Accession    CAGTGGCGCA GCTAACGCAT TAAGCACTCC GCCTGGGGAG TACGGTCGCA AGATTAAAAC
                    ****** * * *     ***     **  *      ******* ******   * ***  * **
```

```
                          850        860        870        880        890        900
Consensus ZC_1_ITR  CC--AGTTAT T--------- CCGAACAA-C GCTCGCCCCC TTCGTATTA- CCGCGGCTGC
JX624245.1          TCAAAGGAAT TGACGGGGGC CCGCACAAGC GGTGGAGCAT GTGGTTTAAT TCGATGCAAC
EU935004.1          TCAAAGGAAT TGACGGGGGC CCGCACAAGC GGTGGAGCAT GTGGTTTAAT TCGATGCAAC
MH843709.1          TCAAAGGAAT TGACGGGGGC CCGCACAAGC GGTGGAGCAT GTGGTTTAAT TCGATGCAAC
Pitman Accession    TCAAAGGAAT TGACGGGGGC CCGCACAAGC GGTGGAGCAT GTGGTTTAAT TCGATGCAAC
                    * **  **    *********    *    *   * * ***** * *  * * * *  **  **

                          910        920        930        940        950        960
Consensus ZC_1_ITR  TGGCACGAAG TTAGCCGGGA CTTCTTCTCC GGATACCGTC ATTA------ -TCTTCTCCG
JX624245.1          GCGCA-GAAC CTTACCAGCC CTTGACATAT AGAGGACGAT ATCAGAGATG GTATTTTCTT
EU935004.1          GCGCA-GAAC CTTACCAGCC CTTGACATAT AGAGGACGAT ATCAGAGATG GTATTTTCTT
MH843709.1          GCGCA-GAAC CTTACCAGCC CTTGACATAT AGAGGACGAT ATCAGAGATG GTATTTTCTT
Pitman Accession    GCGCA-GAAC CTTACCAGCC CTTGACATAT AGAGGACGAT ATCAGAGATG GTATTTTCTT
                    **   *   * * **  * **    **** ** *  ***  **   * ****** * *  *  **

                          970        980        990        1000       1010       1020
Consensus ZC_1_ITR  GCGAAAGAGC TTTACA---- -ACCCTAAGG CCTTCTTCAC TCACGCGGCA TG----GCTG
JX624245.1          TTCGGAGACC TTTATACAGG TGCTGCATGG CTGTCGTCA- GCTCGTGTCG TGAGATGTTG
EU935004.1          TTCGGAGACC TTTATACAGG TGCTGCATGG CTGTCGTCA- GCTCGTGTCG TGAGATGTTG
MH843709.1          TTCGGAGACC TTTATACAGG TGCTGCATGG CTGTCGTCA- GCTCGTGTCG TGAGATGTTG
Pitman Accession    TTCGGAGACC TTTATACAGG TGCTGCATGG CTGTCGTCA- GCTCGTGTCG TGAGATGTTG
                    *****   *      * **** ** *** *    **  *   * ***  * *     **** *

                          1030       1040       1050       1060       1070       1080
Consensus ZC_1_ITR  GATCAGGGTT GCCCCCATTG TCCAATATTC CCCACTGCTG CCTCCCGTAG -----GAGTC
JX624245.1          GGTTAAG--- --TCCCG--- --CAACGAGC GCAACCCCTA CCTCTAGTTG CCATCGAGTT
EU935004.1          GGTTAAG--- --TCCCG--- --CAACGAGC GCAACCCCTA CCTCTAGTTG CCATCAAGTT
MH843709.1          GGTTAAG--- --TCCCG--- --CAACGAGC GCAACCCCTA CCTCTAGTTG CCATCAAGTT
Pitman Accession    GGTTAAG--- --TCCCG--- --CAACGAGC GCAACCCCTA CCTCTAGTTG CCATCAAGTT
                     * * * *** ***   **** **   ****  * *  *** *     **  *  ******   *
                                                                                  +
```

```
                          1090       1100       1110       1120       1130       1140
Consensus ZC_1_ITR  TGGGCCGTGT CTCAGTCCCA G--------- ------TGTG GCTGATCGTC CTCTCAGACC
JX624245.1          TAGATTTTAT CTAGATGTTG GGTACTTTAT AGGGACTGCC GGTGATAATC CG---GAGGA
EU935004.1          TAGATTTTAT CTAGATGTTG GGTACTTTAT AGGGACTGCC GGTGATAATC CG---GAGGA
MH843709.1          TAGATTTTAT CTAGATGTTG GGTACTTTAT AGGGACTGCC GGTGATAATC CG---GAGGA
Pitman Accession    TAGATTTTAT CTAGATGTTG GGTACTTTAT AGGGACTGCC GGTGATAATC CG---GAGGA
                     * **** *    *** ****  ********* ******  **  *    **    *********

                          1150       1160       1170       1180       1190       1200
Consensus ZC_1_ITR  AGCTATAGA- ---------- --TCGTAGCC TTGGTAGGCA TTTACCCCAC CAACTAGCTA
JX624245.1          AGGTGGGGAT GACGTCAAGT CCTCATGGCC CTTATGGGC- --TGGGCTAC ACACGTGCTA
EU935004.1          AGGTGGGGAT GACGTCAAGT CCTCATGGCC CTTATGGGC- --TGGGCTAC ACACGTGCTA
MH843709.1          AGGTGGGGAT GACGTCAAGT CCTCATGGCC CTTATGGGC- --TGGGCTAC ACACGTGCTA
Pitman Accession    AGGTGGGGAT GACGTCAAGT CCTCATGGCC CTTATGGGC- --TGGGCTAC ACACGTGCTA
                      * ***  * ********** **  * *    * ** *   * ** *** *   **  **

                          1210       1220       1230       1240
Consensus ZC_1_ITR  ATCTAACGCG GGCTCATCTC TCTCCAAT-- ------AAAT CTTTCCCC
JX624245.1          ---CAATGGT GG-------- -TTACAATGG GTTGCGAAGT CGCGAGGC
EU935004.1          ---CAATGGT GG-------- -TTACAATGG GTTGCGAAGT CGCGAGGC
MH843709.1          ---CAATGGT GG-------- -TTACAATGG GTTGCGAAGT CGCGAGGC
Pitman Accession    ---CAATGGT GG-------- -TTACAATGG GTTGCGAAGT CGCGAGGC
                    ****  * **   ******** ** *    ** ******  *   ******
```

Figure 4.2. Muscle alignment sequencing results of Consensus ZC_1_ITR (Single-step PCR product of ZC-symptomatic sample 1 inner tuber region (trimmed and edited to 955 from 1,220 bp)) in comparison to accessions JX624245.1 (Nelson *et al.*, 2013), EU935004.1 (Liefting *et al.*, 2008) and HM246509.2 (Pitman *et al.*, 2011). * Denotes the difference between sample 1 and the stated accession sequences; + denotes the difference between accession sequence.

```
                                10         20         30         40         50         60
JX624245.1                ATAACGCACG GAAACGTGTG CTAATACCGT ATACGCCCTG AGAAGGGGAA AGATTTATTG
MG701016.1                ATAACGCACG GAAACGTGTG CTAATACCGT ATACGCCCTG AGAAGGGGAA AGATTTATTG
HM246509.2                ATAACGCACG GAAACGTGTG CTAATACCGT ATACGCCCTG AGAAGGGGAA AGATTTATTG
Consensus ZC_1_OTR        ATAACGCACG GAAACGTGTG CTAATACCGT ATACGCCCTG AGAAGGGGAA AGATTTATTG

                                70         80         90         100        110        120
JX624245.1                GAGAGAGATG AGCCCGCGTT AGATTAGCTA GTTGGTGGGG TAAATGCCTA CCAAGGCTAC
MG701016.1                GAGAGAGATG AGCCCGCGTT AGATTAGCTA GTTGGTGGGG TAAATGCCTA CCAAGGCTAC
HM246509.2                GAGAGAGATG AGCCCGCGTT AGATTAGCTA GTTGGTGGGG TAAATGCCTA CCAAGGCTAC
Consensus ZC_1_OTR        GAGAGAGATG AGCCCGCGTT AGATTAGCTA GTTGGTGGGG TAAATGCCTA CCAAGGCTAC

                                130        140        150        160        170        180
JX624245.1                GATCTATAGC TGGTCTGAGA GGACGATCAG CCACACTGGG ACTGAGACAC GGCCCAGACT
MG701016.1                GATCTATAGC TGGTCTGAGA GGACGATCAG CCACACTGGG ACTGAGACAC GGCCCAGACT
HM246509.2                GATCTATAGC TGGTCTGAGA GGACGATCAG CCACACTGGG ACTGAGACAC GGCCCAGACT
Consensus ZC_1_OTR        GATCTATAGC TGGTCTGAGA GGACGATCAG CCACACTGGG ACTGAGACAC GGCCCAGACT

                                190        200        210        220        230        240
JX624245.1                CCTACGGGAG GCAGCAGTGG GGAATATTGG ACAATGGGGG CAACCCTGAT CCAGCCATGC
MG701016.1                CCTACGGGAG GCAGCAGTGG GGAATATTGG ACAATGGGGG CAACCCTGAT CCAGCCATGC
HM246509.2                CCTACGGGAG GCAGCAGTGG GGAATATTGG ACAATGGGGG CAACCCTGAT CCAGCCATGC
Consensus ZC_1_OTR        CCTACGGGAG GCAGCAGTGG GGAATATTGG ACAATGGGGG CAACCCTGAT CCAGCCATGC

                                250        260        270        280        290        300
JX624245.1                CGCGTGAGTG AAGAAGGCCT TAGGGTTGTA AAGCTCTTTC GCCGGAGAAG ATAATGACGG
MG701016.1                CGCGTGAGTG AAGAAGGCCT TAGGGTTGTA AAGCTCTTTC GCCGGAGAAG ATAATGACGG
HM246509.2                CGCGTGAGTG AAGAAGGCCT TAGGGTTGTA AAGCTCTTTC GCCGGAGAAG ATAATGACGG
Consensus ZC_1_OTR        CGCGTGAGTG AAGAAGGCCT TAGGGTTGTA AAGCTCTTTC GCCGGAGAAG ATAATGACGG
```

```
                                310        320        330        340        350        360
JX624245.1                TATCCGGAGA AGAAGTCCCG GCTAACTTCG TGCCAGCAGC CGCGGTAATA CGAAGGGGGC
MG701016.1                TATCCGGAGA AGAAGTCCCG GCTAACTTCG TGCCAGCAGC CGCGGTAATA CGAAGGGGGC
HM246509.2                TATCCGGAGA AGAAGTCCCG GCTAACTTCG TGCCAGCAGC CGCGGTAATA CGAAGGGGGC
Consensus ZC_1_OTR        TATCCGGAGA AGAAGTCCCG GCTAACTTCG TGCCAGCAGC CGCGGTAATA CGAAGGGGGC

                                370        380        390        400        410        420
JX624245.1                GAGCGTTGTT CGGAATAACT GGGCGTAAAG GGCGCGTAGG CGGGTAATTA AGTTAGGGGT
MG701016.1                GAGCGTTGTT CGGAATAACT GGGCGTAAAG GGCGCGTAGG CGGGTAATTA AGTTAGGGGT
HM246509.2                GAGCGTTGTT CGGAATAACT GGGCGTAAAG GGCGCGTAGG CGGGTAATTA AGTTAGGGGT
Consensus ZC_1_TR         GAGCGTTGTT CGGAATAACT GGGCGTAAAG GGCGCGTAGG CGGGTAATTA AGTTAGGGGT

                                430        440        450        460        470        480
JX624245.1                GAAATCCCAA GGCTCAACCT TGGAACTGCC TTTAATACTG GTTATCTAGA GTTTAGGAGA
MG701016.1                GAAATCCCAA GGCTCAACCT TGGAACTGCC TTTAATACTG GTTATCTAGA GTTTAGGAGA
HM246509.2                GAAATCCCAA GGCTCAACCT TGGAACTGCC TTTAATACTG GTTATCTAGA GTTTAGGAGA
Consensus ZC_1_OTR        GAAATCCCAA GGCTCAACCT TGGAACTGCC TTTAATACTG GTTATCTAGA GTTTAGGAGA

                                490        500        510        520        530        540
JX624245.1                GGTGAGTGGA ATTCCGAGTG TAGAGGTGAA ATTCGCAGAT ATTCGGAGGA ACACCAGTGG
MG701016.1                GGTGAGTGGA ATTCCGAGTG TAGAGGTGAA ATTCGCAGAT ATTCGGAGGA ACACCAGTGG
HM246509.2                GGTGAGTGGA ATTCCGAGTG TAGAGGTGAA ATTCGCAGAT ATTCGGAGGA ACACCAGTGG
Consensus ZC_1_OTR        GGTGAGTGGA ATTCCGAGTG TAGAGGTGAA ATTCGCAGAT ATTCGGAGGA ACACCAGTGG
```

```
                                  550        560        570
JX624245.1                CGAAGGCGGC TCACTGGCCT GATACTGACG C
MG701016.1                CGAAGGCGGC TCACTGGCCT GATACTGACG C
HM246509.2                CGAAGGCGGC TCACTGGCCT GATACTGACG C
Consensus ZC_1_OTR        CGAAGGCGGC TCACTGGCCT GATACTGACG A
                                                          *
```

Figure 4.3. Geneious multiple alignment sequencing results of Consensus ZC_1_OTR (Nested PCR product of ZC-symptomatic sample 1 outer tuber region (trimmed and edited from 582 bp to 571bp)) in comparison to accessions JX624245.1 (Nelson *et al*., 2013), MG701016.1 (Haapalainen *et al*., 2018) and HM246509 (Pitman *et al*., 2011). * Denotes the difference between sample 1 and the stated accession sequences**.**

```
                          10         20         30         40         50         60
Consensus ZC_4_OTR TTTCTACGGG ATAACGCACG GAATCGTGTG CTAATACCGT ATACGCCCTG AGAAGGGGAA
JX624245.1         TTTCTACGGG ATAACGCACG GAAACGTGTG CTAATACCGT ATACGCCCTG AGAAGGGGAA
MG701016.1         TTTCTACGGG ATAACGCACG GAAACGTGTG CTAATACCGT ATACGCCCTG AGAAGGGGAA
HM246509.2         TTTCTACGGG ATAACGCACG GAAACGTGTG CTAATACCGT ATACGCCCTG AGAAGGGGAA

                          70         80         90         100        110        120
Consensus ZC_4_OTR AGATTTATTG CGAGAGAGAT GAGCCCGCGT TAGATTAGCT AGTTGTGTGG GGTAAATGCC
JX624245.1         AGATTTATTG -GAGAGAGAT GAGCCCGCGT TAGATTAGCT AGTTG-GTGG GGTAAATGCC
MG701016.1         AGATTTATTG -GAGAGAGAT GAGCCCGCGT TAGATTAGCT AGTTG-GTGG GGTAAATGCC
HM246509.2         AGATTTATTG -GAGAGAGAT GAGCCCGCGT TAGATTAGCT AGTTG-GTGG GGTAAATGCC
                             *                                       *
                          130        140        150        160        170        180
Consensus ZC_4_OTR TACCAAGGCT ACGATCTATA GCTGGTCTGA GAGGACGATC AGCCACACTG GGACTGAGAC
JX624245.1         TACCAAGGCT ACGATCTATA GCTGGTCTGA GAGGACGATC AGCCACACTG GGACTGAGAC
MG701016.1         TACCAAGGCT ACGATCTATA GCTGGTCTGA GAGGACGATC AGCCACACTG GGACTGAGAC
HM246509.2         TACCAAGGCT ACGATCTATA GCTGGTCTGA GAGGACGATC AGCCACACTG GGACTGAGAC

                          190        200        210        220        230        240
Consensus ZC_4_OTR ACGGCCCAGA CTCCTACGGG AGGCAGCAGT GGGGAATATT GGACAATGGG GGCAACCCTG
JX624245.1         ACGGCCCAGA CTCCTACGGG AGGCAGCAGT GGGGAATATT GGACAATGGG GGCAACCCTG
MG701016.1         ACGGCCCAGA CTCCTACGGG AGGCAGCAGT GGGGAATATT GGACAATGGG GGCAACCCTG
HM246509.2         ACGGCCCAGA CTCCTACGGG AGGCAGCAGT GGGGAATATT GGACAATGGG GGCAACCCTG

                          250        260        270        280        290        300
Consensus ZC_4_OTR ATCCAGCCAT GCCGCGTGAG TGAAGAAGGC CTTAGGGTTG TAAAGCTCTT TCGCCGGAGA
JX624245.1         ATCCAGCCAT GCCGCGTGAG TGAAGAAGGC CTTAGGGTTG TAAAGCTCTT TCGCCGGAGA
MG701016.1         ATCCAGCCAT GCCGCGTGAG TGAAGAAGGC CTTAGGGTTG TAAAGCTCTT TCGCCGGAGA
HM246509.2         ATCCAGCCAT GCCGCGTGAG TGAAGAAGGC CTTAGGGTTG TAAAGCTCTT TCGCCGGAGA
```

```
                          310        320        330        340        350        360
Consensus ZC_4_OTR AGATAATGAC GGTATCCGGA GAAGAAGTCC CGGCTAACTT CGTGCCAGCA GCCGCGGTAA
JX624245.1         AGATAATGAC GGTATCCGGA GAAGAAGTCC CGGCTAACTT CGTGCCAGCA GCCGCGGTAA
MG701016.1         AGATAATGAC GGTATCCGGA GAAGAAGTCC CGGCTAACTT CGTGCCAGCA GCCGCGGTAA
HM246509.2         AGATAATGAC GGTATCCGGA GAAGAAGTCC CGGCTAACTT CGTGCCAGCA GCCGCGGTAA

                          370        380        390        400        410        420
Consensus ZC_4_OTR TACGAAGGGG GCGAGCGTTG TTCGGAATAA CTGGGCGTAA AGGGCGCGTA GGC-GGTAAT
JX624245.1         TACGAAGGGG GCGAGCGTTG TTCGGAATAA CTGGGCGTAA AGGGCGCGTA GGCGGGTAAT
MG701016.1         TACGAAGGGG GCGAGCGTTG TTCGGAATAA CTGGGCGTAA AGGGCGCGTA GGCGGGTAAT
HM246509.2         TACGAAGGGG GCGAGCGTTG TTCGGAATAA CTGGGCGTAA AGGGCGCGTA GGCGGGTAAT
                                                                           *
                          430        440        450        460        470        480
Consensus ZC_4_OTR TAAGTTAGGG GTGAAATCCC AAGGCTCAAC CTTGGAACTG CCTTTAATAC TGGTTATCTA
JX624245.1         TAAGTTAGGG GTGAAATCCC AAGGCTCAAC CTTGGAACTG CCTTTAATAC TGGTTATCTA
MG701016.1         TAAGTTAGGG GTGAAATCCC AAGGCTCAAC CTTGGAACTG CCTTTAATAC TGGTTATCTA
HM246509.2         TAAGTTAGGG GTGAAATCCC AAGGCTCAAC CTTGGAACTG CCTTTAATAC TGGTTATCTA

                          490        500        510        520        530        540
Consensus ZC_4_OTR GAGTTTAGGA GAGGTGAGTG GAATTCCGAG TGTAGAGGTG AAATTCGCAG ATATTCGGAG
JX624245.1         GAGTTTAGGA GAGGTGAGTG GAATTCCGAG TGTAGAGGTG AAATTCGCAG ATATTCGGAG
MG701016.1         GAGTTTAGGA GAGGTGAGTG GAATTCCGAG TGTAGAGGTG AAATTCGCAG ATATTCGGAG
HM246509.2         GAGTTTAGGA GAGGTGAGTG GAATTCCGAG TGTAGAGGTG AAATTCGCAG ATATTCGGAG
```

```
                          550        560        570        580
Consensus ZC_4_OTR GAACACCAGT GGCGAAGG-G GATCACTGGC CTGATAACTG ACGA
JX624245.1         GAACACCAGT GGCGAAGGCG GCTCACTGGC CTGAT-ACTG ACGC
MG701016.1         GAACACCAGT GGCGAAGGCG GCTCACTGGC CTGAT-ACTG ACGC
HM246509.2         GAACACCAGT GGCGAAGGCG GCTCACTGGC CTGAT-ACTG ACGC
                                      *                  *        *
```

Figure 4.4. Geneious multiple alignment results of Consensus HL_4_OTR (Nested PCR product of visibly healthy-looking plant sample 4 outer tuber region (trimmed and edited from 589 bp to 582)) in comparison to accessions JX624245.1 (Nelson *et al*., 2013), MG701016.1 (Haapalainen *et al*., 2018) and HM246509.2 (Pitman *et al*., 2011). * Denotes the difference between sample 1 and the stated accession sequences.

4.3.1.3 Comparison between PCR and IST

None of the leaf samples produced a positive result for CaLso. Of the 100% (n=8) stained leaf samples from the ZC-symptomatic plants, none (n=0) tested positive for the presence of CaLso from the single-step and the subsequent nested PCR. Similarly, no CaLso was detected in the leaf samples of *R. solani* symptomatic nor visibly healthy-looking plants (Table 4.2).

Table 4.2. Comparison between 3% IST staining of leaf lamina samples from ZC-symptomatic, *R. solani*-symptomatic and visibly healthy-looking plants, with the single-step and nested PCR results.

Sample	Sample Number	Iodine Result [1]	Single step PCR [a]	Nested PCR [a]
ZC-symptomatic plants	1	+	-	-
	2	+	-	-
	3	+	-	-
	4	+	-	-
	5	+	-	-
	6	+	-	-
	7	+	-	-
	8	+	-	-
Rhizoctonia solani symptomatic plants	1	-	-	-
	2	-	-	-
	3	-	-	-
	4	-	-	-
	5	-	-	-
	6	-	-	-
	7	+	-	-
	8	-	-	-
Visibly healthy-looking plants	1	-	-	-
	2	+	-	-
	3	-	-	-
	4	-	-	-
	5	-	-	-
	6	+	-	-
	7	-	-	-

	8	-		-		-

Note : [1] Positive or negative results denoted as +/–, respectively. Samples with no staining on the leaf lamina were considered negative.

[a] Positive or negative results denoted as +/–, respectively. Samples with no visual band displayed on an agarose gel were considered negative. The primers used were adapted from Pitman *et al*. (2011).

PCR amplification product from each tuber sample was produced. Of the 100% (n=8) ZC-symptomatic tubers that stained with 3% iodine solution, 87.5% (n=7) tested positive for CaLso. Of the eight *R. solani* symptomatic tubers, none were positive for CaLso. However, one stained tuber was suspect as it did stain blackish-purple between the vascular traces and the periderm. With regards to the healthy-looking plants, 2 false-negatives (no staining but PCR-positive) and 2 false-positives (stained but PCR-negative) were observed (Table 4.3). The nested PCR appeared to be 12.5% more sensitive in CaLso detection when compared to the single-step PCR.

Table 4.3. Comparison between 3% IST staining of tuber samples from ZC-symptomatic, *Rhizoctonia solani* symptomatic and healthy-looking plants with single-step and nested PCR results.

Sample	Sample Number	Iodine Result [1]	Single step PCR [a]		Nested PCR [a]	
			Outer Region	Inner Region	Outer Region	Inner Region
Liberibacter symptomatic plants	1	+	+	+	+	+
	2	+	-	+	-	+
	3	+	+	-	+	-
	4	+	-	-	-	-
	5	+	+	-	+	+
	6	+	+	+	+	+
	7	+	-	+	-	+
	8	+	-	-	-	+
Rhizoctonia solani symptomatic plants	1	-	-	-	-	-
	2	-	-	-	-	-
	3	-	-	-	-	-
	4	-	-	-	-	-
	5	-	-	-	-	-
	6	-	-	-	-	-

	7	+	-	-	-	-
	8	-	-	-	-	-
Visibly healthy-looking plants	1	-	-	-	+	-
	2	+	-	-	-	-
	3	-	-	-	-	-
	4	-	-	-	+	-
	5	-	-	-	-	-
	6	+	-	-	-	-
	7	-	-	-	-	-
	8	-	-	-	-	-

Note: [1] Positive or negative results denoted as +/–, respectively. Samples with no staining on the leaf lamina were considered negative.

[a] Positive or negative results denoted as +/–, respectively. Samples with no visual band displayed on an agarose gel were considered negative. The primers used were adapted from Pitman *et al*. (2011).

4.3.2 Leaf midrib and petiolule

The leaf lamina, midribs and petiolule of the uninfected and CaLso infected plants did not show the presence of CaLso with amplification in the single-step PCR with primers, OA2 and OI2c. Only the CaLso infected petiolule sample (Appendix A and B), showed a 580 base pair amplification from the nested PCR.

4.4 Discussion

4.4.1 PCR results

The average 260/280 ratio value of 1.3, yielded by the Chelex extraction method is observed to be less than the optimum 1.8 (Gupta, 2019). This value indicates that the sample might have a lesser titre of the DNA and might also have a protein contamination (Gupta, 2019) and as such, alternative extraction techniques could have been utilised. The gel electrophoresis results from the single step PCR using primers OA2 and OI2c showed an amplification between 1,000 bp and 1,500 bp. Editing and BLASTn of sequence, yielded a 955 bp product, that showed a >98.75% identity to *Candidatus* Liberibacter solanacearum (CaLso) (Table 4.1). The length of 955bp is less than 1,160bp observed by Pitman *et al.* (2011) and Liefting *et al.* (2008). However, the sequencing results confirm its identity as CaLso. Thus, it can be concluded that all 6 samples, that showed an amplification, between 1,000 bp and 1,500 bp, were positive for CaLso.

With regards to the nested PCR results, all ZC-symptomatic tubers showed an amplification of around 580 bp except sample 7, and the 2 false-negative samples from the visibly healthy-looking plants that showed an amplification of about 700 bp. In comparison to the 700 bp, the 580 bp amplification is similar to the nested PCR results presented in the study by Pitman *et al*. (2011) and Liefting *et al*. (2009). However, editing and megablasting the 700 bp and 580 bp nested PCR products yielded 582 bp and 571 bp sequences, that showed a >99.82% and 98.80% identity to CaLso respectively (Table 4.1). Possible reasons for the 700 bp amplification could either be due to contamination of genomic DNA or carryover of PCR product. However, the latter cannot be true as the sequencing results showed an identity to CaLso with no indication of contamination.

Furthermore, the comparative results of the edited sequences from the single step and nested PCR products, with that of the previous studies (Figure 4.2, 4.3 and 4.4), showed that the 955 bp sequence had more discrepancies in nucleotide arrangement in comparison to the 582 bp and 571 bp. The inconsistency observed in the 955 bp sequence with previous studies made it uncertain to confirm CaLso identity. But, the high similarity with one nucleotide difference in the 571 bp edited sequence and three difference in nucleotide arrangement along the 582 bp edited sequence comparisons, help in confirming the identity of the amplified product to CaLso. The difference in nucleotide arrangement along sequences from previous studies used for comparison were also observed (Figure 4.2). However, the reason for this observation is not known and will need to be investigated in future studies.

From the gel electrophoresis results, primer dimers and smearing of amplified DNA were also observed. Some possible reasons for primers dimers could either be, that the primer concentration is high, or the primers possess complementary overlapping sequences. The latter could be the reason, as the Mastermix prepared for the single-step PCR used [0.1 µM] of each primer, as opposed to [0.2 µM] used by Pitman *et al*., (2011). If the primers did possess complementary overlapping sequences, it could be rectified by increasing the annealing temperature (Apte & Daniel 2009) in future studies. Another possible reason for primer dimers could be because of the MgCl concentration in the Mastermix. However, this could not be adjusted in this study as the Dream Taq used for the PCR assays had a pre-allocated MgCl concentration. With regards to the smearing of amplified DNA, a few

possible reasons could include, too much DNA was loaded on the gel, the template DNA added to each PCR product prepared could have been more, the annealing temperature was low, thermal cycling conditions were not optimal for the thermal cycler, primer concentration was too high, extension time was too high, or the DNA template quality was low (Roux 2009). In future studies, to optimise the gel results with no smearing, preliminary trials with different conditions mentioned above will need to be tested out to obtain optimized results. Similarly, in some of the gels (Appendix B) from the single step PCR, the position of the amplified band between 1,000 bp and 1,500 bp is not clearly seen and can vary. An example of this can be seen on gel images A and B of Figure 1 in Appendix B. Here, the amplification observed on Lane 3 (Appendix B, Figure. 1-A), appears to be in-between 1000 bp and 1500 bp, while in Lane 3 (Appendix B, Figure. 1-B) it appears to be above 1500 bp. This observation can either be due to the different loading quantities on the gel of the 1kb+ ladder (2 µl) and the PCR product (3 µl), or difference in density of the PCR product with respect to the gel, or a human error in loading the PCR product incorrectly into the lane of the gel. Though the exact reason is not known for this observation, in future studies, this can be solved by conducting preliminary tests by amplifying PCR products with different loading quantities and different gel weights. Thus, it can be concluded that each reaction is a unique experiment and the optimal conditions required to generate a product can vary. Also, understanding the variables in a reaction will greatly enhance troubleshooting efficiency, and thus increase the chance in obtaining the desired result (Lorenz 2012).

In each nested PCR reaction, the PCR products of the single-step PCR were used as the template for the second round of amplification. This PCR method had been proven to have a higher detection sensitivity than other molecular detection assays, in diagnosing diseases (Hong *et al*., 2019). This statement is further supported by the results from this study, where a 12.5 % increase in CaLso detection sensitivity is observed using nested PCR in comparison to the single-step PCR. Furthermore, this observation is similar to that observed in the study by Liefting *et al.* (2009) and Pitman *et al*. (2011), where nested PCR presented an increased sensitivity in detecting CaLso in potato plants. This increased sensitivity in using the nested PCR can be attributed to the two sets of primers used, and the two rounds of PCR performed (Ding *et al*., 2017; Lam *et al*., 2007).

4.4.2 Comparison of PCR and 3% Iodine Starch Test

None of the leaves tested by PCR were positive for CaLso. Of the 8 ZC-symptomatic tubers that stained with 3% Iodine solution, 7 tubers tested positive for CaLso by PCR. These results indicate that the IST is 87.5% accurate for ZC-symptomatic plants, but it is expected that increased accuracy will be achieved with larger sample numbers. Future research is implicated. With regards to *R. solani*-symptomatic plants, all tubers tested negative for CaLso by PCR, including the one sample that stained blackish-purple (Appendix A). This false positive made the IST 12.5% inaccurate with regards to *R. solani*-symptomatic plants. With regards to the visibly healthy plant samples, two tubers, that stained blackish-purple, did not test positive for CaLso with PCR, making them false-positives. Furthermore, two tubers that did not stain blackish-purple, tested positive by PCR for CaLso, making them false negatives.

All false-positive samples (ZC-symptomatic tuber 4, *R. solani*-symptomatic tuber 7 and visibly healthy plant tubers 2 and 6 (Appendix A)) suggested the presence of starch (possibly amylopectin) in the leaves and tubers through the dark blackish-purple stain from the iodine starch test (Chapter 3), with no presence of CaLso from PCR results. This observation could be ascribed to the bacteria's life cycle, the anatomical changes occurring in the leaf as a consequence of CaLso infection and the titre of CaLso in the plant.

Once a potato plant is infected with CaLso, it takes approximately 7 days for the bacterium to translocate from the infected leaves to the main stem through the phloem vessels (Levy *et al*., 2011). Similar to CLas infected Citrus trees (Etxeberria *et al*., 2009; Folimonova and Achor, 2010; Schneider, 1968), visible symptoms of starch accumulation will most likely occur only after damage has occurred to the phloem vessels during CaLso movement from source (leaves) to sink (tubers and roots) in the plant. Damage to phloem vessels will most likely impair the movement of sucrose from the source leaves to the tubers or roots, leading to high starch accumulation in the aerial parts of the plant (Levy *et al*., 2011; Gao *et al*., 2016). Thus, for starch accumulation to occur, the bacterium would need to have moved from the leaves to the stem causing phloem vessel damage. It is also important to note that during the process of symptom development, CaLso are unevenly distributed within the vascular system (Levy *et al*., 2011) with titre levels potentially varying

throughout the plant (Gao *et al*., 2016). Furthermore, they could be unevenly distributed throughout the growing season similar to CLas in citrus trees (Gonzalez *et al*., 2012).

In this study, the samples used were collected from open fields with no specific date of infection. Thus, implying that any of the plant samples could have been infected at any point of time before sampling. In a scenario where a plant is infected 7 days or more prior to sampling is sufficient time for the bacteria to move from the leaves and into the stem, causing phloem vessel damage in the stem and increasing starch content. Furthermore, this could also mean that the bacterium has moved from the leaves and is in the stem. In this potential scenario, CaLso is not present in the stem nor in the tubers, but has caused phloem vessel damage causing starch accumulation. A similar observation for the stated scenario is seen in Etxeberria et al. (2009), where plugging of phloem tissue along the stem resulted in the accumulation of starch in leaves acropetally from the initial CLas-infected leaf, likely resulting in symptomatic leaves without DNA signal above the initial infection point. Furthermore, CaLso could be unevenly distributed in the phloem vessels of the plant in low titre and not be present in the leaves or tubers that were used for detection in PCR. Another supporting observation to the above-mentioned hypothesis is the dark blackish-purple colour stain observed in these false positive samples (Chapter 3). A previous study by Braun *et al*. (2016), showed that a nitrogen deficiency led to increased starch accumulation in potato (‘Asterix’ and 'Atlantic’) leaves. This aspect should be considered in future studies.

The only potential explanation for the two false-negatives (no staining but PCR-positive) results could be that the leaf sample selected from the potato plant were from a secondary stem, which might not have yet been infected with CaLso. The false negative and false positive misclassification need to be further examined in future studies to perfect the IST.

With regards to plant sampling for PCR, study by Wen *et al.* (2009) with 12 ZC-symptomatic potato plants collected from commercial fields in the United States and Mexico from 2005 through 2008, found CaLso detection in plant stolons, stems and petioles to higher, when compared to midribs with a minimum detection and no detection in leaf samples. CaLso in the study was done using a single-step PCR with primers OA2 and OI2c. However, in the same study CaLso in leaf samples were detected using a real-time/quantitative PCR and a

conventional PCR with primers LpFrag4- 1611F/480R. Pitman *et al*. (2011), was also able to detect CaLso in leaf samples of ZC infected potato leaves using a nested PCR (Lib16S01F and Lib16S01R primers). Though, in this study a nested PCR was performed, CaLso was unable to be detected, in any of the 24 samples used in the study. The bacterium, however, was detected in the petiolule from nested PCR, in the leaf sample from a CaLso infected potato plant (section 4.3.2). Thus, sample selection of tubers, stolons and stems, and improved detection techniques will need to be considered to improve PCR efficiency in future studies.

With regards to tuber sampling for PCR detection, a piece from the inner region with less staining (peri-medullary region) and the outer region with more staining (vascular region) were selected. The results showed that the CaLso can vary within tubers, as, in some samples CaLso was detected in both the outer and inner region (e.g. ZC-symptomatic sample 1), while in some, it is detected only in the inner (e.g. ZC-symptomatic sample 2) and outer region respectively (e.g. ZC-symptomatic sample 3) (Table 4.3). Thus, it can be stated that the bacterium is not limited to only the vascular bundle in the tuber region as discussed in section 3.4.1. For future studies, it is recommended that a radial cross-section from the peri-medullary region through to the periderm (Figure 2.3) be taken for PCR testing to increase detection efficiency. Furthermore, these results also indicate that the difference in staining colour is possibly influenced by CaLso, as 63.64% of samples that showed a dark blackish-purple staining tested positive and 84.62% of samples that showed a faint blueish-purple stain tested negative with PCR (Table 4.3). This, however, will need to be evaluated in future studies. Also, it is also recommended that this study be conducted on different potato cultivars, as only 'Russet Burbank' was used in this study.

4.4.3 Leaf midrib and petiolule results

The petiolule of the CaLso-infected potato plant tested positive for CaLso, indicating that the 3% IST works. The staining observed along the phloem region of the midrib (Figure 3.9 A) and on the petiolule (Figure 3.9-B), suggests that CaLso caused phloem vessel damage leading to the accumulation of starch in the aerial parts of the plant as it moves from the infected leaves to the stem through the phloem, but future research efforts would need to confirm this. Furthermore, the correlation between the staining colour of dark blackish-

purple in CaLso-positive plants is consistent. This, again could indicate the presence of excess amylopectin in the accumulated starch grains, as discusses in Chapter 3, but future studies are implicated.

5 GENERAL DISCUSSION AND CONCLUSIONS

Results from this study confirmed that the 3% IST is 87.5% accurate in detecting CaLso when potato plants are symptomatic of ZC and 12.5% inaccurate (showed staining but were PCR negative) when symptomatic of *Rhizoctonia solani*. The false-positives and false-negatives observed with visibly healthy-looking plants, made the 3% IST less accurate on symptomless plants, but this is less of a concern as roguing of a small number of healthy looking false positives is an insignificant economic loss, thus erring on the side of caution. With regards to the PCR analysis, CaLso was never detected in leaves of any samples, despite some testing positive for CaLso in the tubers. This suggests that future studies should sample tubers, and specifically radial sections from the peri-medullary region through to the periderm. Although single-step PCR and nested PCR were useful in this study, more accurate detection methods such as qPCR might improve detection sensitivity (Wen *et al.,* 2009). Furthermore, leaf and the tuber samples used for PCR assay in this study were sampled from the stained region which included iodine. This iodine contamination may have played a role as a PCR inhibitor and future investigation should examine this aspect. Research on different DNA extraction methods in human forensics found that PowerClean® DNA Clean-Up kit and DNA IQ™ System were more successful than the Chelex®-100 method (Hu *et al*., 2015) in removing PCR inhibitors. Future research should also investigate this aspect, but also iodine-free samples should be tested by PCR.

In this study, the 3% IST was not 100% accurate, but for a rapid field bioassay, the sensitivity is more than adequate and will enable timely and efficient roguing of plants. This would reduce the primary source of inoculum. Potato leaflets rather than tubers should be stained due to ease of sampling and accuracy of the stain (87.5%). Furthermore, destructive sampling of tubers by digging can be avoided when leaves do not stain blackish-purple. With false-negatives, the bioassay will not negatively impact the economics of the potato paddock.

Where epidemiology of ZC is concerned, future research should consider optimizing the staining efficiencies of asymptomatic plants, to determine how long (days) it will take for a leaf on a secondary stem to stain once the pant is infected with CaLso. With regards to the samples that were *R. solani*-symptomatic, the staining and PCR results rid the myth

amongst the Canterbury growers in New Zealand, that *R. solani* symptomatic potato plants are a precursor to CaLso. However, it will need to be further confirmed with more samples with greenhouse trials in future studies. The samples termed *R. solani* symptomatic in this study were based on their visual symptom and were not confirmed with PCR.

Results from this study confirm that a rapid field bioassay using 3% iodine can be used to determine CaLso infection in potato plants. Armed with this information, growers, fieldman and scouts will be able to accurately identify and immediately rogue infected potato plants, including tubers, thus preventing the build-up, and spread of CaLso. Furthermore, adjacent plants can also be tested inexpensively and rogued if necessary. All this will have a major positive effect on the need for chemical control in Canterbury, New Zealand, and the excessive number of insecticidal sprays will be reduced from the current 18, per growing season.

ACKNOWLEDGEMENTS

I would like to thank my supervisor Dr Clive Kaiser and co-supervisor Dr Seona Casonato for advising and guiding me throughout this study. I have also learnt the importance of paying attention to detail while doing research, and also the importance of keeping on track with the study to complete it on time.

I would like to thank Professor Hamish Gow (Agribusiness and Commerce, Lincoln University) for his assistance in initially setting up the study. Roger Blyth (Seed and field services South Island Ltd, Canterbury, New Zealand) is acknowledged for helping with gathering the potato samples for this study.

I would also like to thank Sarah Cairns (Research Technician, Lincoln University, New Zealand) for helping and guiding me perform the PCR assays in this study, Ping Ying Koay (Research Technician, Lincoln University, New Zealand) for assisting in collecting CaLso leaves for the iodine testing, and Norma Merrick for helping in sequencing the PCR results.

Finally, I would like to thank my family, friends, and my girlfriend Suhasna Palihakkara for supporting and helping me throughout the year.

REFERENCES

Achor, D., Etxeberria, E., Wang, N., Folimonova, S., Chung, K., & Albrigo, L. (2010). Sequence of anatomical symptom observations in citrus affected with huanglongbing disease. *Plant Pathol. J, 9*(2), 56-64.

Alfaro-Fernández, A., Verdeguer, M., Rodríguez-León, F., Ibáñez, I., Hernández, D., Teresani, G. R., Bertolini, E., Cambra, M., & Font, M. I. (2017b). Search for reservoirs of '*Candidatus* Liberibacter solanacearum'and mollicutes in weeds associated with carrot and celery crops. *European Journal of Plant Pathology, 147*(1), 15-20.

Alvarado, V. Y., Odokonyero, D., Duncan, O., Mirkov, T. E., & Scholthof, H. B. (2012). Molecular and physiological properties associated with zebra complex disease in potatoes and its relation with *Candidatus* Liberibacter contents in psyllid vectors. *PLoS One, 7*(5), e37345.

Apte, A., & Daniel, S. (2009). PCR primer design. *Cold Spring Harbor Protocols, 2009*(3), pdb. ip65.

Artschwager, E. F. (1918). Anatomy of the potato plant, with special reference to the ontogeny of the vascular. *Journal of Agricultural Research, 14*, 221.

Ashworth, R. (1963). Investigations into Midvein Anatomy and Ontogeny of Certain Species of the Genus Ilex L. *Journal of the Elisha Mitchell Scientific Society, 79*(2), 126-138.

Barnes, A.-M., Taylor, N., & Vereijssen, J. (2015). Non-crop host plants: prime real estate for the tomato potato psyllid in New Zealand. *New Zealand Plant Protection, 68*, 441.

Beard, S., Pitman, A., Kraberger, S., & Scott, I. (2013). SYBR Green real-time quantitative PCR for the specific detection and quantification of '*Candidatus* Liberibacter solanacearum'in field samples from New Zealand. *European Journal of Plant Pathology, 136*(1), 203-215.

Bertolini, E., Cambra, M., Serra, P., López, M., Lopes, S., Duran-Vila, N., Ayres, J., & Bové, J. (2010). Direct procedures for specific detection of '*Candidatus* Liberibacter'spp. using immobilized targets and real-time PCR and detection kit. *Spanish patent, 201001157*.

Bové, J. M. (2006). Huanglongbing: a destructive, newly-emerging, century-old disease of citrus. *Journal of plant pathology*, 7-37.

Brown, C. (2005). Antioxidants in potato. *American journal of potato research, 82*(2), 163-172.

Buchman, J. L., Fisher, T. W., Sengoda, V. G., & Munyaneza, J. E. (2012). Zebra chip progression: from inoculation of potato plants with liberibacter to development of disease symptoms in tubers. *American journal of potato research, 89*(2), 159-168.

Buchman, J. L., Sengoda, V. G., & Munyaneza, J. E. (2011). Vector transmission efficiency of liberibacter by *Bactericera cockerelli* (Hemiptera: Triozidae) in zebra chip potato disease: effects of psyllid life stage and inoculation access period. *Journal of Economic Entomology, 104*(5), 1486-1495.

Campos, H., & Ortiz, O. (2020). *The potato crop: its agricultural, nutritional and social contribution to humankind*. Springer Nature. https://doi.org/

Casteel, C. L., Hansen, A. K., Walling, L. L., & Paine, T. D. (2012). Manipulation of plant defense responses by the tomato psyllid (Bactericerca cockerelli) and its associated endosymbiont *Candidatus* Liberibacter psyllaurous. *PLoS One, 7*(4), e35191.

Casteel, C. L., Hansen, A. K., Walling, L. L., & Paine, T. D. (2012). Manipulation of plant defense responses by the tomato psyllid (Bactericerca cockerelli) and its associated endosymbiont *Candidatus* Liberibacter psyllaurous. *PLoS One, 7*(4), e35191.

Cating, R. A., Rondon, S. I., & Hamm, P. B. (2015). High-fidelity PCR improves the detection of '*Candidatus* Liberibacter solanacearum'in potato tubers. *American journal of potato research, 92*(3), 451-454.

Chaffey, N. (2014). *Raven biology of plants* (8 ed., Vol. 113). https://doi.org/doi:10.1093/aob/mcu090

Cicero, J. M., Fisher, T. W., Qureshi, J. A., Stansly, P. A., & Brown, J. K. (2017). Colonization and intrusive invasion of potato psyllid by '*Candidatus* Liberibacter solanacearum'. *Phytopathology, 107*(1), 36-49.

Cooper, W. R., Alcala, P. E., & Barcenas, N. M. (2015). Relationship between plant vascular architecture and within-plant distribution of '*Candidatus* Liberibacter solanacearum'in potato. *American journal of potato research, 92*(1), 91-99.

Cooper, W. R., Horton, D. R., Miliczky, E., Wohleb, C. H., & Waters, T. D. (2019). The weed link in zebra chip epidemiology: Suitability of non-crop Solanaceae and Convolvulaceae to potato psyllid and "*Candidatus* Liberibacter solanacearum". *American journal of potato research, 96*(3), 262-271.

Cooper, W. R., Sengoda, V. G., & Munyaneza, J. E. (2014). Localization of '*Candidatus* Liberibacter solanacearum'(Rhizobiales: Rhizobiaceae) in *Bactericera cockerelli* (Hemiptera: Triozidae). *Annals of the Entomological Society of America, 107*(1), 204-210.

Crosslin, J., Hamm, P., Eggers, J., Rondon, S., Sengoda, V., & Munyaneza, J. (2012a). First report of zebra chip disease and "*Candidatus* Liberibacter solanacearum" on potatoes in Oregon and Washington State.

Crosslin, J., Olsen, N., & Nolte, P. (2012b). First report of zebra chip disease and "*Candidatus* Liberibacter solanacearum" on potatoes in Idaho. *Plant Disease, 96*(3), 453-453.

Cruzado, R. K., Rashidi, M., Olsen, N., Novy, R. G., Wenninger, E. J., Bosque-Pérez, N. A., Karasev, A. V., Price, W. J., & Rashed, A. (2020). Effect of the level of "*Candidatus* Liberibacter solanacearum" infection on the development of zebra chip disease in different potato genotypes at harvest and post storage. *PLoS One, 15*(4), e0231973.

Ding, F., Paul, C., Brlansky, R., & Hartung, J. S. (2017). Immune tissue print and immune capture-PCR for diagnosis and detection of *Candidatus* Liberibacter asiaticus. *Scientific Reports, 7*(1), 1-9.

Eng, L. (2008). A presumptive field test for Huanglongbing (Citrus Greening Disease). *Jabatan Pertanian Sarawak*, 1-10.

Esmarch-Bromberg, F. (1919). Contributions to the anatomy of healthy and diseased potato plants. I. *Anatomy of the vegetative organs. Agricultural* Yearb *54* 161-266.

Etxeberria, E., Gonzalez, P., Achor, D., & Albrigo, G. (2009). Anatomical distribution of abnormally high levels of starch in HLB-affected Valencia orange trees. *Physiological and Molecular Plant Pathology, 74*(1), 76-83.

Etxeberria, E., Gonzalez, P., Dawson, W. O., & Spann, T. (2008). An iodine-based starch test to assist in selecting leaves for HLB testing. *EDIS, 2008*(2).

Fedec, P., Ooraikul, B., & Hadziyev, D. (1977). Microstructure of raw and granulated potatoes. *Canadian Institute of Food Science and Technology Journal, 10*(4), 295-306.

Fleischer, H. (2019). The Iodine Test for Reducing Sugars–A Safe, Quick and Easy Alternative to Copper (II) and Silver (I) Based Reagents. *World J Chem Educ, 7*, 45-52.

Frodin, D. G. (2004). History and concepts of big plant genera. *Taxon, 53*(3), 753-776.

Gancarz, M., & Konstankiewicz, K. (2007). Changes of cellular structure of potato tuber parenchyma tissues during storage. *Research in Agricultural Engineering, 53*(2), 75.

Gancarz, M., Konstankiewicz, K., & Zgórska, K. (2014). Cell orientation in potato tuber parenchyma tissue. *International Agrophysics, 28*(1).

Gao, F., Jifon, J., Yang, X., & Liu, T. X. (2009). Zebra chip disease incidence on potato is influenced by timing of potato psyllid infestation, but not by the host plants on which they were reared. *Insect Science, 16*(5), 399-408.

Gao, F., Zhao, Z.-H., Jifon, J., & Liu, T.-X. (2016). Impact of potato psyllid density and timing of infestation on zebra chip disease expression in potato plants. *Plant Protection Science, 52*(4), 262-269.

Garhwal, A. S., Pullanagari, R. R., Li, M., Reis, M. M., & Archer, R. (2020). Hyperspectral imaging for identification of Zebra Chip disease in potatoes. *biosystems engineering, 197*, 306-317.

Gilkes, J. M., Frampton, R. A., Smith, G. R., & Dobson, R. C. (2018). Potential pathogenicity determinants in the genome of '*Candidatus* Liberibacter solanacearum', the causal agent of zebra chip disease of potato. *Australasian Plant Pathology, 47*(2), 119-134.

Glynn, J., Islam, M., Bai, Y., Lan, S., Wen, A., Gudmestad, N., Civerolo, E., & Lin, H. (2012). Multilocus sequence typing of'*Candidatus* Liberibacter solanacearum'isolates from North America and New Zealand. *Journal of plant pathology*, 223-228.

Gonzalez, P., Reyes-De-Corcuera, J., & Etxeberria, E. (2012). Characterization of leaf starch from HLB-affected and unaffected-girdled citrus trees. *Physiological and Molecular Plant Pathology, 79*, 71-78.

Gregory, L. E. (1956). Some factors for tuberization in the potato plant. *American Journal of Botany*, 281-288.

Haapalainen, M. (2014). Biology and epidemics of *Candidatus* Liberibacter species, psyllid-transmitted plant-pathogenic bacteria. *Annals of applied biology, 165*(2), 172-198.

Haapalainen, M., Kivimäki, P., Latvala, S., Rastas, M., Hannukkala, A., Jauhiainen, L., Lemmetty, A., Pirhonen, M., Virtanen, A., & Nissinen, A. I. (2017). Frequency and occurrence of the carrot pathogen '*Candidatus* Liberibacter solanacearum' haplotype C in Finland. *Plant Pathology, 66*(4), 559-570.

Haapalainen, M., Wang, J., Latvala, S., Lehtonen, M. T., Pirhonen, M., & Nissinen, A. (2018). Genetic variation of '*Candidatus* Liberibacter solanacearum' haplotype C and identification of a novel haplotype from Trioza urticae and stinging nettle. *Phytopathology, 108*(8), 925-934.

Harris, K. F., Esbroeck, P.-V., & Duffus, J. E. (1996). Morphology of the sweet potato whitefly, *Bemisia tabaci* (Homoptera, Aleyrodidae) relative to virus transmission. *Zoomorphology, 116*(3), 143-156.

Harrison, K., Tamborindeguy, C., Scheuring, D. C., Herrera, A. M., Silva, A., Badillo-Vargas, I. E., Miller, J. C., & Levy, J. G. (2019). Differences in zebra chip severity between '*Candidatus* Liberibacter solanacearum' haplotypes in Texas. *American journal of potato research, 96*(1), 86-93.

Hawkes, J. (1999). The economic importance of the family Solanaceae. *Solanaceae IV*, 1-8.

He, X., Wratten, S., Zhu, Z., Zhou, W., Emiliano, V., & Gao, Y. (2019). The risk posed by the potato psyllid *Bactericera cockerelli* (Hemiptera: Triozidae) an important invasive pest of solanaceous crops. *Chinese Journal of Applied Entomology, 56*(6), 1422-1429.

Henderson, C., Cripps, M., & Casonato, S. (2019). Distribution of Puccinia punctiformis in above-ground tissue of Cirsium arvense (Californian thistle). *New Zealand Plant Protection, 72*, 265-270.

Henson, J. M., & French, R. (1993). The polymerase chain reaction and plant disease diagnosis. *Annual review of phytopathology, 31*(1), 81-109.

Hong, Y., Luo, Y., Yi, J., He, L., Dai, L., & Yi, T. (2019). Screening nested-PCR primer for '*Candidatus* Liberibacter asiaticus' associated with citrus Huanglongbing and application in Hunan, China. *PLoS One, 14*(2), e0212020.

Howard, R. A. (1974). The stem-node-leaf continuum of the Dicotyledoneae. *Journal of the Arnold Arboretum, 55*(2), 125-181.

Hu, Q., Liu, Y., Yi, S., & Huang, D. (2015). A comparison of four methods for PCR inhibitor removal. *Forensic science international: Genetics, 16*, 94-97.

Huaman, Z. (1986). Systematic botany and morphology of the potato. Technical information bulletin 6. *International Potato Center. Lima-Peru. 12pp*.

Industries, M. o. P. (2022, March 18). *Plant Health and Environment Laboratory tests and charges*. https://www.mpi.govt.nz/science/laboratories/plant-health-and-environment-laboratory/send-a-sample-for-laboratory-testing/tests-and-charges/

Jackson, S. D., James, P., Prat, S., & Thomas, B. (1998). Phytochrome B affects the levels of a graft-transmissible signal involved in tuberization. *Plant Physiology, 117*(1), 29-32.

Jagoueix, S., Bové, J. M., & Garnier, M. (1996). PCR detection of the two *Candidatus* Liberibacter species associated with greening disease of citrus. *Molecular and cellular probes, 10*(1), 43-50.

Kaur, N., Cooper, W. R., Duringer, J. M., Badillo-Vargas, I. E., Esparza-Diaz, G., Rashed, A., & Horton, D. R. (2018). Survival and development of potato psyllid (Hemiptera: Triozidae) on Convolvulaceae: effects of a plant-fungus symbiosis (Periglandula). *PLoS One, 13*(9), e0201506.

Kawabe, K., Truc, N. T. N., Lan, B. T. N., Hong, L. T. T., & Onuki, M. (2006). Quantification of DNA of citrus huanglongbing pathogen in diseased leaves using competitive PCR. *Journal of General Plant Pathology, 72*(6), 355-359.

Keremane, M. L., Ramadugu, C., Rodriguez, E., Kubota, R., Shibata, S., Hall, D. G., Roose, M. L., Jenkins, D., & Lee, R. F. (2015). A rapid field detection system for citrus huanglongbing associated '*Candidatus* Liberibacter asiaticus' from the psyllid vector, *Diaphorina citri* Kuwayama and its implications in disease management. *Crop Protection, 68*, 41-48.

Killiny, N., Hijaz, F., Ebert, T. A., & Rogers, M. E. (2017). A plant bacterial pathogen manipulates its insect vector's energy metabolism. *Applied and environmental microbiology, 83*(5), e03005-03016.

Konstankiewicz, K., Czachor, H., Gancarz, M., Król, A., Pawlak, K., & Zdunek, A. (2002). Cell structural parameter of potato tuber tissue. *International Agrophysics, 16*(2).

Ladd Jr, T., & Rawlins, W. (1965). The effects of the feeding of the potato leafhopper on photosynthesis and respiration in the potato plant. *Journal of Economic Entomology, 58*(4), 623-628.

Lam, W., Yeung, A. C., Tang, J. W., Ip, M., Chan, E. W., Hui, M., & Chan, P. K. (2007). Rapid multiplex nested PCR for detection of respiratory viruses. *Journal of clinical microbiology, 45*(11), 3631-3640.

Levy, J., Ravindran, A., Gross, D., Tamborindeguy, C., & Pierson, E. (2011). Translocation of '*Candidatus* Liberibacter solanacearum', the zebra chip pathogen, in potato and tomato. *Phytopathology, 101*(11), 1285-1291.

Li, W., Abad, J. A., French-Monar, R. D., Rascoe, J., Wen, A., Gudmestad, N. C., Secor, G. A., Lee, M., Duan, Y., & Levy, L. (2009). Multiplex real-time PCR for detection, identification and quantification of '*Candidatus* Liberibacter solanacearum'in potato plants with zebra chip. *Journal of Microbiological Methods, 78*(1), 59-65.

Li, W., Hartung, J. S., & Levy, L. (2007). Evaluation of DNA amplification methods for improved detection of "*Candidatus* Liberibacter species" associated with citrus huanglongbing. *Plant Disease, 91*(1), 51-58.

Liefting, L. W., Sutherland, P. W., Ward, L. I., Paice, K. L., Weir, B. S., & Clover, G. R. (2009a). A new '*Candidatus* Liberibacter'species associated with diseases of solanaceous crops. *Plant Disease, 93*(3), 208-214.

Liefting, L. W., Weir, B. S., Pennycook, S. R., & Clover, G. R. (2009b). '*Candidatus* Liberibacter solanacearum', associated with plants in the family Solanaceae. *International Journal of Systematic and Evolutionary Microbiology, 59*(9), 2274-2276.

Liefting, L., Perez-Egusquiza, Z., Clover, G., & Anderson, J. (2008a). A new '*Candidatus* Liberibacter'species in *Solanum tuberosum* in New Zealand. *Plant Disease, 92*(10), 1474-1474.

Liefting, L., Ward, L., Shiller, J., & Clover, G. (2008). A new '*Candidatus* Liberibacter'species in *Solanum betaceum* (tamarillo) and *Physalis peruviana* (cape gooseberry) in New Zealand. *Plant Disease, 92*(11), 1588-1588.

Lin, T., Lashbrook, C. C., Cho, S. K., Butler, N. M., Sharma, P., Muppirala, U., Severin, A. J., & Hannapel, D. J. (2015). Transcriptional analysis of phloem-associated cells of potato. *BMC genomics, 16*(1), 1-24.

Liu, D., Trumble, J. T., & Stouthamer, R. (2006). Genetic differentiation between eastern populations and recent introductions of potato psyllid (*Bactericera cockerelli*) into western North America. *Entomologia Experimentalis et Applicata, 118*(3), 177-183.

López, M. M., Llop, P., Olmos, A., Marco-Noales, E., Cambra, M., & Bertolini, E. (2009). Are molecular tools solving the challenges posed by detection of plant pathogenic bacteria and viruses? *Current issues in molecular biology, 11*(1), 13-46.

Lorenz, T. C. (2012). Polymerase chain reaction: basic protocol plus troubleshooting and optimization strategies. *JoVE (Journal of Visualized Experiments)*(63), e3998.

MacDaniels, L. H., & Cowart, F. F. (1944). Development and structure of the apple leaf.

Maiden, M. C., Bygraves, J. A., Feil, E., Morelli, G., Russell, J. E., Urwin, R., Zhang, Q., Zhou, J., Zurth, K., & Caugant, D. A. (1998). Multilocus sequence typing: a portable approach to the

identification of clones within populations of pathogenic microorganisms. *Proceedings of the National Academy of Sciences, 95*(6), 3140-3145.

McCauley, M. M., & Evert, R. F. (1988a). The anatomy of the leaf of potato, *Solanum tuberosum* L. 'Russet Burbank'. *Botanical Gazette, 149*(2), 179-195.

McCauley, M. M., & Evert, R. F. (1988b). Morphology and vasculature of the leaf of potato (*Solanum tuberosum*). *American Journal of Botany, 75*(3), 377-390.

Miles, G. P., Samuel, M. A., Chen, J., Civerolo, E. L., & Munyaneza, J. E. (2010). Evidence that cell death is associated with zebra chip disease in potato tubers. *American journal of potato research, 87*(4), 337-349.

Miranda, M. L., & Aguilera, J. M. (2006). Structure and texture properties of fried potato products. *Food Reviews International, 22*(2), 173-201.

Mirmajlessi, S. M., Loit, E., Maend, M., & Mansouripour, S. M. (2015). Real-time PCR applied to study on plant pathogens: potential applications in diagnosis-a review. *Plant Protection Science, 51*(4), 177-190.

Mirmajlessi, S. M., Sjölund, M. J., Mänd, M., Loiseau, M., Ilardi, V., Haesaert, G., Karise, R., Gottsberger, R. A., Sumner-Kalkun, J., & Bertaccini, A. (2019). PCR-based diagnostic methods for '*Candidatus* Liberibacter solanacearum'–Review. *Plant Protection Science, 55*(4), 229-242.

Molki, B., Ha, P. T., Cohen, A. L., Crowder, D. W., Gang, D. R., Omsland, A., Brown, J. K., & Beyenal, H. (2019). The infection of its insect vector by bacterial plant pathogen" *Candidatus* Liberibacter solanacearum" is associated with altered vector physiology. *Enzyme and microbial technology, 129*, 109358.

Monger, W. A., & Jeffries, C. J. (2018). A survey of '*Candidatus* Liberibacter solanacearum'in historical seed from collections of carrot and related *Apiaceae* species. *European Journal of Plant Pathology, 150*(3), 803-815.

Mora, V., Ramasamy, M., Damaj, M. B., Irigoyen, S., Ancona, V., Ibanez, F., Avila, C. A., & Mandadi, K. K. (2021). Potato zebra chip: An overview of the disease, control strategies, and prospects. *Frontiers in Microbiology*, 2064.

Munyaneza, J. E. (2012). Zebra chip disease of potato: biology, epidemiology, and management. *American journal of potato research, 89*(5), 329-350.

Munyaneza, J. E. (2015). Zebra chip disease, *Candidatus* Liberibacter, and potato psyllid: A global threat to the potato industry. *American journal of potato research, 92*(2), 230-235.

Munyaneza, J. E., Buchman, J. L., Sengoda, V. G., Fisher, T. W., & Pearson, C. C. (2011). Susceptibility of selected potato varieties to zebra chip potato disease. *American journal of potato research, 88*(5), 435-440.

Munyaneza, J. E., Sengoda, V. G., Buchman, J. L., & Fisher, T. W. (2012). Effects of temperature on '*Candidatus* Liberibacter solanacearum' and zebra chip potato disease symptom development. *Plant Disease, 96*(1), 18-23.

Munyaneza, J., Sengoda, V., Crosslin, J., De la Rosa-Lozano, G., & Sanchez, A. (2009). First report of '*Candidatus* Liberibacter psyllaurous' in potato tubers with zebra chip disease in Mexico. *Plant Disease, 93*(5), 552-552.

Mustafa, T., Horton, D. R., Cooper, W. R., Swisher, K. D., Zack, R. S., Pappu, H. R., & Munyaneza, J. E. (2015a). Use of electrical penetration graph technology to examine transmission of '*Candidatus* Liberibacter solanacearum'to potato by three haplotypes of potato psyllid (*Bactericera cockerelli*; Hemiptera: Triozidae). *PLoS One, 10*(9), e0138946.

Mustafa, T., Horton, D. R., Cooper, W. R., Zack, R. S., Thinakaran, J., Karasev, A. V., & Munyaneza, J. E. (2021). Stylet Probing Behavior of Two Bactericera (Hemiptera: Psylloidea: Triozidae) Species on Host and Nonhost Plants. *Environmental Entomology, 50*(4), 919-928.

Mustafa, T., Horton, D., Cooper, W., Swisher, K., Zack, R., & Munyaneza, J. (2015b). Interhaplotype fertility and effects of host plant on reproductive traits of three haplotypes of *Bactericera cockerelli* (Hemiptera: Triozidae). *Environmental Entomology, 44*(2), 300-308.

Nault, L. (1997). Arthropod transmission of plant viruses: a new synthesis. *Annals of the Entomological Society of America, 90*(5), 521-541.

Navarre, R., & Pavek, M. J. (2014). *The potato: botany, production and uses*. CABI.

Nelson, W. R., Sengoda, V. G., Alfaro-Fernandez, A. O., Font, M. I., Crosslin, J. M., & Munyaneza, J. E. (2013). A new haplotype of "*Candidatus* Liberibacter solanacearum" identified in the Mediterranean region. *European Journal of Plant Pathology, 135*(4), 633-639.

Nielsen, G. R., Fuentes, C., Quebedeaux, B., Wang, Z., & Lamp, W. O. (1999). Alfalfa physiological response to potato leafhopper injury depends on leafhopper and alfalfa developmental stage. *Entomologia Experimentalis et Applicata, 90*(3), 247-255.

Onuki, M., Truc, N. T. N., Nesumi, H., Hong, L., & Kobayashi, H. (2002). Useful histological method for distinguishing citrus yellowing leaves infected with huanglongbing from those caused by other factors. Proceedings of the 2002 annual workshop of JIRCAS Mekong Delta Project,

Ovchinnikova, A., Krylova, E., Gavrilenko, T., Smekalova, T., Zhuk, M., Knapp, S., & Spooner, D. M. (2011). Taxonomy of cultivated potatoes (Solanum section Petota: Solanaceae). *Botanical Journal of the Linnean Society, 165*(2), 107-155.

Pierson, E. A., Cubero, J., Roper, C., Brown, J. K., Bock, C. H., & Wang, N. (2022). '*Candidatus* Liberibacter' Pathosystems at the Forefront of Agricultural and Biological Research Challenges. *Phytopathology®, 112*(1), 7-10.

Pirone, C., Alexander, L., & Lamp, W. (2005). Patterns of starch accumulation in alfalfa subsequent to potato leafhopper (Homoptera: Cicadellidae) injury. *Environmental Entomology, 34*(1), 199-204.

Pitman, A. R., Drayton, G. M., Kraberger, S. J., Genet, R. A., & Scott, I. A. (2011). Tuber transmission of '*Candidatus* Liberibacter solanacearum' and its association with zebra chip on potato in New Zealand. *European Journal of Plant Pathology, 129*(3), 389-398.

Prager, S. M., Cohen, A., Cooper, W. R., Novy, R., Rashed, A., Wenninger, E. J., & Wallis, C. (2022). A comprehensive review of zebra chip disease in potato and its management through

breeding for resistance/tolerance to ‘Candidatus Liberibacter solanacearum’ and its insect vector. *Pest Management Science*.

Prager, S. M., Wallis, C., & Trumble, J. T. (2015). Indirect effects of one plant pathogen on the transmission of a second pathogen and the behavior of its potato psyllid vector. *Environmental Entomology, 44*(4), 1065-1075.

Prager, S., Wallis, C., Jones, M., Novy, R., & Trumble, J. (2018). Examining the potential role of foliar chemistry in imparting potato germplasm tolerance to potato psyllid, green peach aphid, and zebra chip disease. *Journal of Economic Entomology, 111*(1), 327-336.

Rashed, A., Nash, T., Paetzold, L., Workneh, F., & Rush, C. (2012). Transmission efficiency of ‘*Candidatus* Liberibacter solanacearum’and potato zebra chip disease progress in relation to pathogen titer, vector numbers, and feeding sites. *Phytopathology, 102*(11), 1079-1085.

Rashed, A., Olsen, N., Wallis, C. M., Paetzold, L., Woodell, L., Rashidi, M., Workneh, F., & Rush, C. M. (2018). Postharvest development of ‘*Candidatus* Liberibacter solanacearum’ in late-season infected potato tubers under commercial storage conditions. *Plant Disease, 102*(3), 561-568.

Rashed, A., Wallis, C., Paetzold, L., Workneh, F., & Rush, C. (2013). Zebra chip disease and potato biochemistry: tuber physiological changes in response to ‘*Candidatus* Liberibacter solanacearum’ infection over time. *Phytopathology, 103*(5), 419-426.

Rashed, A., Workneh, F., Paetzold, L., & Rush, C. M. (2015). Emergence of ‘*Candidatus* Liberibacter solanacearum’-infected seed potato in relation to the time of infection. *Plant Disease, 99*(2), 274-280.

Rashed, A., Workneh, F., Paetzold, L., Gray, J., & Rush, C. (2014). Zebra chip disease development in relation to plant age and time of ‘*Candidatus* Liberibacter solanacearum’ infection. *Plant Disease, 98*(1), 24-31.

Ravindran, A., Levy, J., Pierson, E., & Gross, D. C. (2011). Development of primers for improved PCR detection of the potato zebra chip pathogen,‘*Candidatus* Liberibacter solanacearum’. *Plant Disease, 95*(12), 1542-1546.

Ravindran, A., Levy, J., Pierson, E., & Gross, D. C. (2012). Development of a loop-mediated isothermal amplification procedure as a sensitive and rapid method for detection of '*Candidatus* Liberibacter solanacearum'in potatoes and psyllids. *Phytopathology, 102*(9), 899-907.

Reddy, B., Mandal, R., Chakroborty, M., Hijam, L., & Dutta, P. (2018). A review on potato (*Solanum tuberosum* L.) and its genetic diversity. *International Journal of Genetics, ISSN*, 0975-2862.

Rehman, M., Melgar, J., Rivera C, J., Idris, A., & Brown, J. (2010). First report of "*Candidatus* Liberibacter psyllaurous" or "Ca. Liberibacter solanacearum" associated with severe foliar chlorosis, curling, and necrosis and tuber discoloration of potato plants in Honduras. *Plant Disease, 94*(3), 376-376.

Reyes Corral, C. A., Cooper, W. R., Horton, D., Miliczky, E., Riebe, J., Waters, T., Wildung, M., & Karasev, A. V. (2021). Association of *Bactericera cockerelli* (Hemiptera: Triozidae) with the perennial weed Physalis longifolia (Solanales: Solanaceae) in the potato-growing regions of western Idaho. *Environmental Entomology, 50*(6), 1416-1424.

Rondon, S. I., Schreiber, A., Jensen, A. S., Hamm, P. B., Munyaneza, J., Nolte, P., Olsen, N., Wenninger, E., Henne, D., & Wohleb, C. (2012). Potato psyllid vector of Zebra Chip Disease in the Pacific Northwest: biology, ecology, and management.

Roux, K. H. (2009). Optimization and troubleshooting in PCR. *Cold Spring Harbor Protocols, 2009*(4), pdb. ip66.

Sandanayaka, W., Moreno, A., Tooman, L., Page-Weir, N., & Fereres, A. (2014). Stylet penetration activities linked to the acquisition and inoculation of C andidatus L iberibacter solanacearum by its vector tomato potato psyllid. *Entomologia Experimentalis et Applicata, 151*(2), 170-181.

Schneider, H. (1968). Anatomy of greening-diseased sweet orange shoots. *Phytopathology, 58*(1), 1555-1160.

Secor, G., Rivera, V., Abad, J., Lee, I.-M., Clover, G., Liefting, L., Li, X., & De Boer, S. (2009). Association of '*Candidatus* Liberibacter solanacearum'with zebra chip disease of potato

established by graft and psyllid transmission, electron microscopy, and PCR. *Plant Disease, 93*(6), 574-583.

Sengoda, V. G., Buchman, J. L., Henne, D. C., Pappu, H. R., & Munyaneza, J. E. (2013). "*Candidatus* Liberibacter solanacearum" titer over time in *Bactericera cockerelli* (Hemiptera: Triozidae) after acquisition from infected potato and tomato plants. *Journal of Economic Entomology, 106*(5), 1964-1972.

Sengoda, V. G., Cooper, W. R., Swisher, K. D., Henne, D. C., & Munyaneza, J. E. (2014). Latent period and transmission of "*Candidatus* Liberibacter solanacearum" by the potato psyllid *Bactericera cockerelli* (Hemiptera: Triozidae). *PLoS One, 9*(3), e93475.

Sengoda, V. G., Munyaneza, J. E., Crosslin, J. M., Buchman, J. L., & Pappu, H. R. (2010). Phenotypic and etiological differences between psyllid yellows and zebra chip diseases of potato. *American journal of potato research, 87*(1), 41-49.

Spooner, D. M., Núñez, J., Trujillo, G., del Rosario Herrera, M., Guzmán, F., & Ghislain, M. (2007). Extensive simple sequence repeat genotyping of potato landraces supports a major reevaluation of their gene pool structure and classification. *Proceedings of the National Academy of Sciences, 104*(49), 19398-19403.

Swisher Grimm, K. D., Mustafa, T., Cooper, W. R., & Munyaneza, J. E. (2020). Growth and yield performance of *Solanum tuberosum* grown from seed potatoes infected with '*Candidatus* Liberibacter solanacearum'haplotypes A and B. *Plant Disease, 104*(3), 688-693.

Swisher Grimm, K., & Garczynski, S. (2019). Identification of a new haplotype of '*Candidatus* Liberibacter solanacearum' in *Solanum tuberosum*. *Plant Disease, 103*(3), 468-474.

Swisher, K. D., Henne, D. C., & Crosslin, J. M. (2014). Identification of a fourth haplotype of *Bactericera cockerelli* (Hemiptera: Triozidae) in the United States. *Journal of Insect Science, 14*(1).

Swisher, K. D., Munyaneza, J. E., & Crosslin, J. M. (2012). High resolution melting analysis of the cytochrome oxidase I gene identifies three haplotypes of the potato psyllid in the United States. *Environmental Entomology, 41*(4), 1019-1028.

Takushi, T., Toyozato, T., Kawano, S., Taba, S., Taba, K., Ooshiro, A., Numazawa, M., & Tokeshi, M. (2007). Scratch method for simple, rapid diagnosis of citrus huanglongbing using iodine to detect high accumulation of starch in the citrus leaves. *Japanese Journal of Phytopathology (Japan)*.

Tang, X.-T., Fortuna, K., Mendoza Herrera, A., & Tamborindeguy, C. (2020). Liberibacter, a preemptive bacterium: Apoptotic response repression in the host gut at the early infection to facilitate its acquisition and transmission. *Frontiers in Microbiology, 11*, 589509.

Tang, X.-T., Longnecker, M., & Tamborindeguy, C. (2020). Acquisition and transmission of two '*Candidatus* Liberibacter solanacearum' haplotypes by the tomato psyllid *Bactericera cockerelli*. *Scientific Reports, 10*(1), 1-8.

Teara.govt.nz. 2022. *Major vegetable crops*. [online] Available at: https://teara.govt.nz/en/market-gardens-and-production-nurseries/page-3. Accessed 9 August 2022.

Thinakaran, J., Yang, X.-B., Munyaneza, J., Rush, C., & Henne, D. (2015). Comparative biology and life tables of "*Candidatus* Liberibacter solanacearum"-infected and-free *Bactericera cockerelli* (Hemiptera: Triozidae) on potato and silverleaf nightshade. *Annals of the Entomological Society of America, 108*(4), 459-467.

Thomas, K., Jones, D., Kumarasinghe, L., Richmond, J., Gill, G., & Bullians, M. (2011). Investigation into the entry pathway for tomato potato psyllid *Bactericera cockerelli*. *New Zealand Plant Protection, 64*, 259-268.

Thompson, S. M., Johnson, C. P., Lu, A. Y., Frampton, R. A., Sullivan, K. L., Fiers, M. W., Crowhurst, R. N., Pitman, A. R., Scott, I. A., & Wen, A. (2015). Genomes of '*Candidatus* Liberibacter solanacearum'haplotype A from New Zealand and the United States suggest significant genome plasticity in the species. *Phytopathology, 105*(7), 863-871.

Torres, G. L., Cooper, W. R., Horton, D. R., Swisher, K. D., Garczynski, S. F., Munyaneza, J. E., & Barcenas, N. M. (2015). Horizontal Transmission of" *Candidatus* Liberibacter solanacearum" by *Bactericera cockerelli* (Hemiptera: Triozidae) on Convolvulus and Ipomoea (Solanales: Convolvulaceae). *PLoS One, 10*(11), e0142734.

Troncoso, E., Zúñiga, R., Ramírez, C., Parada, J., & Germain, J. C. (2009). Microstructure of potato products: Effect on physico-chemical properties and nutrient bioavailability. *Glob. Sci. Books, 3*, 41-54.

Vereijssen, J., Barnes, A., Berry, N., Drayton, G., Fletcher, J., Jacobs, J., Jorgensen, N., Nielsen, M., Pitman, A., & Scott, I. (2015). The rise and rise of *Bactericera cockerelli* in potato crops in Canterbury. *New Zealand Plant Protection, 68*, 85-90.

Walker, G. P., MacDonald, F. H., Wright, P. J., Puketapu, A. J., Gardner-Gee, R., Connolly, P. G., & Anderson, J. A. (2015). Development of action thresholds for management of *Bactericera cockerelli* and Zebra Chip disease in potatoes at Pukekohe, New Zealand. *American journal of potato research, 92*(2), 266-275.

Wallis, C., Rashed, A., & Rush, C. (2012). Large-scale shifts in potato (*Solanum tuberosum*) tuber physiology occur following infection by '*Candidatus* Liberibacter solanacearum'. *Phytopathology, 102*, 129-130.

Wallis, C., Rashed, A., Chen, J., Paetzold, L., Workneh, F., & Rush, C. (2015). Effects of potato-psyllid-vectored '*Candidatus* Liberibacter solanacearum' infection on potato leaf and stem physiology. *Phytopathology, 105*(2), 189-198.

Wallis, C., Rashed, A., Wallingford, A., Paetzold, L., Workneh, F., & Rush, C. (2014). Similarities and differences in physiological responses to '*Candidatus* Liberibacter solanacearum' infection among different potato cultivars. *Phytopathology, 104*(2), 126-133.

Wan, J., Wang, R., Ren, Y., & McKirdy, S. (2020). Potential distribution and the risks of *Bactericera cockerelli* and its associated plant pathogen *Candidatus* Liberibacter Solanacearum for global potato production. *Insects, 11*(5), 298.

Wang, J., Haapalainen, M., Schott, T., Thompson, S. M., Smith, G. R., Nissinen, A. I., & Pirhonen, M. (2017). Genomic sequence of '*Candidatus* Liberibacter solanacearum' haplotype C and its comparison with haplotype A and B genomes. *PLoS One, 12*(2), e0171531.

Wang, N., Pierson, E. A., Setubal, J. C., Xu, J., Levy, J. G., Zhang, Y., Li, J., Rangel, L. T., & Martins Jr, J. (2017). The *Candidatus* Liberibacter–host interface: insights into pathogenesis mechanisms and disease control. *Annual review of phytopathology, 55*, 451-482.

Wen, A., Johnson, C., & Gudmestad, N. C. (2013). Development of a PCR assay for the rapid detection and differentiation of '*Candidatus* Liberibacter solanacearum' haplotypes and their spatiotemporal distribution in the United States. *American journal of potato research, 90*(3), 229-236.

Wen, A., Mallik, I., Alvarado, V., Pasche, J., Wang, X., Li, W., Levy, L., Lin, H., Scholthof, H., & Mirkov, T. (2009). Detection, distribution, and genetic variability of '*Candidatus* Liberibacter' species associated with zebra complex disease of potato in North America. *Plant Disease, 93*(11), 1102-1115.

Wenninger, E. J., Carroll, A., Dahan, J., Karasev, A. V., Thornton, M., Miller, J., Nolte, P., Olsen, N., & Price, W. (2017). Phenology of the potato psyllid, *Bactericera cockerelli* (Hemiptera: Triozidae), and "*Candidatus* Liberibacter solanacearum" in commercial potato fields in Idaho. *Environmental Entomology, 46*(6), 1179-1188.

Wenninger, E. J., Olsen, N., Lojewski, J., Wharton, P., Dahan, J., Rashed, A., & Karasev, A. V. (2020). Effects of potato psyllid vector density and time of infection on zebra chip disease development after harvest and during storage. *American journal of potato research, 97*(3), 278-288.

Whitaker, D. C., Giurcanu, M. C., Young, L. J., Gonzalez, P., Etxeberria, E., Roberts, P., Hendricks, K., & Roman, F. (2014). Starch content of citrus leaves permits diagnosis of huanglongbing in the warm season but not cool season. *HortScience, 49*(6), 757-762.

Xu, X., Vreugdenhil, D., & Lammeren, A. A. v. (1998). Cell division and cell enlargement during potato tuber formation. *Journal of Experimental Botany, 49*(320), 573-582.

Zhang, Z., Schwartz, S., Wagner, L., & Miller, W. (2000). A greedy algorithm for aligning DNA sequences. *Journal of Computational biology, 7*(1-2), 203-214.

Zhao, Z., Prager, S. M., Cruzado, R. K., Liang, X., Cooper, W. R., Hu, G., & Rashed, A. (2018). Characterizing Zebra Chip symptom severity and identifying spectral signatures associated with '*Candidatus* Liberibacter solanacearum'-infected potato tubers. *American journal of potato research, 95*(5), 584-596.

APPENDIX

Appendix A - 3% Iodine Starch Test Results of the 24 'Russet Burbank' plants

1. ZC-symptomatic samples

Figure A. 1. Tuber and leaf lamina of Zebra Chip symptomatic sample 1 immersed in 3% iodine solution.

Figure A. 2. Tuber and leaf lamina of Zebra Chip symptomatic sample 2 immersed in 3% iodine solution.

Figure A. 3. Tuber and leaf lamina of Zebra Chip symptomatic sample 3 immersed in 3% iodine solution.

Figure A. 4. Tuber and leaf lamina of Zebra Chip symptomatic sample 4 immersed in 3% iodine solution.

Figure A. 5. Tuber and leaf lamina of Zebra Chip symptomatic sample 5 immersed in 3% iodine solution.

Figure A. 6. Tuber and leaf lamina of Zebra Chip symptomatic sample 6 immersed in 3% iodine solution.

Figure A. 7. Tuber and leaf lamina of Zebra Chip symptomatic sample 7 immersed in 3% iodine solution.

Figure A. 8. Tuber and leaf lamina of Zebra Chip symptomatic sample 8 immersed in 3% iodine solution.

2. *Rhizoctonia solani* Symptomatic samples

Figure A. 9. Tuber and leaf lamina of *Rhizoctonia solani* Symptomatic sample 1 immersed in 3% iodine solution.

Figure A. 10. Tuber and leaf lamina of *Rhizoctonia solani* Symptomatic sample 2 immersed in 3% iodine solution.

Figure A. 11. Tuber and leaf lamina of *Rhizoctonia solani* Symptomatic sample 3 immersed in 3% iodine solution.

Figure A. 12. Tuber and leaf lamina of *Rhizoctonia solani* Symptomatic sample 4 immersed in 3% iodine solution.

Figure A. 13. Tuber and leaf lamina of *Rhizoctonia solani* Symptomatic sample 5 immersed in 3% iodine solution.

Figure A. 14. Tuber and leaf lamina of *Rhizoctonia solani* Symptomatic sample 6 immersed in 3% iodine solution.

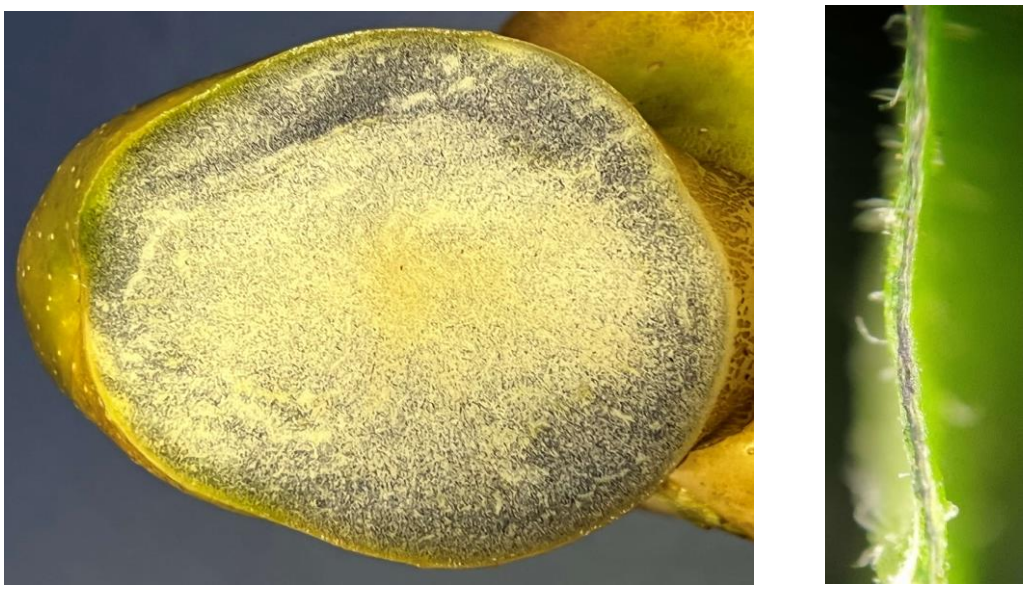

Figure A. 15. Tuber and leaf lamina of *Rhizoctonia solani* Symptomatic sample 7 immersed in 3% iodine solution.

Figure A. 16. Tuber and leaf lamina of *Rhizoctonia solani* Symptomatic sample 8 immersed in 3% iodine solution.

3. Visibly healthy plant samples

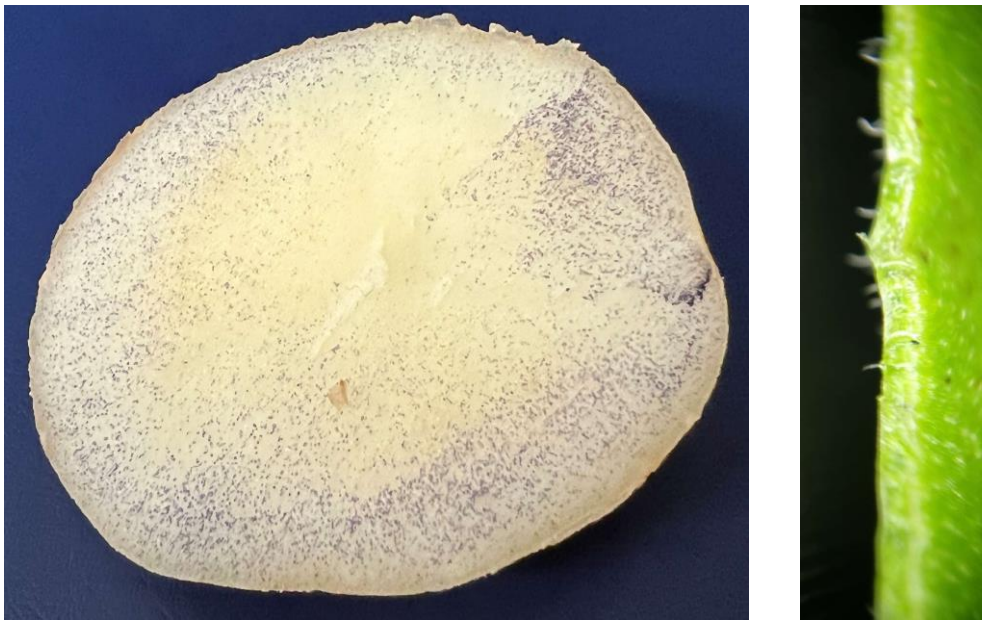

Figure A. 17. Tuber and leaf lamina of visibly healthy-looking plant sample 1 immersed in 3% iodine solution.

Figure A. 18. Tuber and leaf lamina of visibly healthy-looking plant sample 2 immersed in 3% iodine solution.

Figure A. 19. Tuber and leaf lamina of visibly healthy-looking plant sample 3 immersed in 3% iodine solution.

Figure A. 20. Tuber and leaf lamina of visibly healthy-looking plant sample 4 immersed in 3% iodine solution.

Figure A. 21. Tuber and leaf lamina of visibly healthy-looking plant sample 5 immersed in 3% iodine solution.

Figure A. 22. Tuber and leaf lamina of visibly healthy-looking plant sample 6 immersed in 3% iodine solution.

Figure A. 23. Tuber and leaf lamina of visibly healthy-looking plant sample 7 immersed in 3% iodine solution.

Figure A. 24. Tuber and leaf lamina of visibly healthy-looking plant sample 8 immersed in 3% iodine solution.

Appendix B - PCR results

Single step PCR

Tables below denote the PCR products of the sample type and number used for gel electrophoresis. A 1 kb plus ladder was included in all gel results to evaluate the amplification.

1. Gel electrophoresis results of ZC-symptomatic sample 1 and 2, *R. solani*- symptomatic sample 1 and 2, and visibly healthy plant samples 1 and 2.

Table B. 1. Lane number and its single-step PCR product contents of the gel electrophoresis results observed in Fig. 9.

Lane Number	Sample ID
A	
2	L 1 Leaf
3	L 1 Outer tuber region
4	L 1 Inner tuber region
5	L 2 Leaf
6	L 2 Outer tuber region
7	L 2 Inner tuber region
8	R 1 Leaf
9	R 1Outer tuber region
10	R 1 Inner tuber region
12	R 2 Leaf
13	R 2 Outer tuber region
14	R 2 Inner tuber region
15	C 1 Leaf
16	C 1 Outer tuber region
17	C 1 Inner tuber region
18	C 2 Leaf
B	
1	C 2 Outer tuber region
2	L 1 Inner tuber region (Positive Control)
3	R 1 Inner tuber region (Positive Control)
4	C 1 Inner tuber region (Positive Control)
5	Negative control

Note: L: Zebra Chip symptomatic sample
R: *Rhizoctonia solani* symptomatic sample
C: Visibly healthy-looking plant sample

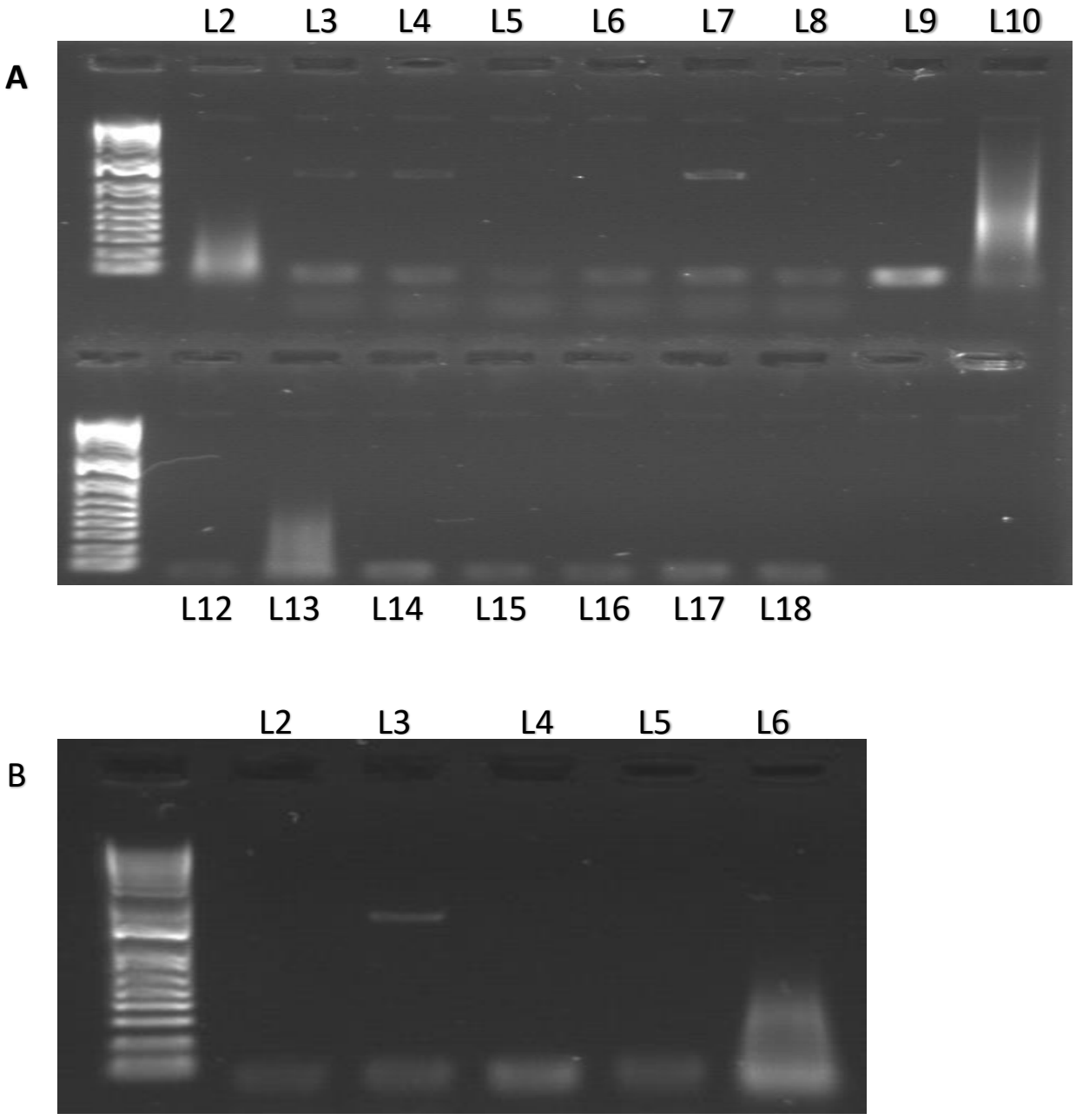

Figure B. 1. Gel electrophoresis results of samples states in table 1. 'L' denotes the lane number.

2. Gel electrophoresis results of ZC-symptomatic sample 3 and 4, *R. solani*-symptomatic sample 3 and 4, and visibly healthy plant samples 2 and 3.

Table B. 2. Lane number and its single-step PCR product contents of the gel electrophoresis results observed in Fig. 10.

Lane Number	ID
A	
2	L 3 Leaf
3	L 3 Outer tuber region
4	L 3 Inner tuber region
5	L 4 Leaf
6	L 4 Outer tuber region
7	L 4 Inner tuber region
8	R 3 Leaf
9	R 3 Outer tuber region
10	R 3 Inner tuber region
12	R 4 Leaf
13	R 4 Outer tuber region
14	R 4 Inner tuber region
15	C 2 Inner tuber region
16	C 3 Leaf
17	C 3 Outer tuber region
18	C 3 Inner tuber region
19	Negative control
B	
1	C 4 Leaf
2	L 1 Inner tuber region (Positive Control)
3	R 1 Inner tuber region (Positive Control)
4	C 1 Inner tuber region (Positive Control)
5	Negative control

Note: L: Zebra Chip symptomatic sample
R: *Rhizoctonia solani* symptomatic sample
C: Visibly healthy-looking plant sample

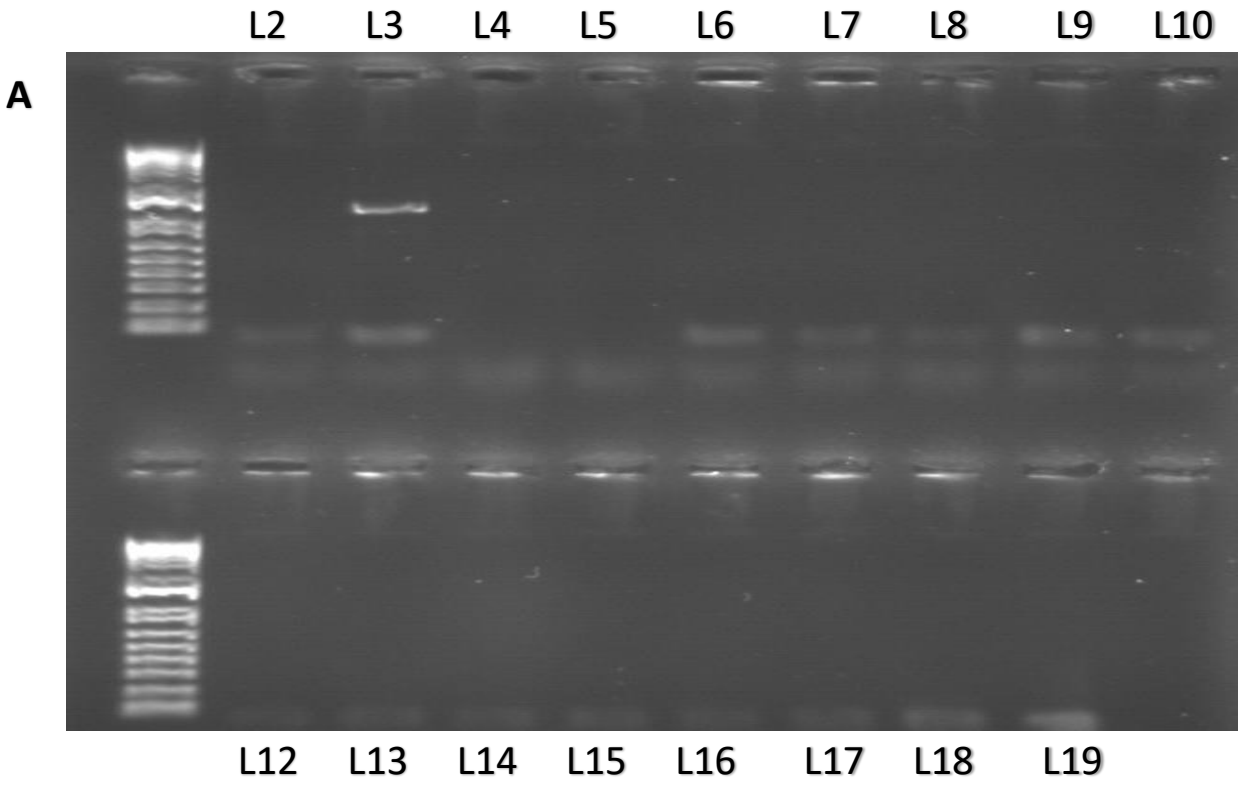

Figure B. 2. Gel electrophoresis results of samples states in table 2. 'L' denotes the lane number.

3. Gel electrophoresis results of ZC-symptomatic sample 5 and 6, *R. solani*-symptomatic sample 5 and 6, and visibly healthy plant samples 4 and 5.

Table B. 3. Lane number and its single-step PCR product contents of the gel electrophoresis results observed in Fig. 11.

Lane Number	ID
A	
2	L 5 Leaf
3	L 5 Outer tuber region
4	L 5 Inner tuber region
5	L 6 Leaf
6	L 6 Outer tuber region
7	L 6 Inner tuber region
8	R 5 Leaf
9	R 5 Outer tuber region
10	R 5 Inner tuber region
12	R 6 Leaf
13	R 6 Outer tuber region
14	R 6 Inner tuber region
15	C 4 Outer tuber region
16	C 4 Inner tuber region
17	C 5 Leaf
B	
2	C 5 Outer tuber region
3	C 5 Inner tuber region
4	L 1 Inner tuber region (Positive Control)
5	R 1 Inner tuber region (Positive Control)
6	C 1 Inner tuber region (Positive Control)
7	Negative control

Note: L: Zebra Chip symptomatic sample
R: *Rhizoctonia solani* symptomatic sample
C: Visibly healthy-looking plant sample

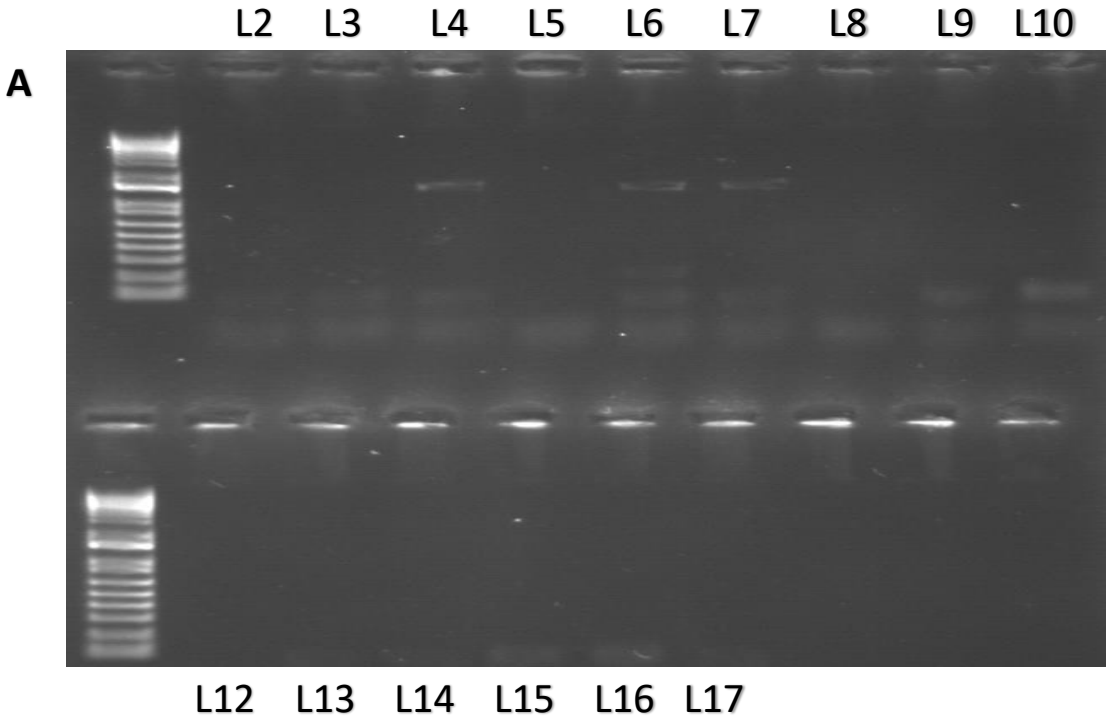

Figure B. 3. Gel electrophoresis results of samples states in table 3. 'L' denotes the lane number.

4. Gel electrophoresis results of ZC-symptomatic sample 7 and 8, *R. solani*-symptomatic sample 7 and 8, and visibly healthy plant samples 6 and 7.

Table B. 4. Lane number and its single-step PCR product contents of the gel electrophoresis results observed in Fig. 12.

Lane Number	ID
A	
2	L 7 Leaf
3	L 7 Outer tuber region
4	L 7 Inner tuber region
5	L 8 Leaf
6	L 8 Outer tuber region
7	L 8 Inner tuber region
8	R 7 Leaf
9	R 7 Outer tuber region
10	R 7 Inner tuber region
12	R 8 Leaf
13	R 8 Outer tuber region
14	R 8 Inner tuber region
15	C 6 Leaf
16	C 6 Outer tuber region
17	C 6 Inner tuber region
B	
2	C 7 Leaf
3	C 7 Outer tuber region
4	L 1 Inner tuber region (Positive Control)
5	R 1 Inner tuber region (Positive Control)
6	C 1 Inner tuber region (Positive Control)
7	Negative control
10	C 7 Inner tuber region
11	C 8 Leaf
12	C 8 Outer tuber region
13	C 8 Inner tuber region
14	L 1 Inner tuber region (Positive Control)
15	R 1 Inner tuber region (Positive Control)
16	C 1 Inner tuber region (Positive Control)
17	Negative control

Note: L: Zebra Chip symptomatic sample
R: *Rhizoctonia solani* symptomatic sample
C: Visibly healthy-looking plant sample

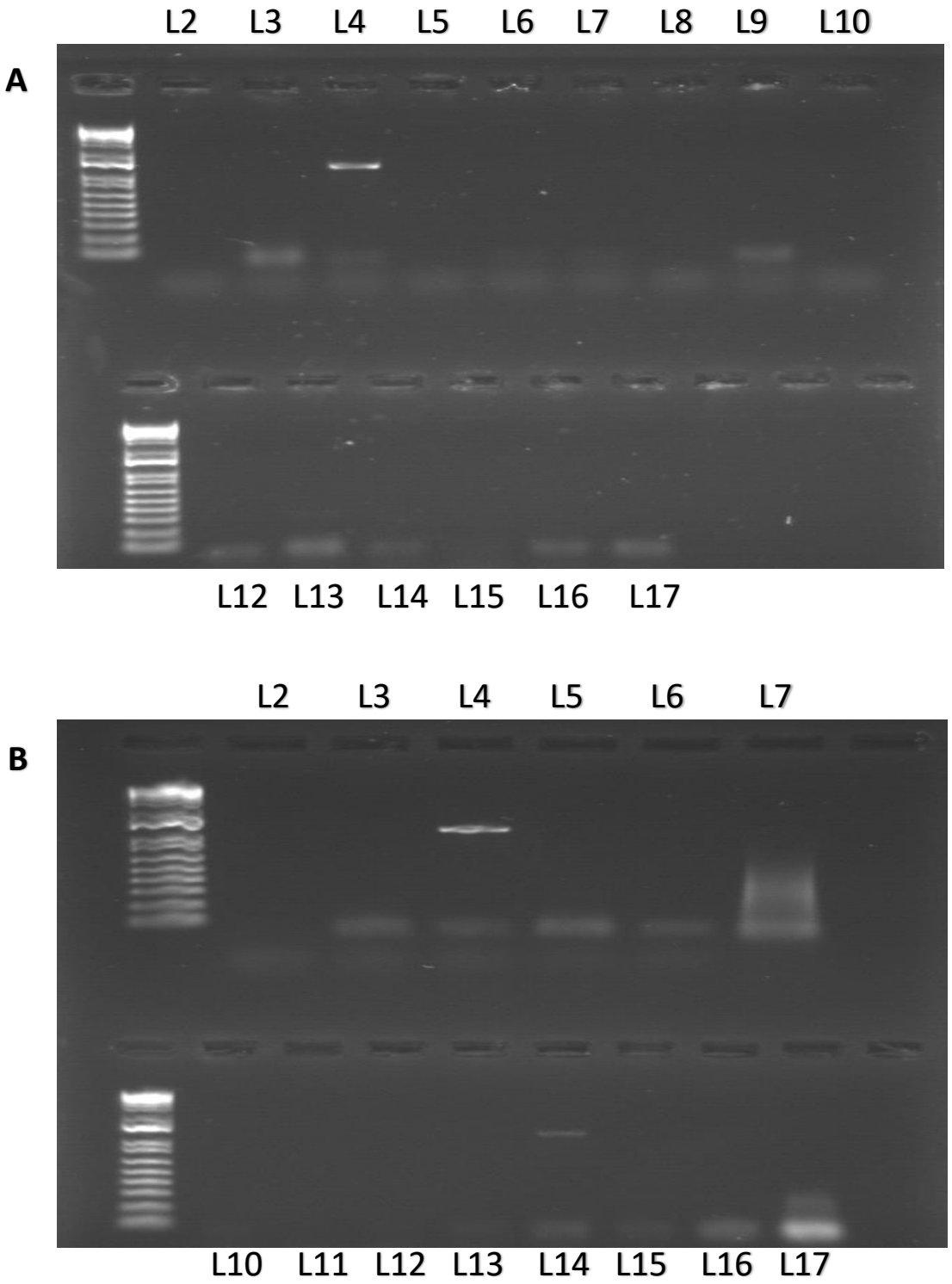

Figure B. 4. Gel electrophoresis results of samples states in table 4. 'L' denotes the lane number.

Nested PCR

Tables below denote the PCR products of the sample number and type used for gel electrophoresis.

1. Gel electrophoresis results of ZC-symptomatic sample 1 and 2, after nested PCR.

Table B. 5. Lane number and its nested PCR product contents of the gel electrophoresis results observed in Fig. 13.

Lane Number	ID
	A
2*	L 1 Leaf
3*	L 1 Outer tuber region
4*	L 1 Inner tuber region
5*	L 2 Leaf
6*	L 2 Outer tuber region
7*	L 2 Inner tuber region
8	L 1 Leaf
9	L 1 Outer tuber region
12	L 1 Inner tuber region
13	L 2 Leaf
14	L 2 Outer tuber region
15	L 2 Inner tuber region
16	Negative control

Note: L: Zebra Chip symptomatic sample
R: *Rhizoctonia solani* symptomatic sample
C: Visibly healthy-looking plant sample
'*****' denotes products that used 1µl (of a 1 in 20 dilution) from the single-step PCR product as a template.

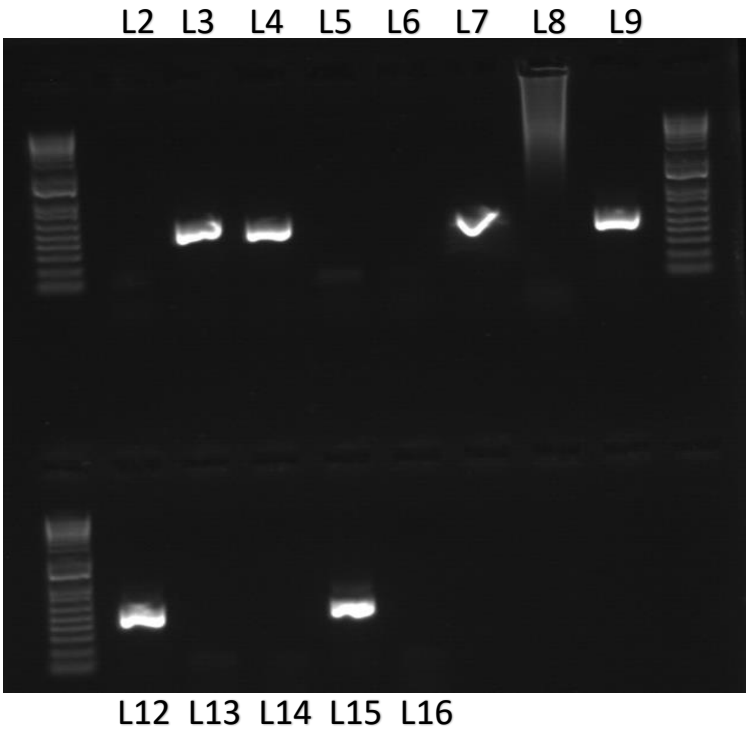

Figure B. 5. Gel electrophoresis results of samples states in table 1. 'L' denotes the lane number.

2. Gel electrophoresis results of ZC-symptomatic sample 1 and 2, *R. solani*-symptomatic sample 1 and 2, and visibly healthy plant samples 1 and 2.

Table B. 6. Lane number and its single-step PCR product contents of the gel electrophoresis results observed in Fig. 9.

Lane Number	ID
	A
2	L 3 Leaf
3	L 3 Outer tuber region
4	L 3 Inner tuber region
5	L 4 Leaf
6	L 4 Outer tuber region
7	L 4 Inner tuber region
8	L 5 Leaf
10	L 5 Outer tuber region
11	L 5 Inner tuber region
12	C 2 Leaf
13	C 2 Outer tuber region
14	C 2 Inner tuber region
15	Negative control

Note: L: Zebra Chip symptomatic sample
R: *Rhizoctonia solani* symptomatic sample
C: Visibly healthy-looking plant sample

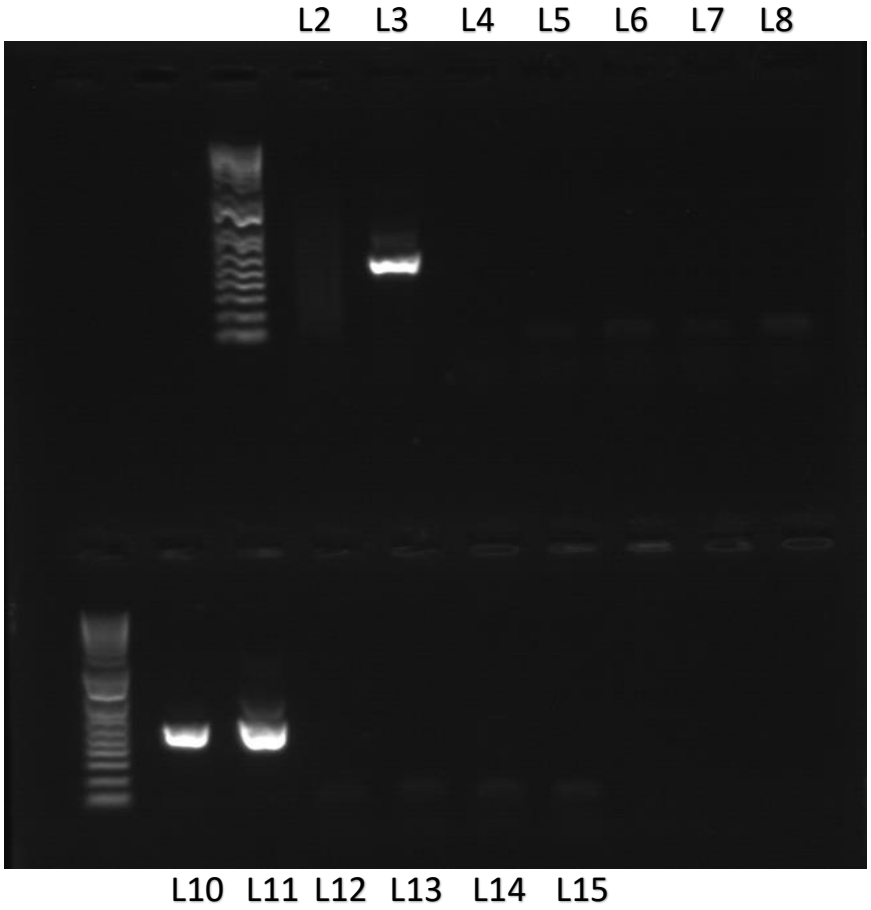

Figure B. 6. Gel electrophoresis results of samples states in table 1. 'L' denotes the lane number.

3. Gel electrophoresis results of ZC-symptomatic sample 1 and 2, *R. solani*-symptomatic sample 1 and 2, and visibly healthy plant samples 1 and 2.

Table B. 7. Lane number and its single-step PCR product contents of the gel electrophoresis results observed in Fig. 9.

Lane Number	ID
	A
2	L 6 Leaf
3	L 6 Outer tuber region
4	L 6 Inner tuber region
5	L 7 Inner tuber region
6	L 7 Outer tuber region
7	L 7 Leaf
8	L 8 Leaf
9	L 8 Outer tuber region
10	L 8 Inner tuber region

11	C 1 Leaf
13	C 1 Outer tuber region
14	C 1 Inner tuber region
15	C 3 Leaf
16	C 3 Outer tuber region
17	C 3 Inner tuber region
18	C 4 Leaf
19	C 4 Outer tuber region
20	C 4 Inner tuber region
21	C 5 Leaf
22	Positive control (L 1 Outer tuber region)
23	Negative control

Note: L: Zebra Chip symptomatic sample
R: *Rhizoctonia solani* symptomatic sample
C: Visibly healthy-looking plant sample

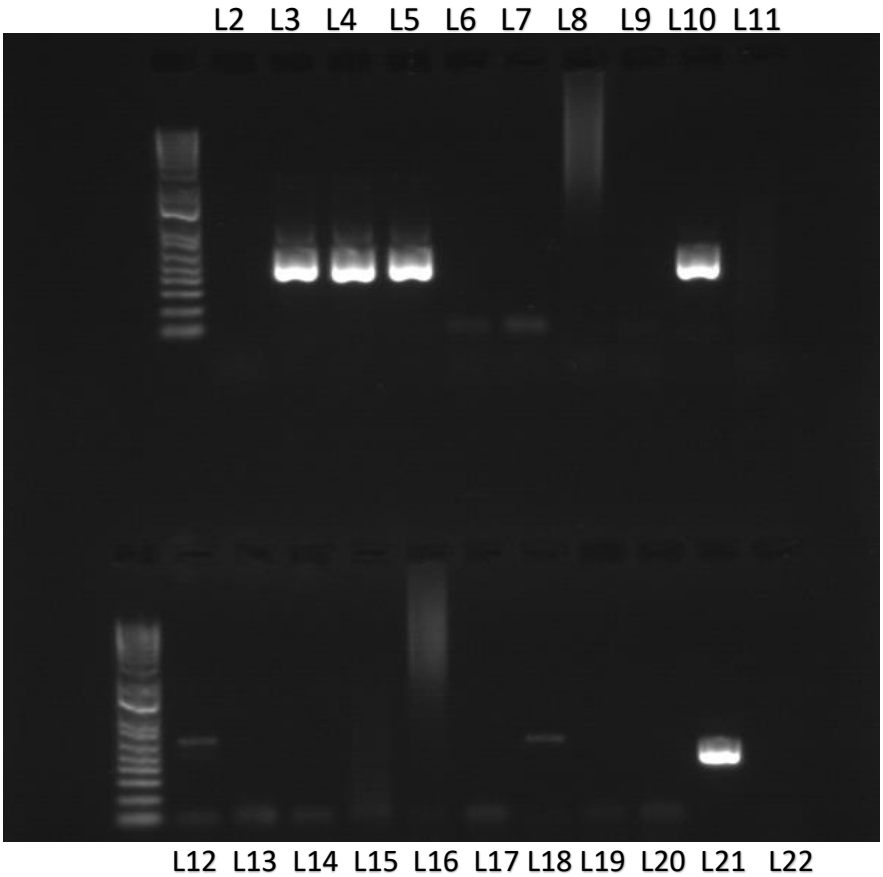

Figure B. 7. Gel electrophoresis results of samples states in table 1. 'L' denotes the lane number.

4. Gel electrophoresis results of ZC-symptomatic sample 1 and 2, *R. solani*-symptomatic sample 1 and 2, and visibly healthy plant samples 1 and 2.

Table B. 8. Lane number and its single-step PCR product contents of the gel electrophoresis results observed in Fig. 9.

Lane Number	ID
A	
2	Positive control (L 1 Outer tuber region)
3	Negative control
4	C 5 Inner tuber region
5	C 5 Inner tuber region
6	C 6 Leaf
7	C 6 Outer tuber region
8	C 6 Inner tuber region
9	C 7 Leaf
10	C 7 Outer tuber region
11	C 7 Inner tuber region
12	C 8 Leaf
14	C 8 Outer tuber region
15	C 8 Inner tuber region
16	R 1 Leaf
17	R 1 Outer tuber region
18	R 1 Inner tuber region
19	R 2 Leaf
20	R 2 Outer tuber region
21	R 2 Inner tuber region
22	R 3 Leaf
23	R 3 Outer tuber region

Note: L: Zebra Chip symptomatic sample
R: *Rhizoctonia solani* symptomatic sample
C: Visibly healthy-looking plant sample

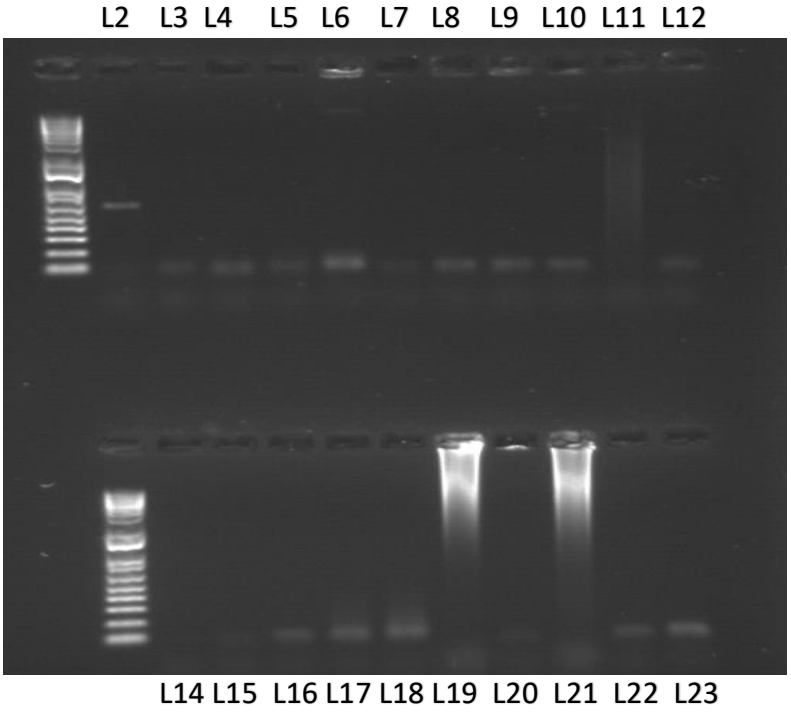

Figure B. 8. Gel electrophoresis results of samples states in table 1. 'L' denotes the lane number.

5. Gel electrophoresis results of ZC-symptomatic sample 1 and 2, *R. solani*-symptomatic sample 1 and 2, and visibly healthy plant samples 1 and 2.

Table B. 9. Lane number and its single-step PCR product contents of the gel electrophoresis results observed in Fig. 9.

Lane Number	ID
A	
2	Positive control (L 1 Outer tuber region)
3	Negative control
4	R 3 Inner tuber region
5	R 4 Leaf
6	R 4 Outer tuber region
7	R 4 Inner tuber region
8	R 5 Leaf
9	R 5 Outer tuber region
10	R 5 Inner tuber region
11	R 6 Leaf
12	R 6 Outer tuber region
14	R 6 Inner tuber region
15	R 7 Leaf
16	R 7 Outer tuber region
17	R 7 Inner tuber region
18	R 8 Leaf

19	R 8 Outer tuber region
20	R 8 Inner tuber region
21	Positive control (L 1 Outer tuber region)
22	Negative control

Note: L: Zebra Chip symptomatic sample
R: *Rhizoctonia solani* symptomatic sample
C: Visibly healthy-looking plant sample

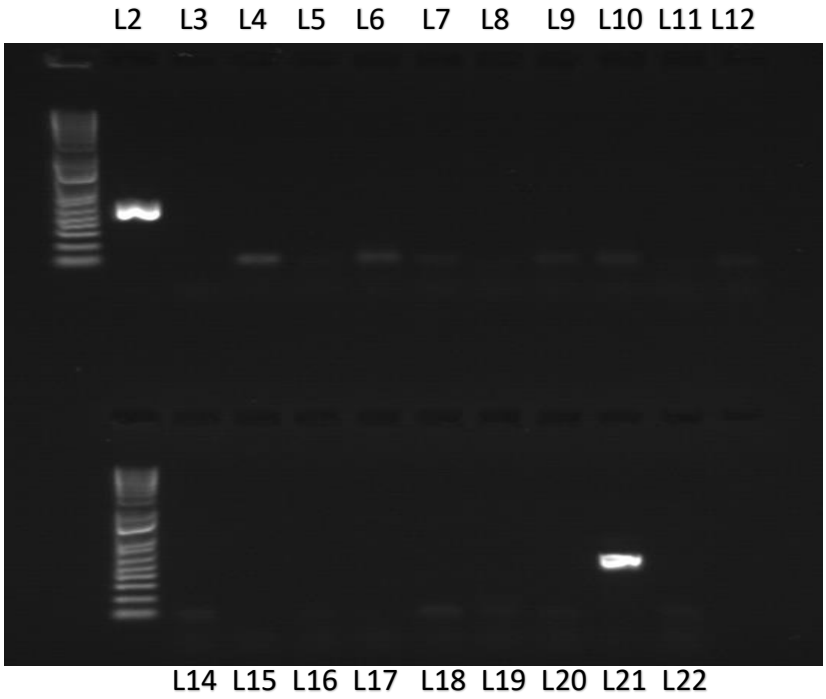

Figure B. 9. Gel electrophoresis results of samples states in table 1. 'L' denotes the lane number.